ISSN 1854-6250

APEM journal

Advances in Production Engineering & Management

Volume 11 | Number 1 | March 2016

University of Maribor

Published by PEI
apem-journal.org

Advances in Production Engineering & Management

Identification Statement

APEM journal

ISSN 1854-6250 | Abbreviated key title: **Adv produc engineer manag** | Start year: 2006
ISSN 1855-6531 (on-line)

Published quarterly by **Production Engineering Institute (PEI)**, **University of Maribor**
Smetanova ulica 17, SI – 2000 Maribor, Slovenia, European Union (EU)

Phone: 00386 2 2207522, Fax: 00386 2 2207990
Language of text: English

University of Maribor

APEM homepage: apem-journal.org
University homepage: www.um.si

APEM Editorial

Subscription Rate: 120 EUR for 4 issues (worldwide postage included); 30 EUR for single copies (plus 10 EUR for postage); for details about payment please contact: info@apem-journal.org
Postmaster: Send address changes to info@apem-journal.org
Cover and interior design: Miran Brezocnik
Printed: Tiskarna Koštomaj, Celje, Slovenia

Advances in Production Engineering & Management is indexed and abstracted in the **WEB OF SCIENCE** (maintained by **THOMSON REUTERS**): **Science Citation Index Expanded**, **Journal Citation Reports** – Science Edition, **Current Contents** – Engineering, Computing and Technology • **Scopus** (maintained by **Elsevier**) • **Inspec** • **EBSCO**: Academic Search Alumni Edition, Academic Search Complete, Academic Search Elite, Academic Search Premier, Engineering Source, Sales & Marketing Source, TOC Premier • **ProQuest**: CSA Engineering Research Database – Cambridge Scientific Abstracts, Materials Business File, Materials Research Database, Mechanical & Transportation Engineering Abstracts, ProQuest SciTech Collection • **TEMA** (**DOMA**) • The journal is listed in **Ulrich's** Periodicals Directory and **Cabell's** Directory

University of Maribor
Production Engineering Institute (PEI)

Advances in Production Engineering & Management

Volume 11 | Number 1 | March 2016 | pp 1–72

Contents

Journal homepage: apem-journal.org

ISSN 1854-6250
ISSN 1855-6531 (on-line)

Scope and topics

Advances in Production Engineering & Management (*APEM journal*) is an interdisciplinary refereed international academic journal published quarterly by the *Production Engineering Institute* at the *University of Maribor*. The main goal of the *APEM journal* is to present original, high quality, theoretical and application-oriented research developments in all areas of production engineering and production management to a broad audience of academics and practitioners. In order to bridge the gap between theory and practice, applications based on advanced theory and case studies are particularly welcome. For theoretical papers, their originality and research contributions are the main factors in the evaluation process. General approaches, formalisms, algorithms or techniques should be illustrated with significant applications that demonstrate their applicability to real-world problems. Although the *APEM journal* main goal is to publish original research papers, review articles and professional papers are occasionally published.

Fields of interest include, but are not limited to:

Additive Manufacturing Processes
Advanced Production Technologies
Artificial Intelligence
Assembly Systems
Automation
Cutting and Forming Processes
Decision Support Systems
Discrete Systems and Methodology
e-Manufacturing
Fuzzy Systems
Human Factor Engineering, Ergonomics
Industrial Engineering
Industrial Processes
Industrial Robotics
Intelligent Systems
Inventory Management
Joining Processes
Knowledge Management
Logistics
Machine Tools
Machining Systems
Manufacturing Systems
Mechanical Engineering
Mechatronics
Metrology
Modelling and Simulation
Numerical Techniques
Operations Research
Operations Planning, Scheduling and Control
Optimisation Techniques
Project Management
Quality Management
Queuing Systems
Risk and Uncertainty
Self-Organizing Systems
Statistical Methods
Supply Chain Management
Virtual Reality

Announcement and acknowledgement

I am very pleased to announce that in December 2016, the journal *Advances in Production Engineering & Management* was positively evaluated for inclusion in the WEB OF SCIENCE scientific citation indexing service maintained by THOMSON REUTERS. The journal will be indexed and abstracted in the *Science Citation Index Expanded*, *Journal Citation Reports – Science Edition*, and *Current Contents – Engineering, Computing and Technology*. The coverage will begin with Vol. 8, No. 1, 2013. I would like to thank the leadership of the *Production Engineering Institute* on *Faculty of Mechanical Engineering – University of Maribo*r, and the laboratories' leaders for the financial support to the journal. My appreciation for the financial support given in the last two years is also directed to the *Slovenian Research Agency – ARRS*. I gratefully acknowledge the journal's founding team members, the current editorial team and the editorial board members for their support, suggestions, and a lot of good advice regarding the journal contents and the technical details. I gratefully acknowledge the reviewers for the time and expertise devoted to reviewing the manuscripts. Many thanks also to the English abstract proofreading experts and to the office personnel in the *Production Engineering Institute* for their contributions to the journal's success.

Miran Brezocnik
Editor-in-Chief

APEM journal
Advances in Production Engineering & Management
Volume 11 | Number 1 | March 2016 | pp 5–14
http://dx.doi.org/10.14743/apem2016.1.205
ISSN 1854-6250
Journal home: apem-journal.org
Original scientific paper

Assessment of mechanical and wear properties of epoxy-based hybrid composites

Agunsoye, J.O.[a], **Bello, S.A.**[a,b,*], **Bello, L.**[a], **Idehenre, M.M.**[a]

[a]Department of Metallurgical and Materials Engineering, University of Lagos, Akoka, Yaba, Lagos Nigeria
[b]Department of Materials Science and Engineering, Kwara State, University, Malete, Kwara State Nigeria

ABSTRACT

Discarded florescent tubes and graphite rods obtained from dumped primary cells have been processed to obtain glass and graphite particles. 80 μm glass and graphite particles were used as reinforcements in epoxy resin, LY 556 cured with HY 931 hardener to produce epoxy resin hybrid composites. The morphology, mechanical properties, thermal stability and wear resistance characteristics of the epoxy resin glass/graphite hybrid composites were studied. The thermogravimetric analyser TGA 701 was used to examine the thermal stability of the epoxy resin glass particle/graphite composites. Addition of graphite and glass particles enhanced the strength, thermal stability and wear resistance of the epoxy resin. However, tensile strain and impact energy absorption of the epoxy resin hybrid composites started declining at 6 wt% of glass particle addition. The increase in wear rate of the composites with an increment in applied loads is attributable to increase in the normal reaction between the examined sample surfaces and the emery paper. Furthermore, the increase in wear resistance with an increment in wt% of glass particle additions is attributable to good interfacial adhesion between matrix and the fillers. The textural and appearance differences between the scanning electron micrographs of the control and epoxy resin hybrid composites is attributable to the presence of new phases due to exothermic and cross linking reaction between the matrix and the fillers. Hence, new vital engineering composites peculiar to automobile, aerospace and building industries have been produced.

ARTICLE INFO

Keywords:
Epoxy resin
Composite
Glass particle
Graphite particle
Mechanical properties
Wear properties

**Corresponding author:*
sefiu.bello@kwasu.edu.ng;
adekunle_b@yahoo.com
(Bello, S.A.)

Article history:
Received 11 June 2015
Revised 8 January 2016
Accepted 19 January 2016

1. Introduction

Epoxy resins belong to a class of polymer under the aegis of thermoset [1]. They possess excellent mechanical strength, electrical and chemical resistance; good thermal characteristic and fine adhesion to many substrates after cure. They are used as matrix resins for reinforced composites, in aerospace industry, adhesives in car, as insulating materials for electrical and electronic industry. However, when compared to other light materials like aluminium, they have low mechanical strength and thermal resistance. Hence, filling of epoxy resin for improved mechanical, wear and thermal resistance properties is imperative. The mechanical performance of the fiber-reinforced composites usually depends on the properties of the matrix and fiber materials [2-4]. Reinforcement such as glass has good thermal resistance, wear resistance and high strength but they have low fracture toughness. Also, in the development of wide variety of composites for application in areas such as aerospace industry, automobile industries and sporting goods, carbon fiber has been used as the reinforcing material [5-6]. Carbon fibre reinforced polymer com-

posites are being used in a wide range of engineering applications because of increase in the impact energy absorption per unit weight, reduce noise and vibrations and excellent resistance to fatigue [7]. Hybridization of particles as a filler for a polymer gives rise to a new polymer based composite with enhanced mechanical properties [8]. Hence, the composites of these three engineering materials, i.e. polymer–matrix composites with small amount and size of glass and carbon particle reinforcements, could improve strength and impact energy of the composites. This is the thrust of this research i.e. to use the good properties offered by both glass and carbon particles to reinforce epoxy resin to develop composites with improved properties. Such composites made from high-performance particles (e.g., carbon and glass particles) embedded in compliant polymeric resins can be used in a wide range of fields such as aerospace engineering and sports utilities. The developed composites are expected to have high specific strength and toughness, superior manufacturability, as well as excellent corrosion resistance and fatigue tolerance.

Agunsoye et al. (2014) worked on the development and characterization of aluminium dross/epoxy resin composite materials [9]. Their results revealed that additions of particulate aluminium dross to epoxy resin enhanced significantly, the thermal and wear resistance of the epoxy resin aluminium dross composites. Hassan et al. (2012) worked on development of polyester/eggshell particulate composites [10]. Their results show that the addition of eggshell to the polyester slightly improved the mechanical properties of the produced composites. Allaouis et al. (2002) fabricated and studied mechanical and electrical properties of epoxy resin/carbon nanotube composites [11]. Results of the experimental examination revealed that the Young's modulus and the yield strength of the composites have been doubled and quadrupled for composites with respectively 1 wt% and 4 wt% nanotubes, compared to the pure resin matrix samples. Conductivity measurements on the composite samples showed that the insulator-to-conductor transition took place for nanotube concentration between 0.5 wt% and 1 wt%. Valášek et al. 2015 studied two-body abrasive wear of polymeric composites using waste abrasive Al_2O_3 particles as a filler [12]. Their results indicated 16 % improvement in hardness with composite made from 284 μm sized Al_2O_3 particles.

Many worked have been focused on enhancement of thermoset properties, the use of florescent tube glass particles and graphite particles obtained from discarded primary cell as reinforcements in epoxy is rare or not found. However, in this work, thermoset hybrid composites have been produced from epoxy resin (LY 556) reinforced with 80 μm glass and graphite particles. The mechanical properties, wear behaviour, phase morphology and distribution in the epoxy matrix of the produced composites were investigated. The glass particles used were obtained from processed discarded fluorescent tubes which have the potential of causing serious environmental harm due to mercury. The mercury from just one fluorescent tube is enough to pollute 30,000 l of underground water so that the water is no longer safe to drink [13]. Hence, this research was also aimed at eliminating this challenge by making use of this potential harmful material (discarded fluorescent tube) as reinforcement in the production of composites for engineering applications.

2. Materials and methodology

Materials used in this work are discarded florescent tube procured from Waste Dumping Centre of University of Lagos; graphite rods were obtained from discarded primary cells. Epoxy resin (LY 556), HY931 hardener and distilled water were purchased from Tony Nigeria Chemicals, Ojota Lagos. The major equipment used includes scanning electron microscope (SEM), Instron extensometer, model 3319; hot press, X-ray diffractometer and Avery Denison Universal Impact Testing Machine.

Broken glasses obtained from florescent tubes were submerged in a 100 l of boiling water contained in a plastic drum covered with 0.5 kg ground sulphur powder. This attempt was made to remove mercury from the florescent tube. The resulted suspension containing black particles was decanted off the drum after 24 h, leaving behind the broken glasses. The broken glasses were sundried at average daily temperature of 25 °C for 2 days. They were ground into powder using 87002 LIMOGES planetary ball mill, model 28A20 92 in accordance with [14]. Glass pow-

ders were classified using a set of sieves arranged in descending order of mesh sizes ranging from 50-300μm. Sieves were vibrated for 30 min using a sine shaker. Solid graphite electrodes were ground and sieved. Fig. 1 and Fig. 2 present glass and graphite particles.

Epoxy resin (LY 556) and hardener (HY 931) were mixed inside a beaker at 3:1 in accordance with manufacturer specification. The mixture was stirred by a hot plate and stirrer, model Jenway 1000 at 120 °C for 1 h and then poured into a metallic mould coated with petroleum jelly. Epoxy resin/hardener blends were left in the mould for 2 days at room temperature to obtain epoxy/hardener preforms.

Epoxy preforms were placed in a mould with different cavities patterned to the standard shapes for mechanical property analyses. The preforms were heated to 150 °C, held at the temperature for 1 h and then forged to obtain the standard samples for analyses (in accordance with ASTM D 3039 M959 and ASTM D 790-90), using a hot press.

For composite production, a mixture containing 80 μm sized graphite and glass particles were dispersed in 50 cm^3 of water in a beaker and then stirred manually with a glass rod for a period of 10 min. The mixture was added to 250 cm^3 epoxy resin (LY 556) in another beaker and then stirred for 15 min. 30 % HY931 hardener was added to the epoxy resin/filler mixture. The resulting mixture was stirred using magnetic mantle shaker for 1 h at a temperature of 120 °C to evaporate water molecules. The epoxy resin mixture was poured into a mild steel mould (coated with petroleum jelly as a dispatching/releasing agent) and then left in the mould for 2 days at room temperature. Epoxy graphite/glass particles hybrid composite preforms were placed in a forming mould. They were heated to 150 °C, held at the temperature for 1 h and then forged to obtain standard samples for mechanical property investigation. Six different composite samples produced contained 2 wt% graphite particles with increasing wt% of glass particles from 2-12 % at 2 % interval.

Phase identification of the produced epoxy samples were carried out using a Panalytical Empyrean X- ray diffractometer (XRD) in accordance with [15]. Morphology of the samples was examined with the aids of scanning electron microscope, ASPEX 3020 in line with [16].

Tensile samples of 80 mm gauge length and 7 mm width were subjected to tensile test using Instron extensometer, model 3369. Samples were gradually loaded at a strain rate of 10^{-3} 1/s [17]. This resulted in the simultaneous elongation and reduction in the cross section of the sample until the samples became fractured. The flexural test was carried out on the bended 100 mm square samples. The samples were loaded at the bended centre point until fracture occurred at the point. 150 mm diameter samples were subjected to compressive load using Instron extensometer.

The impact energies of the produced samples were determined with the aids of Avery Denison Universal Impact Testing Machine. The notched 60 × 10 × 10 mm^3 dimensioned samples were subjected to the Charpy impact test. First, the hammer pendulum was released to set the scale to zero point. Each sample was impacted with hammer pendulum of weight 300 J, released from the upper position of the machine. The impact energy absorbed by each sample was read and then recorded.

Fig. 1 Photograph of glass particles

Fig. 2 Photograph of graphite particles

The wear resistance of 60 × 10 × 10 mm^3 dimensioned samples of the control, epoxy resin hybrid composites containing 2, 4 and 12 % glass particles were investigated using Pin on Disc wear machine. Densities and the initial masses of the examined samples are expressed in two Cartesian system as follows (1.33 g/cm^3, 8 g); (1.28 g/cm^3, 7.7 g); (1.27 g/cm^3, 7.64 g) and (1.24 g/cm^3, 7.43 g) respectively.

The wear test was carried out on a 200 mm circular rotating disc with attached emery paper of 220 grit size according to [2]. The surface of the test sample was placed against the rotating disc for a period of 60 s under different loads at a speed of 2.36 m/s. The final mass after each test was measured and recorded. The mass loss during the investigation was calculated and recorded using the Eq. 1.

$$Mass\ loss\ =\ initial\ mass - final\ mass \tag{1}$$

The thermal stability of the control and the epoxy resin hybrid composites containing 2 and 12 % glass particles were examined using TGA 701. Each sample was heated from room temperature to a maximum of 900 °C for 200 min. The thermal stability was studied as a function of weight loss with heating temperature and time.

3. Results and discussion

3.1 X-ray diffractograms

X-ray diffractogram in Fig. 3 reveals the phases present in the epoxy resin (control) sample. It was observed from the result obtained that aluminium manganese titanium ($Al_3Ti_{0.78}Mn_{0.25}$), burnt lime (CaO), pyrolusite (P_2O_5), sodium aluminium sulphide (Na_4AlS_5) were identified at diffraction angles of 44.23°, 46.24°, 27.81° and 14.02° respectively.

Fig. 4 shows the X-Ray diffractogram of the epoxy resin hybrid composite containing 12 % glass particles. There are two peaks with many shoulders at their sides. This indicates higher degree of phase segregation and or straining within the matrix. They are attributable to chemical interaction among epoxy resin, glass and graphite particles. It was observed from the result that the phases were Iron titanium (FeTi), anatase (TiO_2), Titanium Zinc ($Zn_{0.6}Ti_{0.4}$). These phases were identified at diffraction angles of 50.01°, 28.23° and 85.23° respectively.

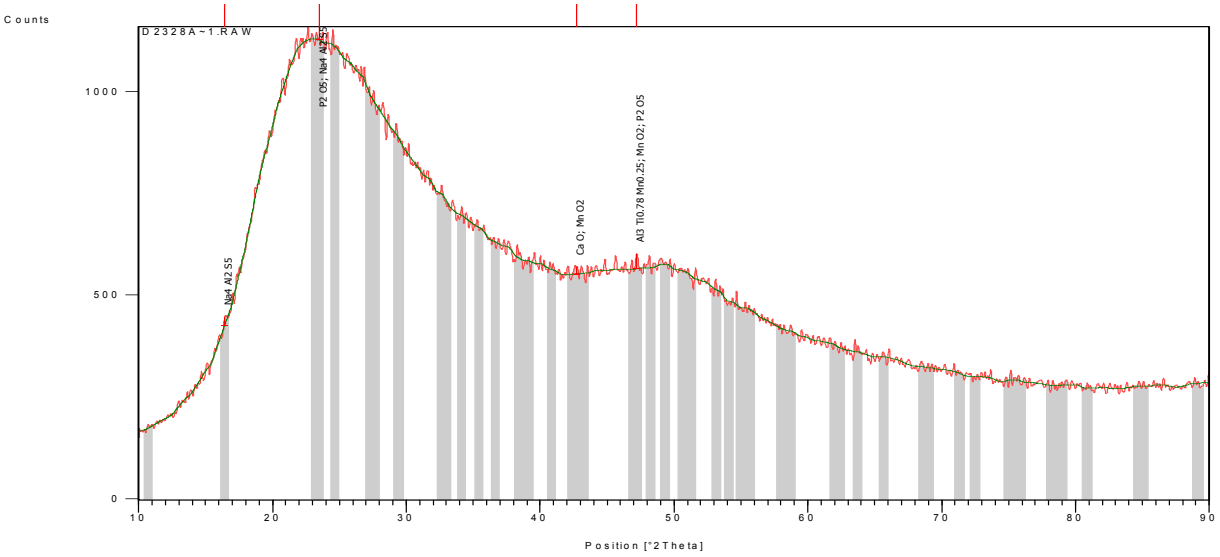

Fig. 3 X-ray diffractogram of the unfilled epoxy resin [2]

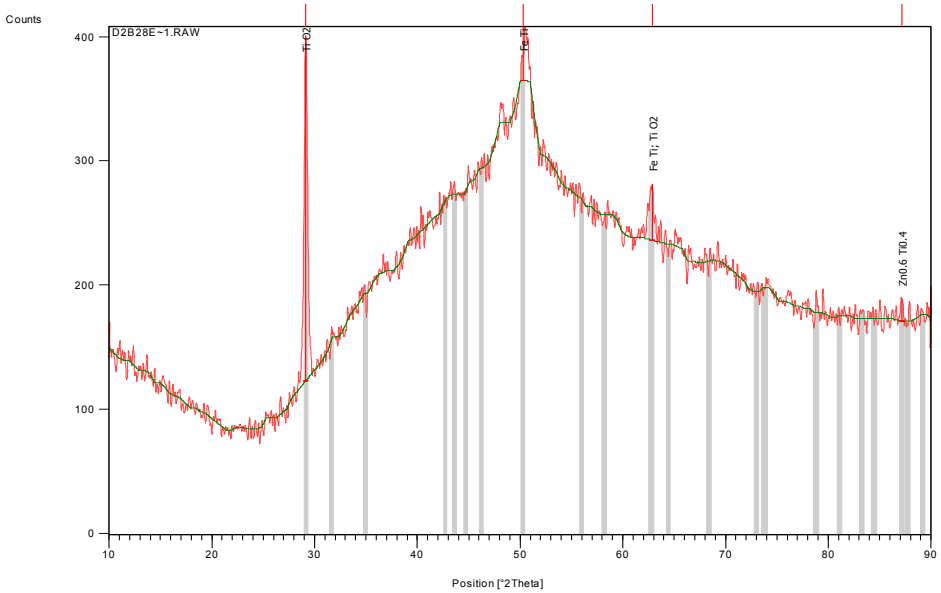

Fig. 4 X-ray diffractogram of the epoxy resin hybrid composite of 2 % graphite and 12 % glass particle additions

3.2 SEM micrographs

Microstructure of epoxy resin control sample is presented in Fig. 5. The structure reveals the white phases within the black matrix. The white phases are attributable to $Al_3Ti_{0.78}Mn_{0.25}$, CaO and Na_4AlS_5 as indicated by the diffractogram in Fig. 3. Fig. 6 presents the microstructure of the filled epoxy resin. The facial difference of the microstructure in Fig. 7 from that in Fig. 6 is attributable to glass and graphite particle additions. The microstructure appears rocky which indicates a good interfacial adhesion between the matrix and reinforcements.

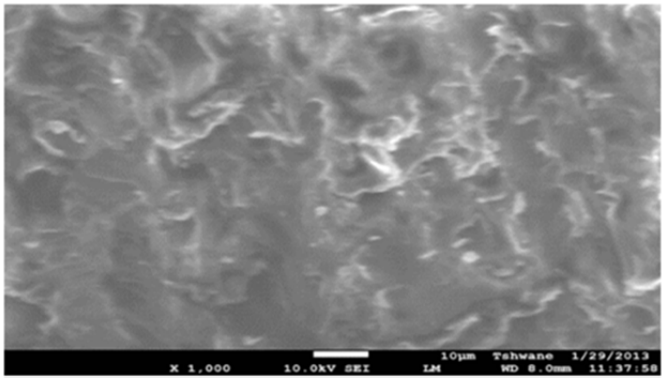

Fig. 5 Unfilled epoxy resin SEM micragh

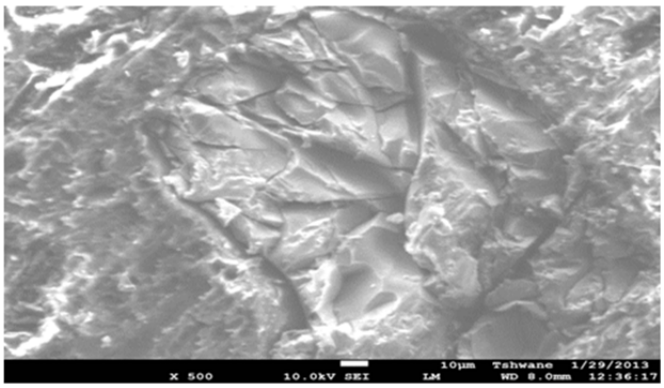

Fig. 6 Epoxy resin hybrid composite micrograph obtained from SEM

3.3 Mechanical properties

It was observed from Fig. 7, Fig. 8, and Fig. 9 that filling of epoxy resin with graphite and glass particles produced epoxy resin hybrid composites with enhanced tensile, flexural and compressive strengths. Strength of the epoxy hybrid composites increased with an increment in wt% of glass particle additions up to 10 wt% when the ultimate tensile and flexural strength start declining. This indicated epoxy resin saturation level. However, the increase in compressive strength beyond 10 wt% of glass particles may be attributable to brittleness of the phases within the matrix which enhance the strength in compression. Fig. 10 and Fig. 11 depicted that impact energy and tensile strain started declining at 6 wt% glass particle addition. This indicated a critical glass filling level such that glass particle addition above this level embrittled the epoxy hybrid composites. The decline in impact energy and tensile strain could be associated with brittleness of glass and graphite particles. During loading, the hybridized particles allowed the crack propagation in a more rapid manner than that in the case of epoxy hybrid composites at lower wt% of glass particle additions. This caused the 2 % graphite-6 % glass particle epoxy composites to fail at lower absorbed energy and percentage elongation.

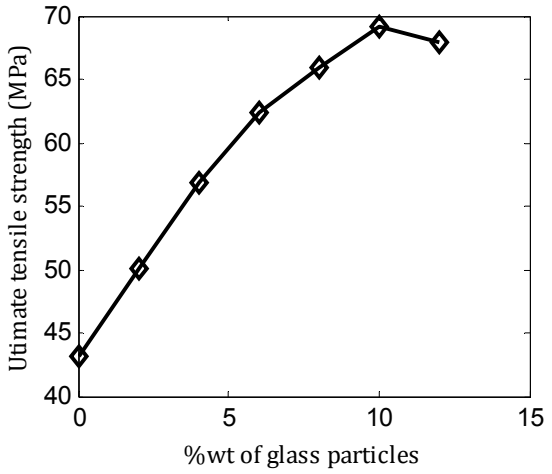

Fig. 7 Ultimate tensile with wt% of glass particles

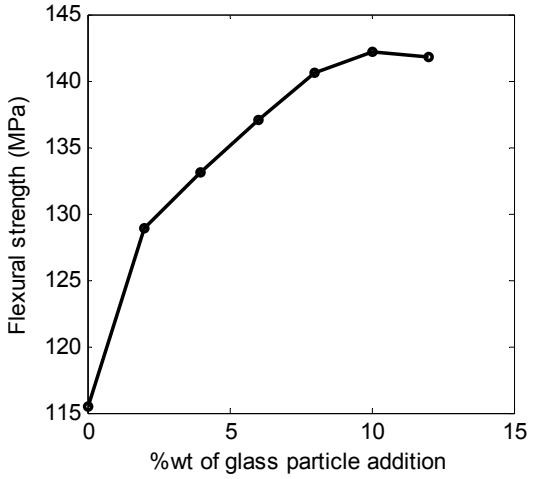

Fig. 8 Flexural strength with wt% of glass particles

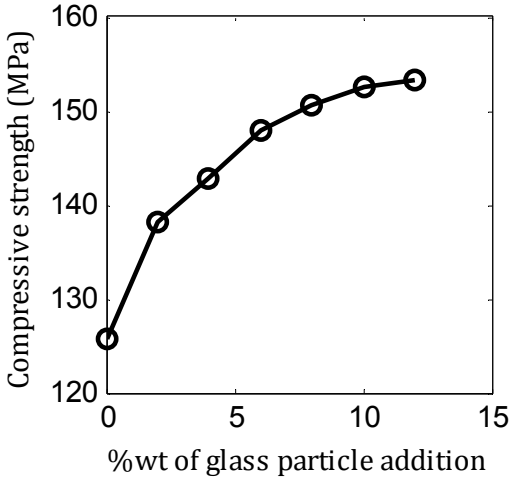

Fig. 9 Compressive strength with wt% of glass particle

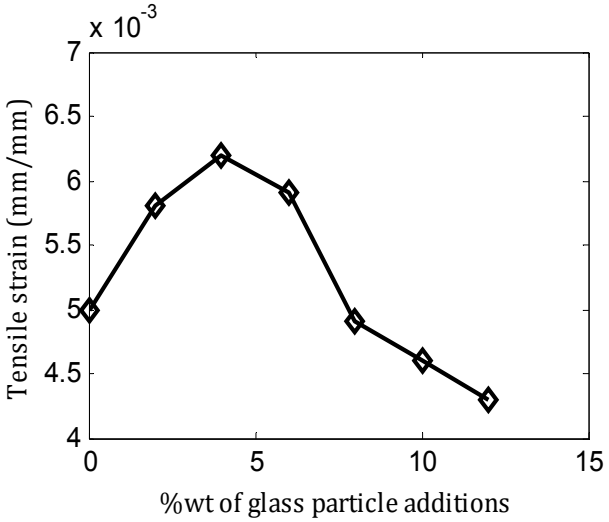

Fig. 10 Tensile strain with wt% of glass particles

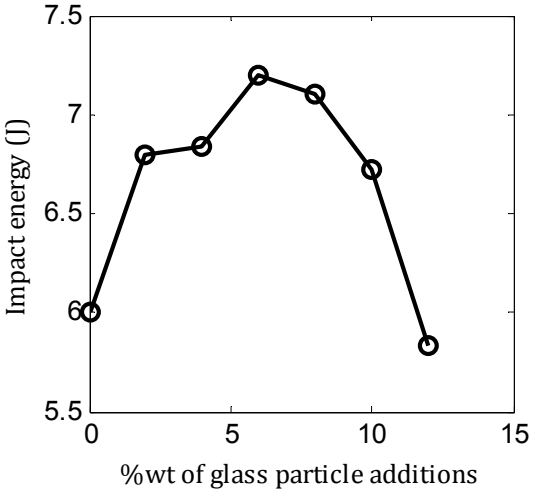

Fig. 11 Impact energy with wt% of glass particles

3.4 Wear resistance properties

It was observed from Fig. 12 that the specific wear rate increased with an increment in applied loads. This may be attributable to increased normal reaction which enhanced the friction between the epoxy samples and the emery paper. However, the decrease in specfic wear rate with an increment in glass particle addition is attributable to good interfacial bonding between matrix and the fillers; tough and rigid surfaces of the epoxy resin graphite-glass particles hybrid composites.

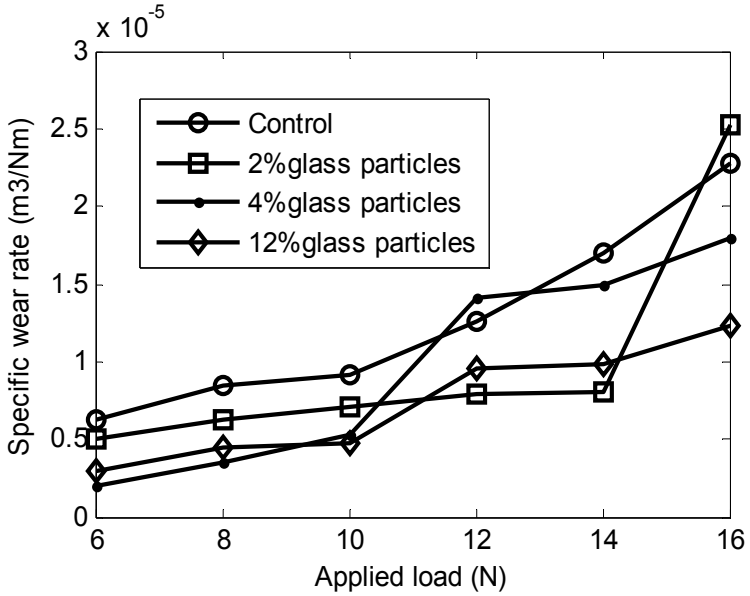

Fig. 12 Specific wear with applied load

3.5 Thermal resistance property

Fig. 13-15 show the variation of weight loss (%/min) as the heating time and temperature increased in a graph known as thermogravimetrogram. Fig. 13 shows the thermogravimetrogram of the epoxy resin (control) in which the weight loss at 900 °C was around 8 %/min, indicated by the highest peak of the curve. The various shoulders around the peak are functions of resistance of the epoxy resin to the thermal decomposition. The intersection of the base line and the curve is a measure of phase transition during heating regime. The maximum temperature at which intersection occurred is the glass transition temperature (Tg) of the examined sample. In Fig. 14, Tg of the control epoxy resin was around 430 °C. Fig. 14 and Fig. 15 show the thermogravimetograms of the epoxy resin hybrid composites of 2 % graphite containing 2 % and 12 % glass

particles respectively. In Fig. 14, the weight loss at 900 °C was around 3 %/min and Tg of the hybrid composite was around 460 °C while in Fig. 18, the weight loss was around 3.5 %/min and Tg is 600 °C. This is an indication of enhancement in thermal resistance of the epoxy resin hybrid composite. This is attributable to inherent refractoriness of the graphite and glass particles.

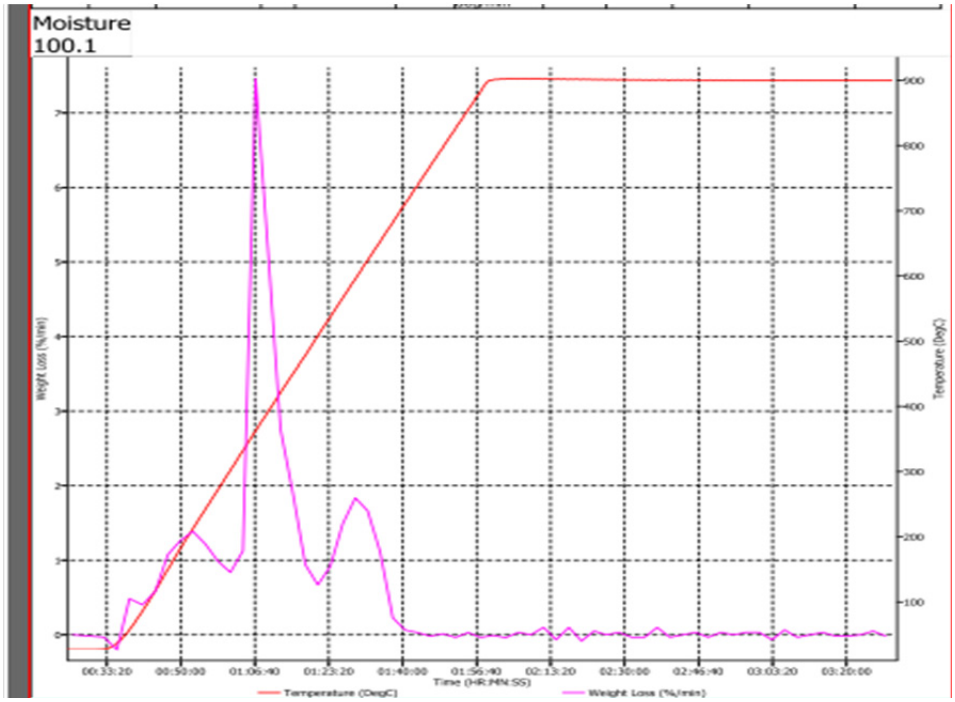

Fig. 13 Thermogravimetrogram of the epoxy resin

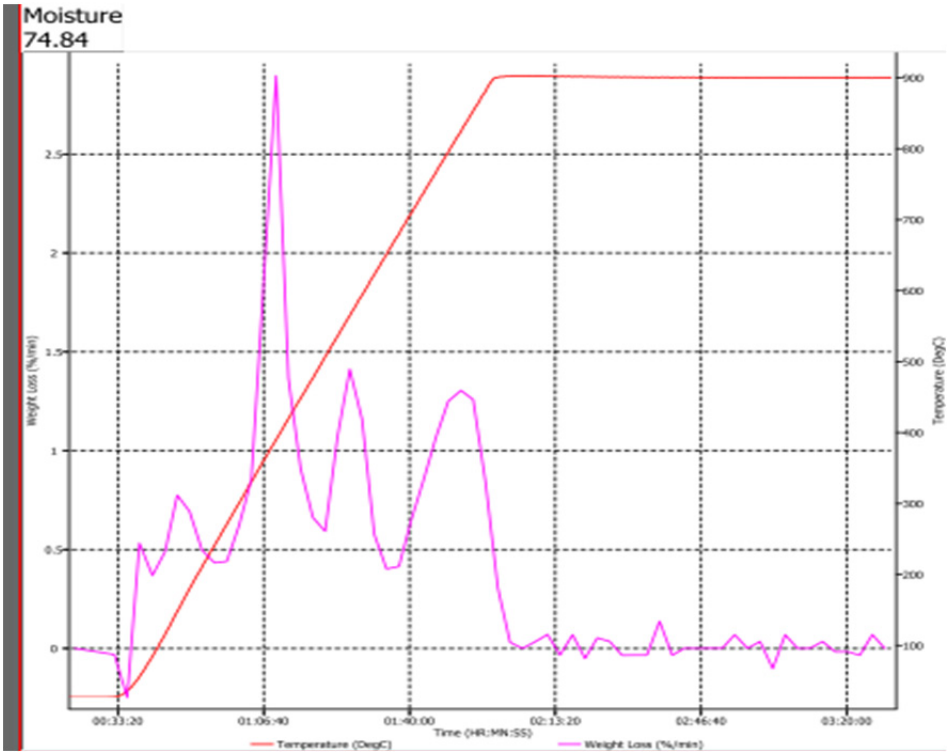

Fig. 14 Thermogravimetrogram of the epoxy resin hybrid composites of 2 % graphite and 2 % glass particles

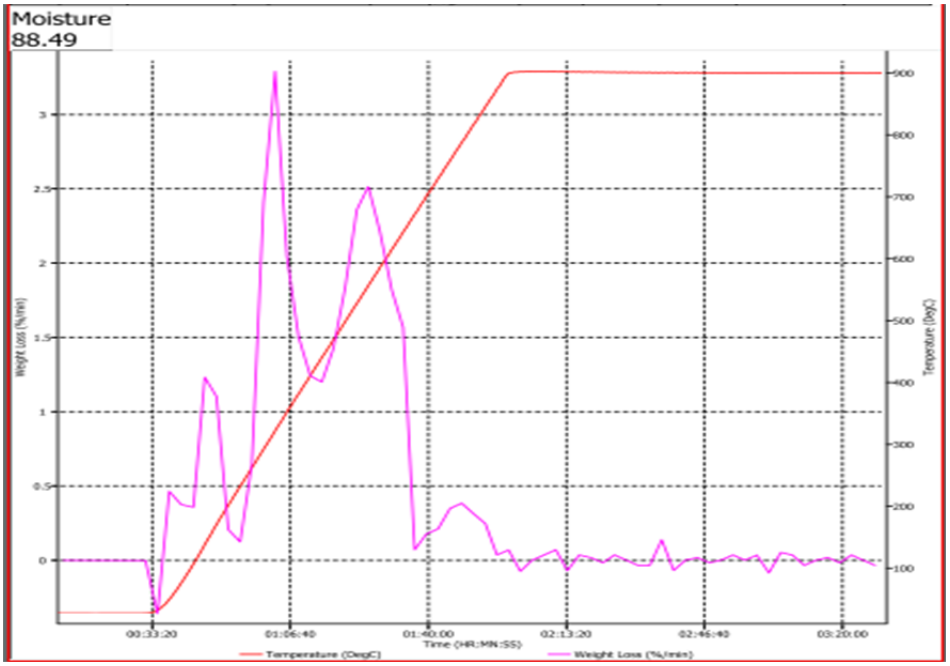

Fig. 15 Thermogravimetrogram of the epoxy resin hybrid composites of 2 % graphite and 12 % glass particles

4. Conclusion

Based on the results of experimental investigations in this work, the following conclusions can be made:

- Recycled materials obtained from graphite rods of discarded primary cells are essentially strong and tough reinforcements for thermoset polymeric materials.
- Recycled glass particles from florescent tube can be harnessed into materials development for various engineering applications
- Additions of graphite and glass particles to epoxy resin led to epoxy hybrid composites with enhanced mechanical, wear and thermal resistant properties of the epoxy resin.
- Compressive strength of the epoxy hybrid composites increased with an increment in wt% of glass particle additions.
- There are formation of new phases in consequent to exothermic reaction taking place during mixing and curing of the filler and the matrix.
- Enhancement in the properties of the epoxy resin is attributable to presence of glass and graphite particles within the matrix.
- The future work in this area will present the empirical model to characterise effects of hybridized particles on mechanical properties of the developed epoxy composites in order to validate the experimental results.

Acknowledgement

Authors appreciate members of staff of Materials Science and Engineering and Mechanical Engineering laboratories of Kwara State University, Metallurgical and Materials Engineering laboratory of University of Lagos, Ceramics Department of Federal Industrial Institute of Research Oshodi (FIIRO) for their assistance in making this study a reality.

References

[1] Bello, S.A., Agunsoye, J.O., Hassan, S.B., Kana, M.G.Z., Raheem, I.A. (2015). Epoxy resin based composites, mechanical and tribological properties: A review, *Tribology in Industry,* Vol. 37, No. 4, 500-524.

[2] Marieta, C., Schulz, E., Irusta, L, Gabilondo, N., Tercjak, A., Mondragon, I. (2005). Evaluation of fiber surface treatment and toughening of thermoset matrix on the interfacial behaviour of carbon-reinforced cyanate matrix composites, *Composite Science Technology*, Vol. 65, No. 14, 2189-2197, doi: 10.1016/j.compscitech.2005.05.008.

[3] Marieta, C., Schulz, E., Mondragon, I. (2002). Characterization of interfacial behaviour in carbon-fibre/cyanate composites, *Composites Science and Technology*, Vol. 62, No. 2, 299-309, doi: 10.1016/S0266-3538(01)00215-9.

[4] Wang, Y., Hahn, T.H. (2007). AFM Characterization of the interfacial properties of carbon fiber reinforced polymer composites subjected to hydrothermal treatments, *Composites Science and Technology*, Vol. 67, No. 1, 92-101, doi: 10.1016/j.compscitech.2006.03.030.

[5] Donnet, J.B., Bansal, R.C. (1990). *Carbon Fibers*, (2nd edition), Mercel Dekker, New York.

[6] Moutier, J., Fois, M., Picard, C. (2009). Characterization of carbon/epoxy materials for structural repair of carbon/BMI structures, *Composites: Part B*, Vol. 40, No. 1, 1-6, doi: 10.1016/j.compositesb.2008.09.003.

[7] Feraboli, P., Masini, A. (2004). Development of carbon/epoxy structural components for a high performance vehicle, *Composites: Part B*, Vol. 35, No. 4, 323-330, doi: 10.1016/j.compositesb.2003.11.010.

[8] Davoodi, M.M., Sapuan, S.M., Ahmad, D., Aidy Ali, Khalina, A., Jonoobi, M. (2010). Mechanical properties of hybrid kenaf/glass reinforced epoxy composite for passenger car bumper beam, *Materials & Design*, Vol. 31, No. 10, 4927-4932, doi: 10.1016/j.matdes.2010.05.021.

[9] Agunsoye, J.O., Talabi, S.I., Hassan, S.B., Awe, I.O., Bello, S.A., Aziakpono, E. (2014). The development and characterisation of aluminium dross-epoxy resin composite materials, *Journal of Materials Science Research*, Vol. 3, No. 2, 23-37, doi: 10.5539/jmsr.v3n2p23.

[10] Hassan, S.B., Aigbodion, V.S., Patrick, S.N. (2012). Development of polyester/eggshell particulate composites, *Tribology in Industry*, Vol. 34, No. 4, 217-225.

[11] Allaoui, A., Bai, S., Cheng, H.M., Bai, J.B. (2002). Mechanical and electrical properties of a MWNT/epoxy composite, *Composites Science and Technology*, Vol. 62, No. 15, 1993-1998, doi: 10.1016/S0266-3538(02)00129-X.

[12] Valášek, P., Müller, M., Hloch, S. (2015). Recycling of corundum particles – two-body abrasive wear of polymeric composites based on waste, *Tehnički vjesnik – Technical Gazette*, Vol 22, No. 3, 2015, 567-572, doi: 10.17559/TV-20131111140048.

[13] Parkinson, M., Visco, C. (2002). *Sustainable markets for waste glass from fluorescent tubes and lamps*, Final Report, The National Centre for Business and Sustainability (NCBS), Manchester, UK.

[14] Hassan, S.B., Agunsoye, J.O., Bello, S.A. (2015). Ball milling synthesis of Al (1050) particles: Morphological study and particle size determination, *Industrial Engineering Letters*, Vol. 5, No. 11, 22-27.

[15] Bello, S.A., Agunsoye, J.O., Hassan, S.B. (2015). Synthesis of coconut shell nanoparticles via a top down approach: Assessment of milling duration on the particle sizes and morphologies of coconut shell nanoparticles, *Materials Letters*, Vol. 159, 514-519, doi: 10.1016/j.matlet.2015.07.063.

[16] Bello, S.A., Hassan, S.B., Agunsoye, J.O., Kana, M.G.Z., Raheem, I.A. (2015). Synthesis of uncarbonised coconut shell nanoparticles: Characterisation and particle size determination, *Tribology in Industry*, Vol. 37, No. 2, 257-263.

[17] Bello, S.A., Raheem, I.A., Raji, N.K. (2015). Study of tensile properties, fractography and morphology of aluminium (1xxx)/coconut shell micro particle composites, (In Press), *Journal of King Saud University – Engineering Sciences*, doi: 10.1016/j.jksues.2015.10.001.

APEM journal
Advances in Production Engineering & Management
Volume 11 | Number 1 | March 2016 | pp 15–28
http://dx.doi.org/10.14743/apem2016.1.206
ISSN 1854-6250
Journal home: apem-journal.org
Original scientific paper

A knowledge-based system for end mill selection

Prasad, K.[a], **Chakraborty, S.**[a,*]

[a]Department of Production Engineering, Jadavpur University, Kolkata, India

ABSTRACT

In the present global competitive environment, manufacturing organizations are being forced to constantly develop newer methods/technologies for producing high quality products/components at the minimum possible cost to satisfy the diverse and dynamic needs of customers. Selection of a proper cutting tool within a process planning system is vital for the productive efficiency and cost effectiveness of a manufacturing process. In this paper, a knowledge-based system is developed in Visual BASIC 6.0 and subsequently implemented for selection of an appropriate end mill for a given machining application from a set of feasible alternatives. Although, there are some published research papers on the applications of knowledge-based systems for selecting of cutting tools, none of them has investigated its scope for choosing a suitable end mill from a comprehensive list of options available on the market. The developed system first narrows down the list of end mills based on some predefined parameters as set by the process planner and then ranks the feasible end mills according to their suitability for the desired machining application. While ranking the end mill alternatives, criteria weights are determined using Shannon's entropy method to avoid subjectivity in judgments. It also guides the process planner in identifying the corresponding speed and feed for different combinations of workpiece material and machining operation.

ARTICLE INFO

Keywords:
End mill
Decision making
Knowledge-based system
Entropy method
Rank

**Corresponding author:*
s_chakraborty00@yahoo.co.in
(Chakraborty, S.)

Article history:
Received 1 September 2015
Revised 21 January 2016
Accepted 25 January 2016

1. Introduction

The business dynamics of manufacturing sector is changing at a lightening pace with advancement in technologies and innovation in product development. Therefore, manufacturing organizations in order to stay relevant in this highly competitive global market have to look ways to achieve manufacturing excellence through producing new cutting-edge products/components more economically. A product/component can be manufactured using a diverse range of processes, like material removal, casting, forging etc. It is observed that material removal through machining operation is the most extensively used manufacturing technique among all the processes because invariably every product undergoes through this operation at one point or the other while utilizing different types of cutting tools [1]. Material removal is an expensive process as it involves removal of substantial amount of material from the workpiece in the form of chips with a view to generate the desired product shape. The expensive nature of material removal can also be attributed due to the considerable amount of energy spent in this process. Besides, effective monitoring of cutting tools facilitates superior efficiency of the machine tools [2, 3]. Therefore, appropriate cutting tool selection and its correct application are the key elements to profitable machining, which are completely in line with the overall objective of achieving manufacturing excellence in an organization.

There are several different kinds of cutting tools available in the market today, each serving diverse purposes and applications. These cutting tools can be broadly classified into two groups, i.e. single point and multi-point cutting tools. End mill is one of the most widely employed multi-point cutting tools, which is indispensible in many industries, like aerospace, ship building and automobile for machining varying complex-shaped components [4]. It is typically mounted vertically on a machine tool and has two or more helical flutes/cutting edges. The main advantage of an end mill is that unlike any other type of milling cutter, it is configured to cut with both its tips and sides. End mill can operate effectively and efficiently only when it is capable to withstand the heat generated during the cutting process. In addition, the material from which the end mill is manufactured must be harder as compared to the material being cut. End mill should have a specific geometry according to the requirements of a considered machining application in order to provide correct clearance angles so that only the cutting edge of the tool makes contact with the workpiece material. It is also crucial to ensure that the end mill is able to machine the complete work surface without any interference [5]. Therefore, the type of end mill and its related geometry depend on the material being cut and complexity of the machining operation being performed.

These are some important factors that the process planners need to consider while selecting an end mill in order to ensure its optimal productive working life. Moreover, there is a wide range of end mill varieties available in the market with respect to design styles and material choices. As the number of influencing criteria and available alternatives increases, it becomes quite hard and almost impossible for a human brain to examine the relation between those criteria and alternatives while making a valid conclusive decision. Additionally, a suitable end mill can drastically minimize the final roughness of a milled surface [6]. Thus, selection of an appropriate end mill for a specific machining application requires a thorough knowledge regarding its applicability, capability and economy, and related effects of the considered evaluation criteria on the machining operation. Besides selection of an inappropriate end mill may lead to infeasible and inconsistent process plans. Incorrect process plans often need to be rejected in the shop floor and the new ones generated on an impromptu basis result in overall cost escalation. So, an adherent need for development of a knowledge-based system which can select an appropriate end mill from a wide range of alternatives available from different manufacturers cannot be ignored. Therefore, this paper proposes development and subsequent deployment of a knowledge-based system for solving end mill selection problems for varying machining applications.

2. Literature review

Arezoo et al. [7] designed a knowledge-based system for identification of cutting tools and conditions for turning operations. Carpenter and Maropoulos [8] proposed a methodology to choose tools for a wide range of milling operations based on a comprehensive set of user-defined selection and optimization criteria. Sorby and Tonnessen [9] presented a methodology for optimization of cutting data of high speed flank milling in order to find out its optimal cutting parameters. Čuš and Balič [10] developed an algorithm to identify the optimal tool version and cutting conditions from different tool manufacturers' commercial databases. For a concurrent engineering environment, Edalew et al. [11] developed a computer-based intelligent system for automatic selection of cutting processes and tools. Wang et al. [12] proposed a new methodology employing genetic algorithms for selection of the optimal cutting conditions and cutting tools in multi-pass turning operations based on a complete set of optimization criteria. Zhao et al. [13] combined a commercial computer-aided design system and an expert system for selection of cutting conditions and tools for turning operation. Byrne et al. [14] reviewed some of the main developments in the domain of cutting technology over the last 50 years in order to provide a roadmap for its future development. Muršec and Čuš [15] developed an integral model for selection of the optimal cutting conditions on the basis of various databases offered by the tool manufactures while taking into account some limitations of the cutting processes. Oral and Cakir [16] determined the computer-aided optimal operation and tool sequences for use in generative process planning system of rotational parts. Svinjarević et al. [17] discussed about the benefits of

implementation of a cutting tool management system in an organization specializing in metal cutting processes. Wang et al. [18] developed a performance-based machining optimization system for predicting the optimal cutting conditions in turning operations. Arshad et al. [19] presented a cutting tool management system to help the end user in selecting the best cutting tool and parameters for cutting operation. Ostojic et al. [20] designed a computer-aided system for efficient selection of cutting tools for machining processes, including turning, drilling, milling and grinding operations. Vukelic et al. [21] presented an integrated software solution for cutting tool selection based on modular principle. Chougule et al. [22] developed an expert system capable of selecting appropriate carbide cutting tools for various turning operations.

It is thus observed from the past literature review that an extensive work on cutting tool selection and optimization of various cutting parameters for different machining operations has already been carried out. But, it is noteworthy to mention here that those research works are mainly intended to identify the most suitable cutting tools with respect to a set of pre-determined performance criteria, while ignoring the interrelationship between various technical, strategic and economic attributes. Moreover, the published research papers in the area of milling cutter selection are really scarce in number. None of the past researches has proposed a logical and systematic procedure for solving end mill selection problems. Selection of the most appropriate and also theoretically correct end mill is a complex task due to the presence of several evaluation criteria which are often conflicting in nature. Therefore, in this paper, a knowledge-based system is designed and developed in Visual BASIC 6.0 for solving end mill selection problems. It is supported by an exhaustive database for end mills containing information on their various technical specifications and controlled by a set of rules for specific machining applications. Its applicability and potentiality is demonstrated by three real-time industrial examples.

3. Knowledge-based system for end mill selection

Quick and easy access to the pertinent information for decision-making on end mill selection for a given machining application is of vital importance to attain competitive edge and manufacturing excellence. This paper presents a knowledge-based system for selecting end mills in accordance with the specific machining application requirements of the present day manufacturing industries. The developed system generates a set of feasible end mill alternatives for the given application from a comprehensive list of options available in the market, and subsequently provides their ranking preorder. It is often observed that the change in machining conditions and generated shape features of the final component considerably affect the efficiency and productivity of an end mill. Hence, the process planner needs to have a clear understanding about the selection problem. The process planner first provides the required information with respect to tool material, type of use, workpiece material etc. Different evaluation criteria, like number of flutes, cutting diameter, cutting length etc. are then shortlisted. Next, the required ranges of values for those recognized evaluation criteria are specified. This knowledge-based system is designed to first discard those end mills which do not satisfy the identified machining application requirements and gradually narrow down the list of feasible solutions at each step of the selection procedure. Finally, the set of feasible end mill alternatives is ranked with the identification of the most suitable choice. The framework of the developed knowledge-based system for end mill selection is exhibited in Fig. 1.

End mills available in the market can be broadly classified into various categories. Each category may further be divided on the basis of its specific application and special geometry. The initial step in the development process of this knowledge-based system comprises of creation of the related database for various types of end mills available in the market. The pertinent information for the end mills is accumulated from the brochures and catalogues of different manufacturers available online. Then, this collected information is stored into MS-Access option of Visual BASIC 6.0 and an exhaustive database containing technical specifications of a wide variety of end mills is thus documented. With the introduction of new end mills and inclusion of more added features, like geometry of the tool and other related specifications, it can be updated from time to time with the active participation of the knowledge-based system builder.

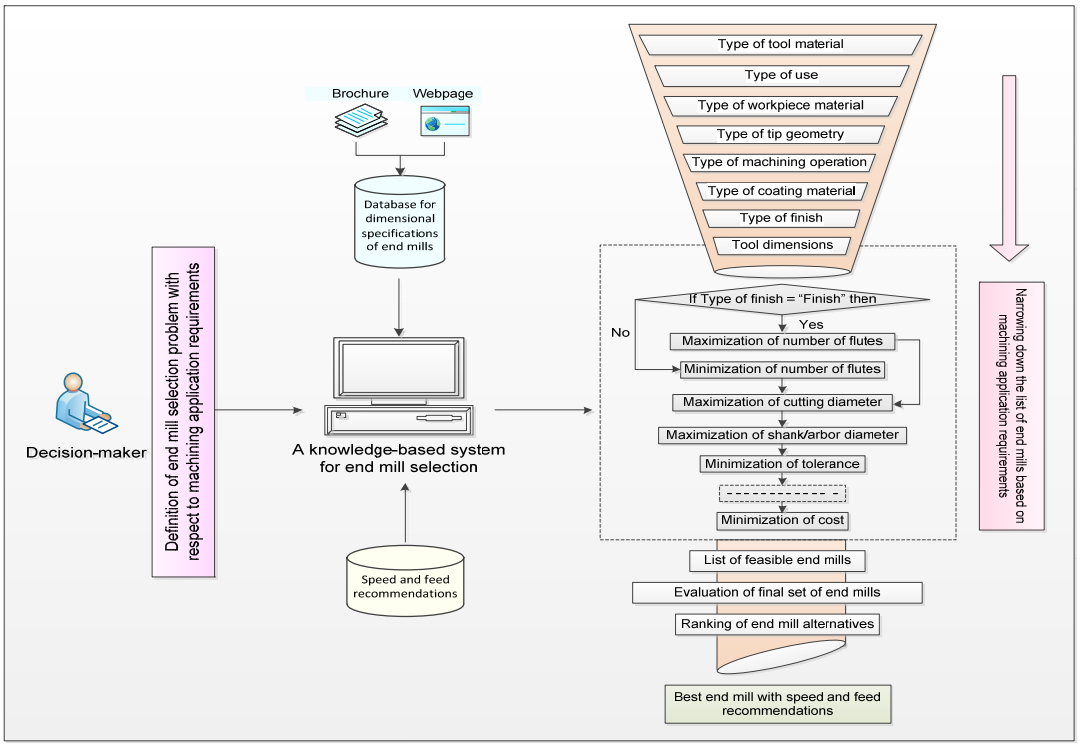

Fig. 1 Framework for knowledge-based system for end mill selection

Once the database is created, the next step is to generate a set of feasible alternative end mills based on various criteria as specified by the process planner according to requirements of a particular machining application. End mill removes material from the workpiece simply by means of shear deformation. So, the material of end mill needs to be harder than that of the workpiece, which is to be machined, and it must also be able to withstand the heat generated during the material removal process. A wide range of materials is being utilized to manufacture end mills. Therefore, tool material is an important consideration while selecting an end mill. Some of the common tool materials used for manufacturing of end mills are listed as below:

a) *Carbide:* It has comparatively higher values for hardness, thermal conductivity and Young's modulus, which facilitate its usability as an efficient tool material. Tools made of carbide can operate at much faster speed because of its extreme hardness. This allows the milling cutters to withstand high cutting temperature and provides excellent wear resistance. Carbide also offers better rigidity than high speed steel (HSS), which enables the end mill to perform the machining operation with higher degree of dimensional accuracy and superior surface finish.

b) *HSS:* It accounts for the largest tonnage of tool materials currently being utilized. It provides good wear resistance and is less expensive than cobalt or carbide end mills. It is used for general purpose milling of both ferrous and non-ferrous materials. HSS tools are tough and suitable for interrupted cutting, and are employed to manufacture tools of complex shapes, such as drills, reamers, taps, dies and gear cutters.

c) *HSSCoM42:* It comprises of molybdenum-series HSS alloy with additional 8 % cobalt content. It provides better wear resistance, and higher hardness and toughness than HSS. There is very less chipping or micro-chipping under severe cutting conditions allowing the tool to run 10 % faster than HSS. This results in achieving excellent material removal rate (MRR) with better surface finish.

d) *HSSCoPM:* Powdered metal (PM) exploits the benefits of both, i.e. toughness of cobalt HSS, and heat and wear resistance properties of micro-grain carbide tools. It is used in those applications, which require higher MRR and are vulnerable to vibrations, like roughing operation. It is a cost effective alternative to solid carbide.

e) *Ceramic:* Many grades of ceramic are utilized for manufacturing of end mills. Ceramic grades are characterized by good wear and abrasive resistance, non-conductivity and superior thermal properties. Ceramic is recommended for machining cast irons and nickel-based superalloys at intermediate cutting speeds.

f) *Diamond:* Industrial diamond grades, such as polycrystalline diamonds (PCD) are normally made by sintering many micro-size single diamond crystals at high temperature and pressure. They have good fracture toughness and thermal stability. They are often used for special applications, like very high-speed machining of aluminium-silicon alloys, composites and other non-metallic materials.

End mills can also be grouped into three categories based on their usage, which are as follows:

a) *General purpose:* It also symbolizes multi-purpose end mills, which can be employed for a wide range of applications and workpiece materials. They favour high productivity while keeping the number of tool changes as minimum as possible. General purpose end mills are quite economical, and at the same time, have high manufacturing flexibility.

b) *Special purpose:* They are employed for specific machining operations, such as thread cutting, die-sinking, corner rounding etc.

c) *High performance:* As the name indicates, they are applied in highly specialized fields for manufacturing components of aircraft, marine structures, turbines etc. where high precision and close tolerances are required.

Manufacturing organizations produce an extremely large variety of products/components which are machined from different workpiece materials. Each workpiece material has a unique set of characteristics that are influenced by its alloying elements, heat treatment process, hardness etc. These factors combine to strongly influence the choice regarding the cutting tool geometry and grade. Therefore, the workpiece materials as considered for this knowledge-based system are divided into the following seven major groups:

a) *Steel:* It refers to a broad category of alloys containing primarily iron with little amount of carbon and other alloying elements. The machinability of steel is normally good, but can differ depending on material hardness, carbon content etc.

b) *Stainless steel:* It is a steel alloy with a minimum of 12 % chromium content by mass and has non-magnetic properties. Stainless steel exhibits superior resistance to corrosion and is available in different grades.

c) *Cast iron:* It is a group of iron-carbon alloy with a carbon content greater than 2 %. Grey cast iron, malleable cast iron and ductile cast iron are quite easy to machine, whereas, white cast iron, compacted cast iron and austempered cast iron are comparatively difficult to machine.

d) *Non-ferrous material:* Softer metals, like aluminum, copper, brass etc. belong to this category. Machinability property of these materials usually fluctuates with their varying alloying elements.

e) *Special alloy:* It comprises of a large number of iron, nickel, cobalt and titanium-based alloy materials. Special alloy is very similar to stainless steel but is much more difficult to cut, which reduces the tool life of end mills.

f) *Hardened steel:* This group includes steels with hardness between 45-65 HRc (Rockwell hardness). Hardened steel is difficult to machine and it generates excessive heat during cutting operation.

g) *Titanium/exotic metal:* This refers to a category of different precious and exotic metals, such as titanium, tungsten, platinum etc.

A number of tip geometry options for end mills are also available for generating the desired shape feature on a given workpiece material. Various kinds of tip geometry options for the end mills are enlisted as below:

a) *Square:* Cutting tips are square or straight-ended with no radius, chamfer or other finish feature.

b) *Ball:* Cutter ends with a hemispherical ball whose radius is one half of the cutter diameter. It is useful for machining semicircular groove or radii on a workpiece.

c) *Radius:* Cutting tool comprises of radius on tips of straight flutes.

d) *Chamfer:* Cutter sides or ends contain an angled section on tip to produce an angled cut or a chamfered edge on the workpiece.

The type of finish is also an important consideration while selecting end mills. There are broadly two finish preferences that can be opted while employing end mills:

a) *Roughing:* Tool material, flutes and/or cutter geometry are designed for rapid and heavy material removal. Roughing cutters are typically utilized to machine workpieces for initial cutting stages, i.e. where cutting somewhat more than the desired dimension is not a problem.

b) *Finishing:* A minimal amount of material leftover after the roughing operation is removed with a finish cut.

Coatings are applied on the end mills to enhance their wear resistance property and isolate the area where heat is generated from the substrate of the tool. If coatings are not applied, heat produced during the machining operation can potentially accumulate to negatively affect the tool life. Most of these coatings are usually referred to by their chemical compositions, such as:

a) *Aluminium Titanium Nitride (AlTiN):* It is ideal for high temperature cutting operation of a diverse range of materials, such as titanium and nickel alloys, steel, stainless steel and cast iron. AlTiN is an extremely tough coating material capable of withstanding extreme machining conditions developed during heavy and interrupted cutting operations.

b) *Aluminium Titanium Nitride + Silicon Nitride (nACo):* This coating material is very well suited for high performance milling applications. It has a great ability to resist at high temperature up to 1200 °C before getting oxidized and worn out.

c) *Physical vapor deposition (PVD) diamond:* Thin diamond films are applied to cutters to increase their service life and abrasive resistance. This coating is a standard choice among the die and mold shops for machining graphite.

d) *Titanium Carbonitride (TiCN):* It has an exceptional high hardness and low coefficient of friction, which provide excellent wear resistance. TiCN's high lubricity facilitates easy chip flow, prevents formation of build-up edges, and reduces cutting forces and temperature.

e) *Zirconium Nitride (ZrN):* ZrN is typically used to coat end mills that are employed for machining non-ferrous materials, such as aluminum, brass, nickel alloys, plastics etc. It also provides good abrasive resistance and lubricity properties.

An assortment of machining operations can be performed using end mills, which comprise of a) side milling, b) slotting, c) profiling, d) radius cutting, e) slotting with radius, f) pocketing, g) chamfering, h) drilling, i) thread cutting, and j) corner rounding.

The developed system narrows down the list of feasible end mill alternatives based on the above-considered parameters with respect to the specified machining application requirements. Then, the selection procedure moves to the next stage where various evaluation criteria with respect to the dimensional specifications of the end mills are shortlisted, and subsequently, ranges of values for those identified criteria are provided. The following 12 important dimensional specifications are considered in this system, which affect the final end mill selection decision.

a) *Number of flutes:* It signifies the number of cutting edges in the end mill.

b) *Cutting diameter* (inch)*:* It is the diameter of the full-tool which cuts the workpiece material.

c) *Shank/arbor diameter* (inch)*:* It refers to the diameter of mounting shank or arbor.

d) *Flute/cutting length* (inch)*:* It is the total length of a cutting edge.

e) *Overall length* (inch)*:* It denotes the total tool length, including integral shank, if present.

f) *Tolerance* (inch)*:* It represents the dimensional closeness to a given specification.

g) *Width of cut* (inch)*:* It is the depth of cut in radial direction.

h) *Cost* (USD)*:* It symbolizes the procurement cost of a single end mill.

i) *Radius/corner size* (inch)*:* It either signifies the dimension of radius of the end mill with radius type tip geometry, or represents the angle of cutter of the end mill having tip geometry as chamfer.

j) *Taper* (°)*:* It measures the gradual reduction in the diameter of a cylinder towards one of its end.

k) *Drill point* (°)*:* It is the angle formed at the tip of the end mill utilized for drilling holes.

l) *Pitch* (inch)*:* It is the distance from the crest of one thread to that of the next thread.

These 12 above-mentioned dimensional specifications may be either beneficial or non-beneficial in nature depending on the machining applications which ultimately affect the shape feature generated on the end product. For example, the number of flutes can range from two to eight. Fewer number of flutes offer efficient chip removal and high MRR, whereas, more number of flutes provide a smoother finish. Beneficial attributes are always required in higher values, whereas, non-beneficial attributes are preferred with smaller values.

Once the list of feasible alternatives is elicited after the ranges of values are entered, it is again required to be critically analyzed and ranked with a view to recognize the most suitable end mill. Evaluation and ranking of the feasible end mills with respect to the given dimensional specifications needs formation of the related decision matrix. This decision matrix is developed while extracting the pertinent information for the feasible end mills from the database integrated with the knowledge-based system.

Shannon's entropy method [23] has a significant role in decision making under uncertain environment. It is a well-accepted technique to estimate criteria weights, particularly in those situations, where obtaining a suitable weight (importance) based on the preferences and decision making experiments are impracticable. In other words, it is capable of measuring uncertainty in the information formulated using probability theory. Moreover, it facilitates comparisons of different criteria through converting different scales and units into common measurable elements. In this paper, the priority weight for each evaluation criterion is calculated using this method to eliminate subjectivity in judgments. The performance scores of the feasible end mills are finally calculated employing the following equation:

$$PS_i = \sum_{j=1}^{n} w_j \times (\text{Normalized value})_{ij} \; (i = 1, 2, \ldots, m; j = 1, 2, \ldots, n) \tag{1}$$

where w_j is the weight for j^{th} criterion, m is the number of feasible end mills, and n is the number of the considered criteria. The normalized value showing the normalized performance of i^{th} end mill with respect to j^{th} criterion is derived from the decision matrix of a given end mill selection problem using linear normalization technique. The ranking of the feasible end mills is then derived based on their descending performance scores, and subsequently, the most appropriate end mill for the given machining application is identified along with its ideal parametric settings.

4. Illustrative examples

The following three end mill selection problems are formulated and subsequently solved to demonstrate the applicability and robustness of the developed knowledge-based system.

4.1 End mill for aerospace applications

In this selection problem, the most suitable end mill for aerospace applications that can perform finishing operations needs to be identified from a wide range of available alternatives. The components used in aerospace industries are generally thin-walled and complex shaped. They need to be machined within close tolerances. Additionally, machining of aerospace components is generally carried out at higher speed with increased MRR and relatively low cutting forces. Further, it is observed that materials utilized for aerospace components should have higher strength, hardness, elasticity, toughness, ductility and malleability, but lower brittleness.

The selection procedure starts with identification of the proper cutting tool material that satisfies the machining requirements of aerospace components. It is observed after careful review that end mills made of HSSCoPM enable in achieving comparatively higher MRR with less power requirement while providing excellent cutting strength and wear resistance. So, 'HSSCoPM' is opted as the cutting tool material in Fig. 2(a). Next, the process planner needs to provide the type of use, which in this case, is 'High performance' as it is in sync with the complex machining requirements of aerospace components. Special alloy, non-ferrous material and Ti/exotic metal are selected as workpiece materials in the subsequent step because they satisfy the physical requirements of materials employed in aerospace industry. The tip geometry for this application is chosen as 'Square' due to its ability to remove material while maintaining excellent finish. 'Finishing' is opted as the type of cut according to the end mill requirement. Coating provides additional protection against corrosion and abrasion, increases hardness, and improves overall life of the end mill. In this case, coating of AlTiN is more effective than any other available option as it facilitates exceptional oxidation resistance and works well in high demanding machining applications. Complex shape geometries often need to be generated on aerospace components, and therefore, 'Pocketing', 'Slotting' and 'Profiling' are chosen as the required machining operations among various options available in the knowledge-based system. 'Tool dimensions' functional key, as exhibited in Fig. 2(b), is now pressed to derive a narrowed down list of end mill alternatives satisfying all the above-mentioned requirements.

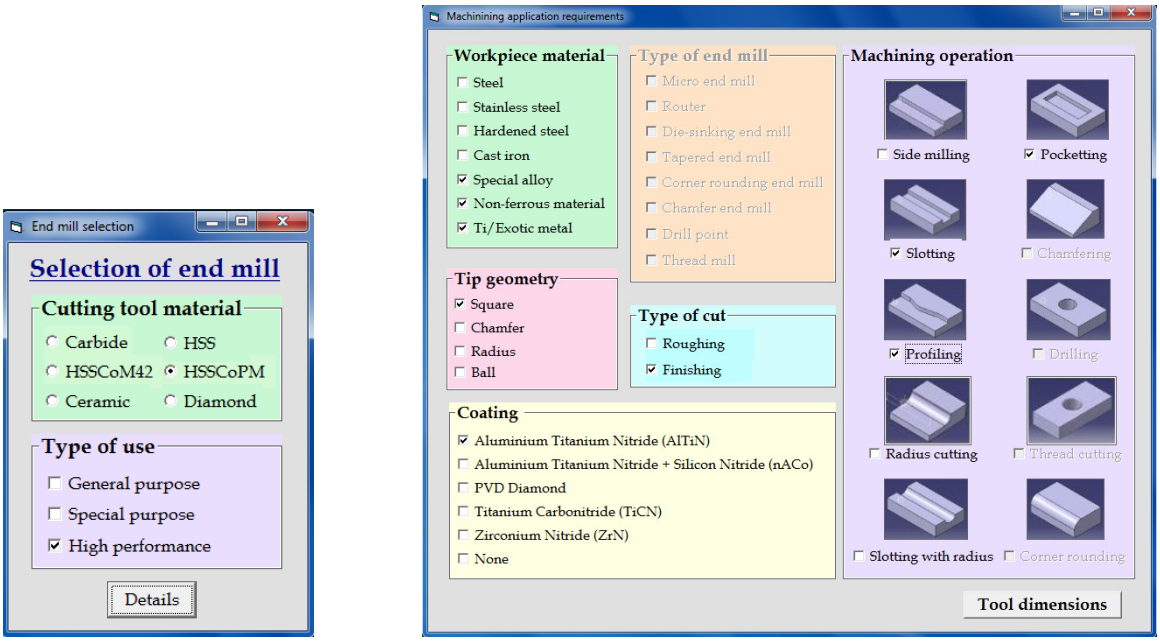

(a) (b)

Fig. 2 Requirements of an end mill for aerospace applications

In the next stage of this selection procedure, the narrowed down list of end mill alternatives is further evaluated based on some important evaluation criteria, which are identified here as shank/arbor diameter, flute/cutting length, overall length, tolerance and width of cut. All these chosen evaluation criteria are beneficial in nature, except tolerance. The desired ranges of values for these five criteria are then entered into the corresponding empty cells, which can be generated on pressing 'Input range' key. Some of the already feasible alternative end mils are discarded at this stage based on their incapability to meet the specified tool dimensional requirements. Finally, a set of 15 end mill alternatives satisfying all the preset machining application requirements is obtained after pressing 'Feasible alternatives' functional key. At this stage, the knowledge-based system provides two options, i.e. either to select all the end mill alternatives by pressing 'Select all' functional key or to choose the end mills individually from the already generated final list. Here, all the end mill alternatives are selected for final evaluation. On pressing of 'Compare' functional key, the corresponding decision matrix is automatically generated from the database, as shown in Fig. 3. The priority weights for the five evaluation criteria and the performance score for each end mill are subsequently calculated at the backend of the developed system to rank all the candidate alternatives.

Here, ERFPM-1616 emerges out as the most suitable end mill for the given aerospace applications. Its technical details along with a real-time figure can be obtained after pressing 'Tool description' key in Fig. 4. The developed system also guides the process planner in deciding the values of surface feet per minute (SFM) and chip load per tooth (CLP), which in turn represents the optimal speed and feed respectively for the finally selected end mill. Although the details regarding SFM and CLP are only the suggested starting points, they can be modified depending on the machine condition, depth of cut, type of coolant etc.

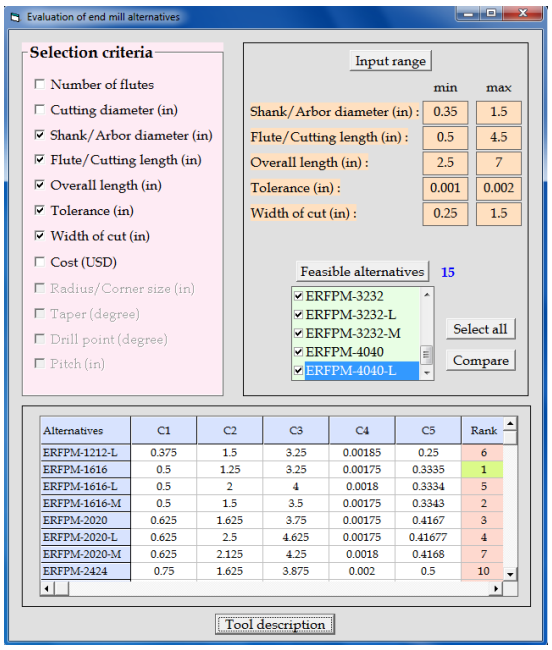

Fig. 3 Decision matrix for selection of end mill for aerospace applications

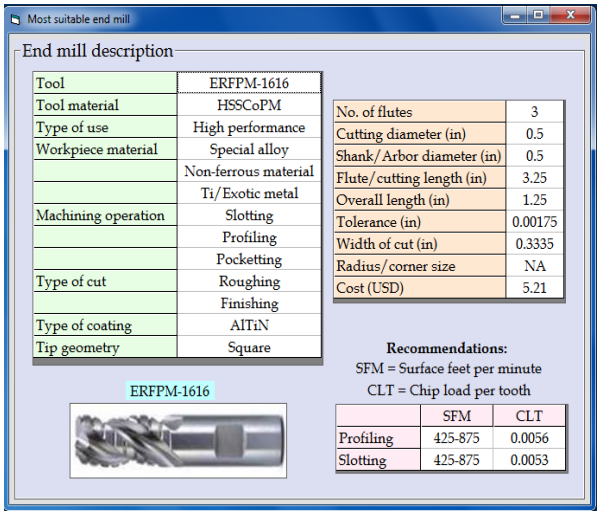

Fig. 4 Most suitable end mill for aerospace applications

4.2 End mill for general purpose milling operation

The aim of this selection problem is to choose the most appropriate end mill that can perform a wide variety of machining operations required in a small-lot-production process. The selected end mills should be versatile and flexible enough to meet the varying demands of small-lot-production. Moreover, these types of machining operations need end mills to be rigid and powerful in order to sustain cutting forces during the material removal process.

The initial step in identifying the best end mill for this selection problem is to choose the cutting tool material as 'HSS'. The advantages of HSS over the other cutting tool materials are its strength to withstand comparatively high cutting forces and relatively low cost. HSS also performs well at intermittent cutting applications from the tool life point of view, which is an important consideration while selecting an end mill. Depending on the type of usage for the end mill, 'General purpose' option is chosen from the opening window of the developed system, as shown in Fig. 5(a). Next, 'Steel' and 'Special alloy' are identified as the workpiece materials owing to their widespread applications in manufacturing industry. The selected end mill should be able to operate for prolonged duration, and hence, tip geometry for the end mill is chosen as 'Chamfer' which offers longer tool life. TiCN film is an excellent all-purpose coating material that induces good repeatability and increases hardness of the end mill considerably. Thus, 'Titanium Carbonitride (TiCN)' is accepted as the coating option for this selection problem. Additionally, the end mills required for general purpose milling operation usually undergo heavy duty machining without any close dimensional tolerance for the end product. Therefore, 'Roughing' is opted as the type of cut to be performed. The machining operations in manufacturing industry usually comprise of production of flat vertical surface on the sides, and generation of key ways, grooves and slots of varying shapes and sizes on the workpieces. So, 'Side milling' and 'Slotting' are chosen as the machining operations to be performed, as exhibited in Fig. 5(b). In order to discard the unsuitable end mill alternatives and move into the next stage of the selection procedure, 'Tool dimensions' functional key is now pressed.

In this stage, five evaluation criteria, i.e. number of flutes, cutting diameter, flute/cutting length, overall length and cost are shortlisted based on which the feasible end mills are further examined for their suitability to perform the intended machining operation. Here, cost and number of flutes are non-beneficial criteria, which are always preferred with lower values. The range of values for each evaluation criterion is then entered into the corresponding empty cells, as exhibited in Fig. 6. A list of nine feasible end mill alternatives which satisfy the specified criteria values appears on pressing of 'Feasible alternatives' functional key. Here, all the nine end mill alternatives are evaluated. The most suitable end mill and the corresponding ranking preorder are obtained while pressing 'Compare' functional key.

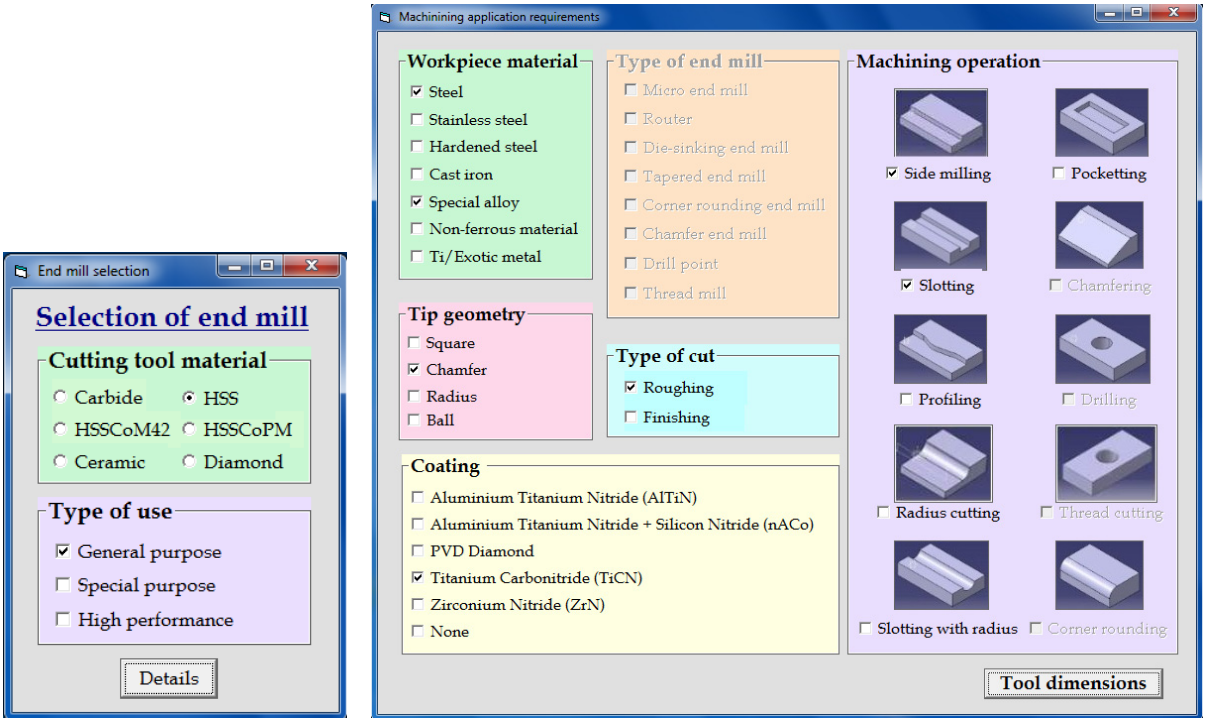

(a) (b)

Fig. 5 End mill selection for general purpose milling operation

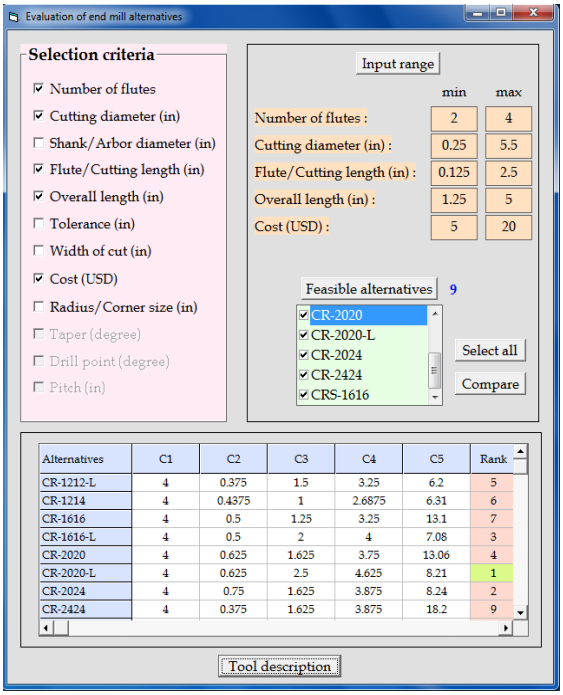

Fig. 6 Decision matrix for selection of end mill for general purpose milling

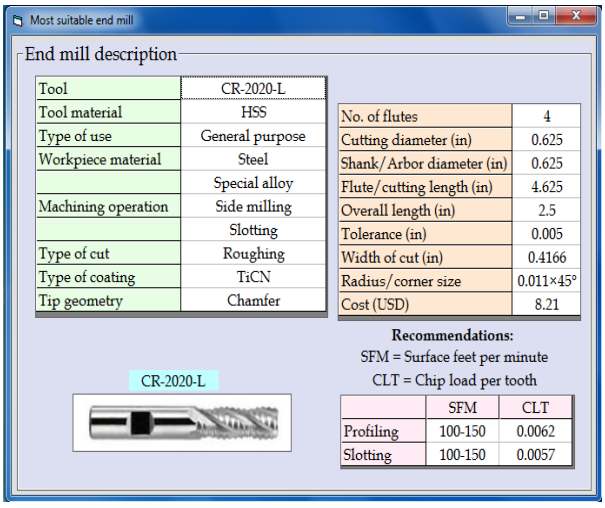

Fig. 7 Selected end mill for general purpose milling operation

It is noticed that CR2020-L is the most suited end mill for performing general purpose milling operations on workpiece materials, like steel and special alloy. The complete details of CR2020-L along with its real-time photograph, and suggestions regarding the corresponding SFM and CLP values are displayed in Fig. 7.

4.3 End mill for corner rounding operation

This example illustrates selection of an end mill which is designed for quick and effective rounding off operation of corners of finished components made of steel and cast iron. The first step in solving this problem is to select the proper cutting tool material. The tools made of carbide are more resistant to abrasive wear, thus protecting them from edge wear caused due to high abrasiveness of cast iron. They also resist cratering and heat deformation that may be caused by long chips of steel at higher cutting speeds. So, 'Carbide' is selected as cutting tool material, as shown in Fig. 8(a), entrusting on the above-mentioned characteristics of carbide tools. Corner rounding is a special category of machining operation performed for high volume production. Therefore, in accordance with the machining application requirements of the said selection problem, 'Special purpose' is chosen as the type of use. Consequently, 'Type of end mill' module is automatically enabled in the developed system with the selection of 'Special purpose' as type of use. Here, 'Corner rounding end mill' is identified as the type of end mill, as exhibited in Fig. 8(b). In this selection process, owing to the fact that the considered end mill variant does not possess specific type of end geometry, 'Tip geometry' option is disabled. Rounding of corner is considered as a finishing operation. Therefore, 'Finish' option is opted as the type of cut to be performed. Coating of AlTiN helps in protecting carbide tools from the detrimental effects of heat. It is acknowledged to be ideal for high speed and hard milling, especially in dry cutting operation. Keeping these properties in mind, AlTiN is chosen as the coating material for carbide tool. Corner rounding is the machining operation to be performed. Therefore, all the other machining operations are disabled except 'Corner rounding', as shown in Fig. 8(b). The end mill alternatives suitable for this machining application are then shortlisted after pressing 'Tool dimensions' key.

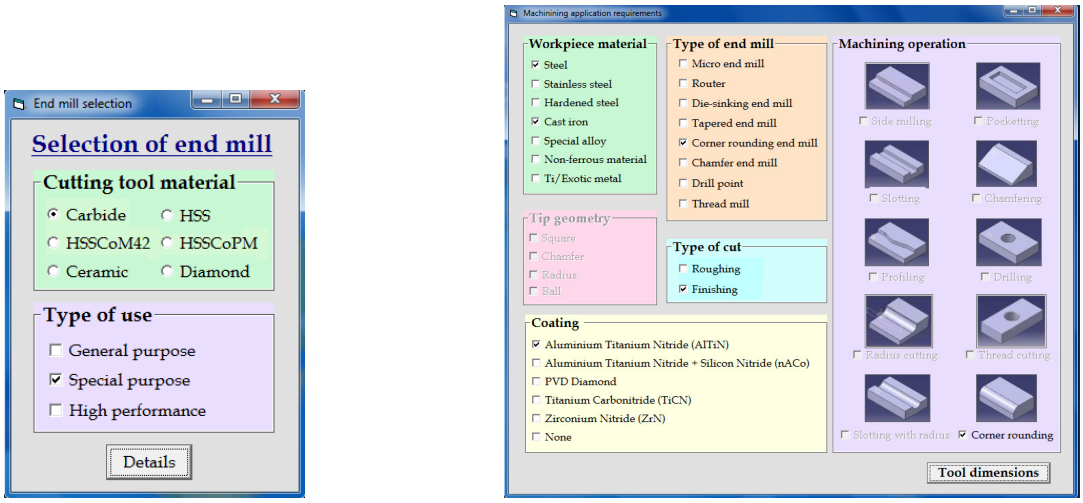

(a) (b)

Fig. 8 End mill selection for corner rounding operation

In this phase of the selection procedure, the extracted end mill alternatives from the first stage are further evaluated with respect to five more criteria, i.e. number of flutes, minor diameter, shank/arbor diameter, radius/corner size and cost. The range of values for each criterion is entered into the respective cells generated on pressing 'Input range' functional key. Once, all the necessary values are entered, this knowledge-based system elicits a list of 23 candidate end mill alternatives capable of performing the task of corner rounding operation on steel and cast iron after pressing of 'Feasible alternatives' functional key. Here, a list of 12 end mill alternatives is selected for final evaluation. Pressing of 'Compare' functional key develops the corresponding decision matrix and calculates the performance score for each alternative to identify the best end mill choice. The ranks of the considered end mill alternatives are displayed in Fig. 9.

Fig. 10 shows the complete description of RCMG-3208, which is identified as the most suitable end mill based on the criteria as set for carrying out corner rounding operation on steel and cast iron. The developed system also assists the process planner in determining the related SFM and CLT values for the considered workpiece materials.

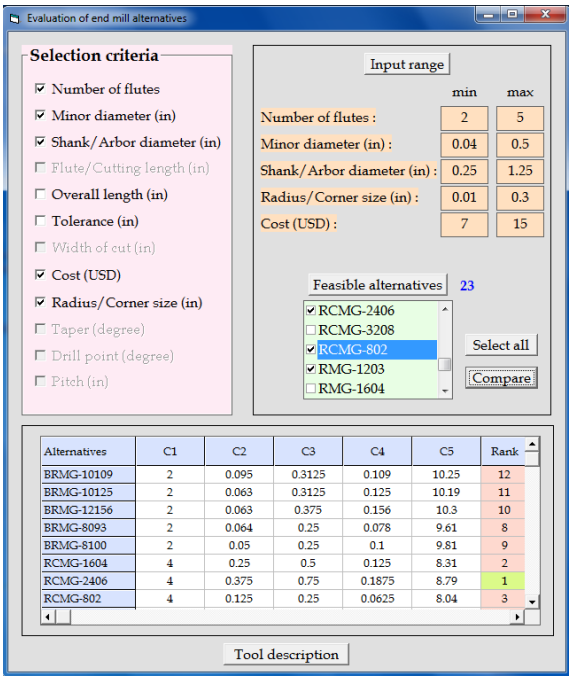

Fig. 9 Decision matrix for selection of end mill for corner rounding operation

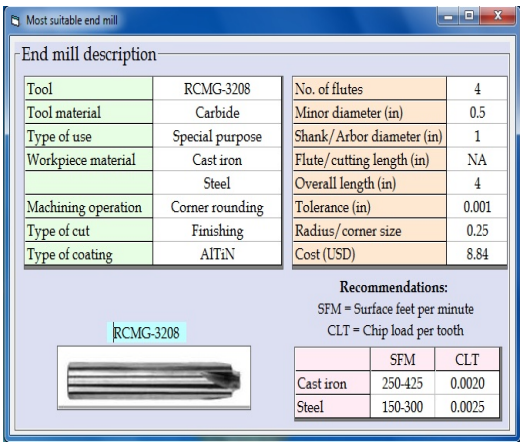

Fig. 10 Selected end mill for corner rounding operation

5. Conclusion

Technological advancements play a critical role in radical growth of the manufacturing sector. There are numerous options for end mills available with respect to their use, coating, workpiece material application etc. So, it becomes quite difficult to see and judge those alternatives one dimensionally. Moreover, this list of alternatives is growing gradually with the arrival of new commercial end mills in the market. Therefore, in this paper, a knowledge-based system is designed in Visual BASIC 6.0 which extracts the end mill alternatives from the database and compares them to identify the most appropriate end mill for a given machining application. The real time implementation of this system on a job floor considerably reduces the time required by the conventional selection procedure and minimizes human error, thus helping in better management of end mills through establishing an effective and productive work culture in the organization. Its utility and solution accuracy are also validated on a real time shop floor satisfying needs of the industrial experts. The database can be periodically upgraded with the changing business environment, thus supporting continuous improvement of the manufacturing enterprise. It ensures that quality of the highest standard is maintained throughout the production process while providing optimal ranges of values for speed and feed combination of the finally selected end mill. This system is flexible enough as it encompasses a wide range of end mill alternatives from different manufacturers into the database. Implementation of this system also results in cost minimization through reduction in manpower requirement, increased personnel efficiency and effective utilization of information. Although, it is designed and developed for an end mill selection process, it can also be employed for selection of other cutting tools, like drill bits, reamers etc. while creating a different module within the same system.

References

[1] Rubio, L., De la Sen, M. (2006). Selection of mill cutter and cutting parameters through an expert system, *Advances in Computer, Information, System Sciences, Engineering*, Springer, Netherlands, doi: 10.1007/1-4020-5261-8_2.

[2] Rao, P.N., (2009). *Manufacturing Technology*, (3rd edition), Tata McGraw-Hill Publishing Company Limited, New Delhi, India.

[3] Klancnik, S., Ficko, M., Balic, J., Pahole, I. (2015). Computer vision-based approach to end mill tool monitoring, *International Journal of Simulation Modelling*, Vol. 14, No. 4, 571-583, doi: 10.2507/IJSIMM14(4)1.301.

[4] Reddy, N.S.K., Rao, P.V., (2005). Selection of optimum tool geometry and cutting conditions using a surface roughness prediction model for end milling, *International Journal of Advanced Manufacturing Technology*, Vol. 26, No. 11, 1202-1210, doi: 10.1007/s00170-004-2110-y.

[5] Li, L.L., Zhang, Y.F. (2006). Cutter selection for 5-axis milling of sculptured surfaces based on accessibility analysis, *International Journal of Production Research*, Vol. 44, No. 16, 3303-3323, doi: 10.1080/00207540500444720.

[6] Novak-Marcincin, J., Janak, M., Novakova-Marcincinova, L., Fecova, V. (2012). Possibility of a quick check on milling strategy suitability, *Tehnički vjestnik – Technical Gazette*, Vol. 19, No. 4, 959-964.

[7] Arezoo, B., Ridgway, K., Al-Ahmari, A.M.A. (2000). Selection of cutting tools and conditions of machining operations using an expert system, *Computers in Industry*, Vol. 42, No. 1, 43-58, doi: 10.1016/S0166-3615(99)00051-2.

[8] Carpenter, I.D., Maropoulos, P.G., (2000). Automatic tool selection for milling operations Part 1: Cutting data generation, *Proceedings of the Institution of Mechanical Engineers, Part B: Journal of Engineering Manufacture,* Vol. 214, No. 4, 271-282, doi: 10.1243/0954405001517667.

[9] Sorby, K., Tonnessen K. (2000). Methodology for selection of cutting tool and machining data for high speed flank milling, In: *Proceedings of the 2nd International Seminar on Improving Machine Tool Performance*, La Baule, France, from *http://imtp.free.fr/imtp2/C1/Sorby_Knut_revised.pdf*, accessed September 1, 2015.

[10] Čuš, F., Balič, J. (2001). Selection of cutting conditions and tool flow in flexible manufacturing system, *Journal of Materials Processing Technology,* Vol. 118, No. 1-3, 485-489, doi: 10.1016/S0924-0136(01)00988-8.

[11] Edalew, K.O., Abdalla, H.S., Nash, R.J. (2001). A computer-based intelligent system for automatic tool selection, *Materials & Design,* Vol. 22, No. 5, 337-351, doi: 10.1016/S0261-3069(00)00106-0.

[12] Wang, X., Da, Z.J., Balaji, A.K., Jawahir, I.S. (2002). Performance-based optimal selection of cutting conditions and cutting tools in multipass turning operations using genetic algorithms, *International Journal of Production Research,* Vol. 40, No. 9, 2053-2065, doi: 10.1080/00207540210128279.

[13] Zhao, Y., Ridgway, K., Al-Ahmari, A.M.A. (2002). Integration of CAD and a cutting tool selection system, *Computers & Industrial Engineering,* Vol. 42, No. 1, 17-34, doi: 10.1016/S0360-8352(01)00061-4.

[14] Byrne, G., Dornfeld, D., Denkena, B. (2003). Advancing cutting technology, *CIRP Annals – Manufacturing Technology*, Vol. 52, No. 2, 483-507, doi: 10.1016/S0007-8506(07)60200-5.

[15] Muršec, B., Čuš, F. (2003). Integral model of selection of optimal cutting conditions from different databases of tool makers, *Journal of Materials Processing Technology,* Vol. 133, No. 1-2, 158-165, doi: 10.1016/S0924-0136(02)00226-1.
[16] Oral, A., Cakir, M.C. (2004). Automated cutting tool selection and cutting tool sequence optimisation for rotational parts, *Robotics and Computer-Integrated Manufacturing,* Vol. 20, No. 2, 127-141, doi: 10.1016/j.rcim.2003.10.006.
[17] Svinjarević, G., Stoić, A., Kopač, J. (2007). Implementation of cutting tool management system, *Journal of Achievements in Materials and Manufacturing Engineering,* Vol. 23, No. 1, 99-102.
[18] Wang, X., Da, Z.J., Balaji, A.K., Jawahir, I.S. (2007). Performance-based predictive models and optimization methods for turning operations and applications: Part 3 – Optimum cutting conditions and selection of cutting tools, *Journal of Manufacturing Processes,* Vol. 9, No. 1, 61-74, doi: 10.1016/S1526-6125(07)70108-1.
[19] Arshad, H., Hassan, R., Omar, N., Sahran, S. (2010). Virtual cutting tool management system for milling process, *International Journal of Computer Science and Network Security*, Vol. 10, No. 2, 148-153.
[20] Ostojic, G., Tadic, B., Luzanin, O., Stankovski, S., Vukelic, D., Budak, I., Miladinovic, L. (2011). An integral system for automated cutting tool selection, *Scientific Research and Essays*, Vol. 6, No. 15, 3240-3251.
[21] Vukelic, D., Tadic, B., Jocanovic, M., Luzanin, O., Simeunovic, N., (2011). A system for computer-aided selection of cutting tools, *ACTA Technica Corviniensis – Bulletin of Engineering,* Vol. 4, No. 3, 89-92.
[22] Chougule, P.D., Kumar, S., Raval, H.K., (2014). An expert system for selection of carbide cutting tools for turning operations, In: *Proceedings of 5th International & 26th All India Manufacturing Technology, Design and Research Conference,* India, (252-1)-(252-6).
[23] Rao, R.V. (2013). *Decision making in the manufacturing environment using graph theory and fuzzy multiple attribute decision making methods*, Volume 2, Springer Series in Advanced Manufacturing, Springer-Verlag, London, UK, doi: 10.1007/978-1-4471-4375-8.

APEM journal
Advances in Production Engineering & Management
Volume 11 | Number 1 | March 2016 | pp 29–37
http://dx.doi.org/10.14743/apem2016.1.207
ISSN 1854-6250
Journal home: apem-journal.org
Original scientific paper

Thermal analysis on a weld joint of aluminium alloy in gas metal arc welding

Ismail, M.I.S.[a,*], **Afieq, W.M.**[a]

[a]Department of Mechanical and Manufacturing Engineering, Faculty of Engineering, Universiti Putra Malaysia, Serdang, 43400, Selangor, Malaysia

ABSTRACT

In this paper, a three-dimensional finite element model has been developed to simulate dynamically the gas metal arc welding (GMAW) process of aluminium alloy sheets. The numerical simulation was conducted using a non-linear transient thermal analysis by changing the welding parameters: namely arc power and welding speed. A moving Gaussian distributed heat source is implemented. All major physical phenomena associated with the GMAW process, such as thermal conduction and convection heat losses are taken into account in the model development. The developed model can calculate the temperature field and predict the weld geometry profile during the welding process. The measurement of weld bead profile from the GMAW experiments was used to validate the developed finite element model. The numerical study reveals that the arc voltage and welding speed have a significant influence on the temperature distribution, weld pool size and shape, and weld bead geometry. The results show that there are good agreements with the weld bead profile between the experimental observation and finite element simulation.

ARTICLE INFO

Keywords:
Gas metal arc welding
Aluminium alloy
Weld bead profile
Finite element model
Thermal analysis

**Corresponding author:*
ms_idris@upm.edu.my
(Ismail, M.I.S.)

Article history:
Received 31 August 2015
Revised 22 January 2016
Accepted 25 January 2016

1. Introduction

Welding ranks high among industrial processes and involves more sciences and variables than those involves in any other industrial process. Today, the welding has four popular processes, which are shielded metal arc welding (SMAW), metal inert gas (MIG), flux core arc welding (FCAW) and tungsten inert gas welding (TIG). MIG welding is one of the gas metal arc welding (GMAW) subtypes which are a welding process that joint two or more parts by melting the filler with the similar type of material of the product. The purpose of the shielding gas during the MIG welding is to protect the process from the contaminants in the air.

The quality of this welding process can also refer to the formation of the welding bead profile. However, the size of welding bead is hard to predict and to measure where it is depend on the power usage and the speed of welding [1, 2]. Experimental work can be one of the techniques to measure welding bead profile from a set of parameter [3, 4]. However, experimental trials have some uncertainties in the data obtained [5]. By doing the experimental work, the heat data that had been generated during the welding process could not be generated. The weld bead also can be predicted by using mathematical approaches [6-9]. Nevertheless, the main disadvantage of the mathematical model, it does not consider the variation of the thermal properties with temperature, which has very little practical or theoretical relevance to describe the real GMAW process.

Thermal analysis is very important to conduct the numerical simulation for welding process [10-12]. Simulation of welding process first appeared in early 1970's, and comprehensive review regarding developments in the welding simulation is by Lindgren [13-15]. Ueda and Yamakawa [16] and Hibbitt and Marcal [17] are among the pioneers who initiated application of finite element technique on simulation of welding. Goldak et al. [18] presented a so-called double ellipsiodal heat source model which is having Gaussian distribution of power density in space. There are many research papers successfully utilized the numerical simulation in the research and development of arc welding [19, 20], friction stir welding [21], laser beam welding [22], and electron beam welding [23], which deal with the temperature field and weld bead geometry of welding by using numerical models. By carrying out the thermal analysis using the finite element method, the thermal field data could easily be generated. Moreover, the weld bead size could also be easily measured by measuring the area of melting point of material.

In this study, the MIG welding process was investigated through finite element analysis. A three-dimensional finite element model has been developed to simulate the MIG welding process. The effect of heat input on MIG welding process also has been study in this project. In order to validate the finite element model, the experimental work of MIG welding process of thin plate aluminium alloy AA6061 was carried out to investigate the welding bead profile. The weld bead geometry was measured at different power input and welding speed.

2. Finite element model

2.1 Heat transfer analysis

The transient temperature field of the welded specimen is a function of time t and Cartesian coordinate system with y-axis along the welding direction, z-axis along the thickness direction and the origin locating on the specimen on the specimen surface. The governing equation for the transient heat conduction can be expressed as Eq. 1:

$$\rho c \frac{\delta \theta}{\delta t} = k\left(\frac{\delta^2 \theta}{\delta x^2} + \frac{\delta^2 \theta}{\delta y^2} + \frac{\delta^2 \theta}{\delta z^2}\right) + Q \tag{1}$$

where θ is the temperature, ρ is the material density, c is the specific heat, k is the thermal conductivity, and Q is the internal heat generation per unit volume. The thermal analysis was conducted using temperature dependent thermal material properties as shown in Fig. 1, which were taken from Afieq [24].

In this study, the heat source can be modelled by using Gaussian distribution at any time t, for the heat source of welding arc. The points that are lying on the surface of the specimen are within the arc radius r_a receive distribution of heat flux $q(t)$ according to the Eq. 2 [25],

$$q(t) = \frac{3Q_A}{\pi {r_a}^2} exp\left[-\left(\frac{r(t)}{r_a}\right)^2\right] \tag{2}$$

where $r(t)$ is the radial distance measured from the arc centre of the specimen, and Q_A is the total heat input of the welding process, and it can be written as Eq. 3,

$$Q_A = \eta VI \tag{3}$$

where Q_A is the heat input, V is the voltage, and I is the current radius. The efficiency η value for this welding process is 0.9 due to GMAW process [26].

The boundary condition of the heat transfer Eq. 1 was assumed as the heat flux generated by the welding arc, which is only applied on the top surface of the specimen and is defined by Eq. 2. While, on the non-welded top surface, the heat flux was assumed to be only the convective heat flux q_c, and can be expressed as $q_c = h_c\,(\theta - \theta_0)$, where h_c is the coefficient of the heat convection

(h_c = 10 W/m²K) [27, 28] and θ_0 is the room temperature of the surrounding environment. The initial temperature of specimen was also assumed as θ_0.

In order to obtain the solution to the thermal equilibrium equation, the initial and boundary conditions are needed. The finite element equation for the thermal analysis can be expressed as follows:

$$[C]\{\dot{\theta}\} + [K]\{\theta\} = \{Q\} \tag{4}$$

where $[C]$, $[K]$, $\{Q\}$, $\{\theta\}$ and $\{\dot{\theta}\}$ are heat capacity matrix, heat conduction matrix, heat flux column, nodal temperature column and nodal temperature rate column, respectively.

2.2 Model development

A three-dimensional (3D) finite element model was developed using ANSYS finite element software. The model was created under the similar dimension with the specimen of experimental work. It has 100 mm in width, 125 mm in length and 3 mm in thickness. The mesh was graded finest in the region of highest and most rapid temperature gradient near the heat input, and a coarse mesh was used outside the heating zone as illustrated in Fig. 2. The mesh generation was carried out first on the upper or lower surface of the specimen. Then, 3D mesh was generated by taking offsets across the specimen thickness. In order to capture the characteristics of GMAW process accurately, the mesh size increases exponentially across the thickness of the specimen, being finer near the heated side of the specimen. The mesh was composed of a total number of 29312 elements. The elements were the thermal analysis element PLANE77 and SOLID70 for 2D eight-node thermal solid and 3D eight-node thermal solid, respectively. The extrapolation method which was established by Richardson in 1926 and widely used for assessing the solution accuracy of many problems in finite volumes [29-31] and finite elements [32, 33] analyses. However, in the numerical modeling of welding process, the accuracy of mesh size has been proposed by Moraitis and Labeas [34] and Malik et al. [35]. In this method, the peak temperature is the parameter being studied in sensitivity analysis of the mesh size. Application of a finer mesh in this work led to less than 2% difference in the peak temperatures. Therefore, the presented mesh was used. An ANSYS Parametric Design Language (APDL) was used to model the moving heat source. The distributed heat flux moves with time. When the distributed heat flux moves to the next step, the former distributed heat flux step is deleted. In the present case, a moving laser beam heat source with small steps is adopted in order to simulate its continuous scanning.

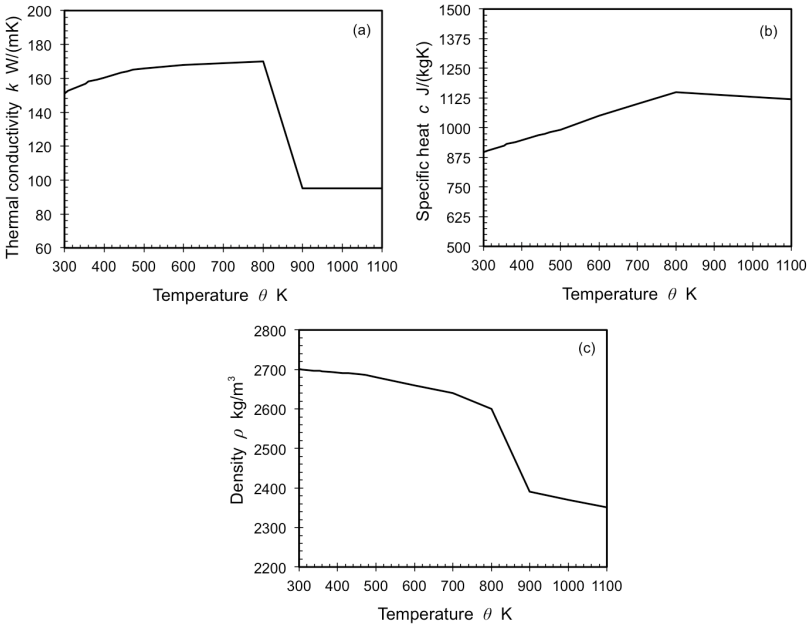

Fig. 1 Thermophysical properties of aluminium alloy AA6061

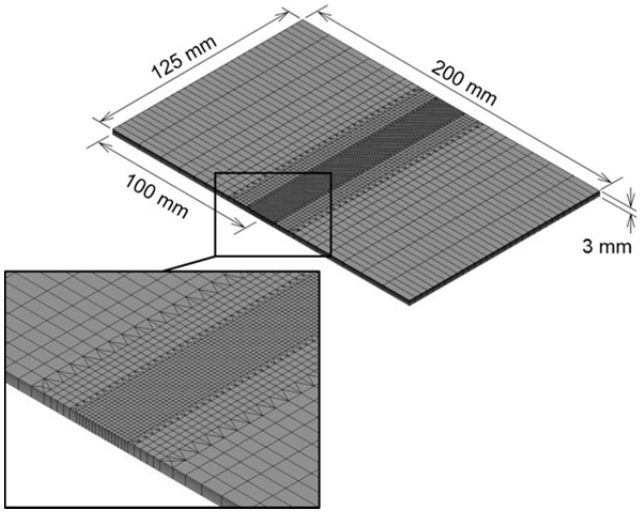

Fig. 2 Finite element model of gas metal arc welding process

3. Experimental work

A schematic diagram of experimental setup is shown in Fig. 3. In this study, the GMAW process was performed by using KempoWeld machine with 1 mm aluminium wire electrode under a shielding gas of argon. The orientation of welding torch was aligned 45 degree to the perpendicular axis of specimen top surface. The welding experiments were carried out with a motorize translations stage to execute the consistent welding speed. The workpiece material used in this study was aluminium alloy AA6061. The chemical composition is listed in Table 1. The aluminium alloy with thickness of 3 mm was cut to two plates of 100 mm x 125 mm. The butt-joint weld design was welded as shown in Fig. 3.

Welding experiments were conducted according to welding conditions as shown in Table 2. The selected welding speeds were 30 mm/s and 40 mm/s. The arc voltage were varied from 18 V to 22 V. Welding current, wire electrode feed rate and flow rate of shielding gas remained constant throughout the experiment. After the welding process, the welded specimens were cut perpendicular to the welding direction for the observation of weld bead by optical microscope.

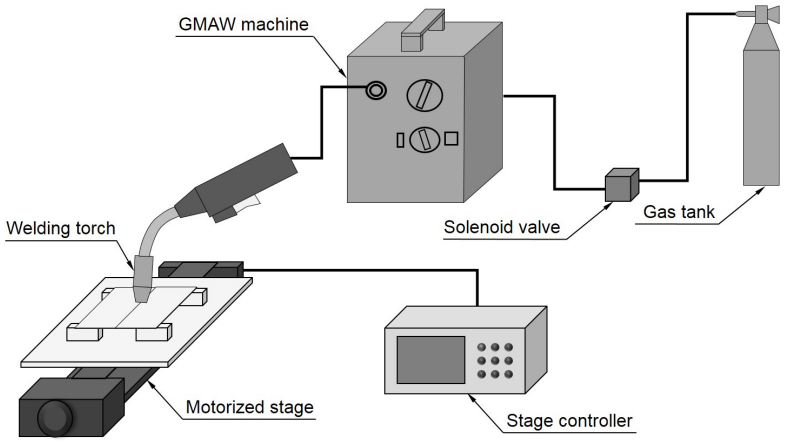

Fig. 3 Schematic diagram of experimental setup

Table 1 Chemical composition of aluminium alloy AA6061 (wt.%)

Al	Cu	Fe	Mg	Mn	Si	Ti	Zn
Bal.	0.15	≤0.7	0.8-1.2	0.15	0.4-0.8	0.15	0.25

Table 2 Welding condition

Parameter	Value
Welding speed (mm/s)	30, 40
Welding voltage (V)	18, 20, 22
Welding current (A)	140
Flow rate (l/min)	18
Shielding gas	Argon
Wire electrode feed rate (mm/s)	148
Wire electrode diameter (mm)	1

4. Results and discussion

Fig. 4 shows the temperature distribution at the top surface of the cross-section of the specimen along the welding path along *x*-axis for the 22 V welding power and 30 mm/s welding speed at the location of 94 mm from the starting point (x = 0 mm). The iteration time of each step for this analysis is 0.033 mm/s due to the welding speed. The temperature on the surface along the welding path is increasing rapidly after it is been heated by the welding arc, where the heat is then distributed throughout the plate. In this analysis, the cooling process has immediately taken place after the welding has finish at 5.17 s where it undergoes convection of heat transfer on the surface. The highest reading of temperature heating the plate almost reaches 8000 K where it is located on the centre of the arc. The convection of heat transfer are taken place during the welding process where there are difference in temperature reading where the highest reading is on the arc location, meanwhile the temperature at locations which already undergo the welding process are already slightly reduced.

Fig. 5 shows the temperature histories for three points located transversally to the weld direction. The peak temperature is at the "heel" of the center of the welding arc. In this period, the peak temperature remains constant and already in the quasi-steady state. For the same period, the velocity of the rising temperature decreases at the bottom surface as shown in Fig. 6. Since the temperature at the top surface is much higher than that at the bottom surface, the larger temperature difference between the top and bottom surfaces leads to a high temperature gradient. This significant temperature difference through the specimen thickness can also affect the final deformation of the specimen [36].

Fig. 7 shows the temperature field of heating phase and cooling phase in the welding process. The time period of heating during welding process for this parameter only takes 5.17 s which then the cooling process are taken place immediately. The heat from the heat source is distributed through the plate by the heat conduction. The temperature reading during the heating phase becomes stable when the welding process reaches the middle location of the plate on the welding path. The heat are been removed to the surrounding during the cooling phase by the heat convection process where the plate are been left at the room temperature for the cooling process.

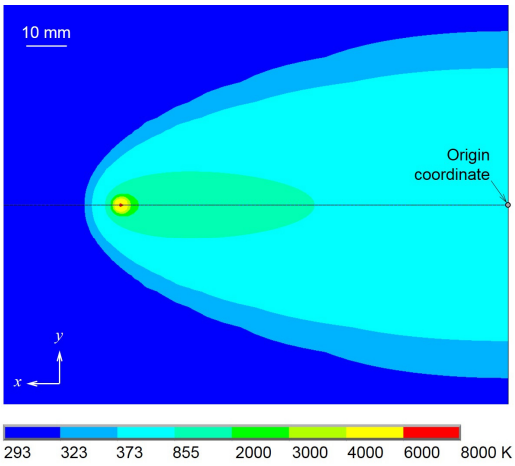

Fig. 4 Temperature distribution at the top surface along the weld direction (Voltage: 22 V, Speed: 30 mm/s)

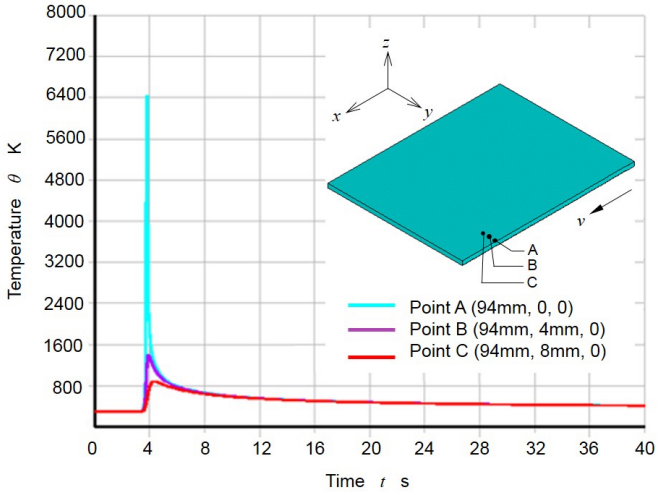

Fig. 5 Temperature histories of the three evaluated points transverse to the direction (Voltage: 22 V, Speed: 30 mm/s)

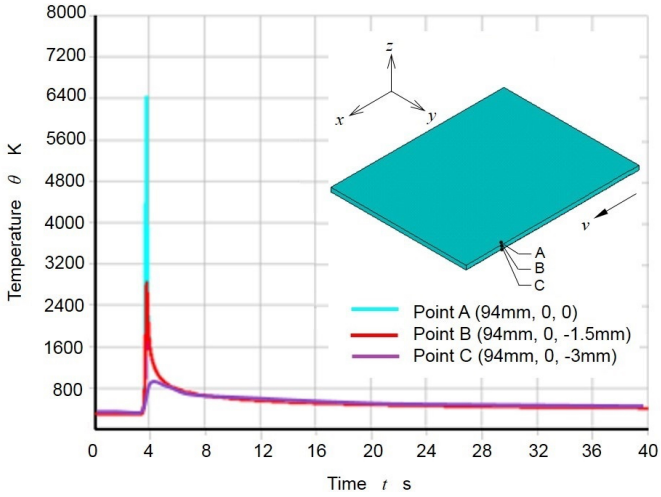

Fig. 6 Temperature histories of the three evaluated points of the cross-section of plate (Voltage: 22 V, Speed: 30 mm/s)

In Fig. 8, by having different heat input even though the similar welding speed is used due to different in the welding voltage during the welding process. The faster the welding is having lower heat input compare to the slower welding speed which is having higher heat input. This is because the welding speed is inversely proportional with the heat input. The different in the temperature distribution can be only seen on the top surface of the plate since the heat are been distributed throughout a large volume. The depth of the penetration for all parameter are similar due to the plate are thin, which the heat only throughout small volume.

In order to verify the developed model, the simulation and experimental weld geometry were compared. Fig. 9 shows the comparison of bead profile between the simulation and experimental. From this comparison, the highest heat input makes the bead formation wider when comparing parameter used in the similar welding speed. Whereas at a higher speed with the similar power usage the bead was reduce in its size. The bead profile from the experimental was viewed by using optical microscope. The height of the bump of the welding bead depended on the voltage usage and the speed of welding. The voltage of 18 V showed the highest bump formation for each speed. This was due to the low power usage to melt the filler so that it could bond completely with the plate. The usage of voltage 20 V and 22 V showed that the bump formations were smaller in sizes where the filler was completely bonded with the plate. Thus those power were more preferable to be used since the quality of welding process was been referred by the formation of bumps.

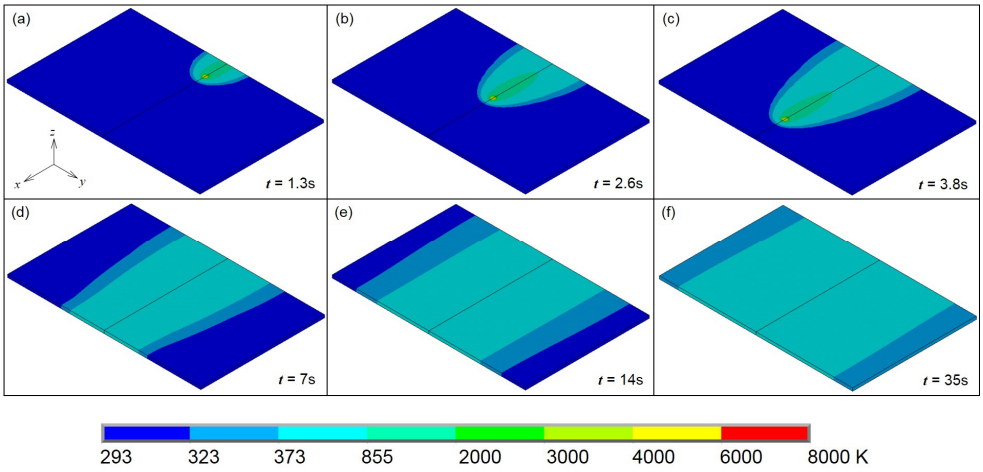

Fig. 7 Temperature distributions during welding (a-c) and cooling (d-f) (Voltage: 22 V, Speed: 30 mm/s)

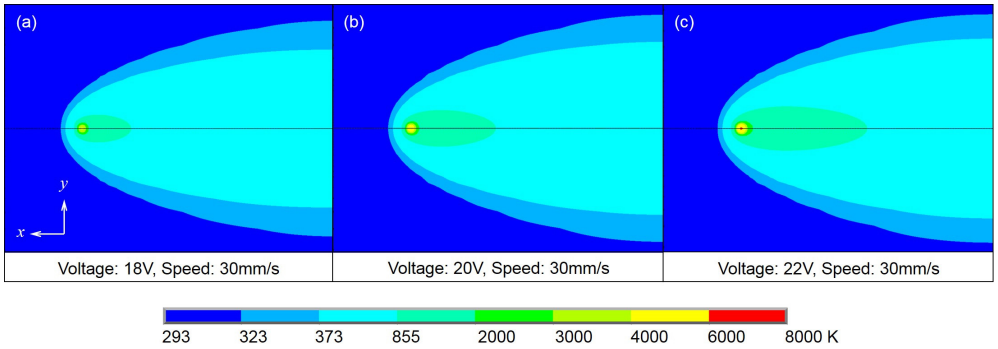

Fig. 8 Temperature distributions for welding conditions with the speed of 30 mm/s and different voltage of (a) 18 V, (b) 20 V, and (c) 22 V

Most of the percentage of error is less than 20 % and the least error is at the voltage of 18 V speed of 40 mm/s with the percentage of error of 0.05 %. The results from the analysis become the theoretical result which was used as the reference to calculate the percentage of errors. The percentage of error varies among the parameter due to some problems that occurred during the experimental which affect the results.

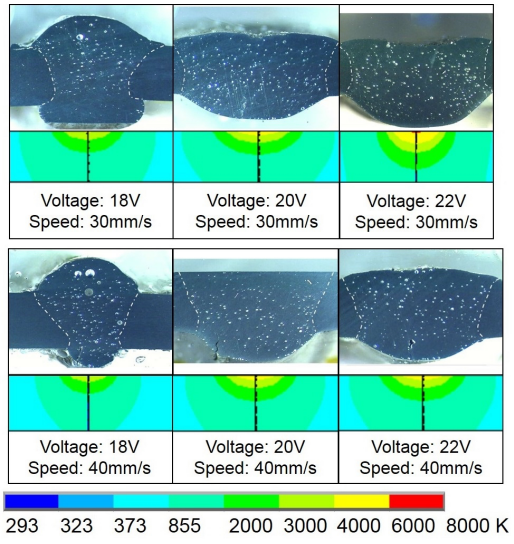

Fig. 9 Comparison between experimental and simulated weld bead profiles

The voltage that was used during the welding process may differ from the analysis since the welding machine could not maintain the power output. The power used during the welding was set by setting the arc voltage with the tolerance of ± 1 V so that the result could be acceptable. The welding process was done manually where the height of the nozzle was not static, affecting the torch arc diameter which lead to the error in the size of bead.

5. Conclusion

A three-dimensional finite element model has been developed to simulate the thermal history during gas metal arc welding of aluminium alloy sheet. Main conclusions obtained in this study are as follows:

- The developed numerical model using a Gaussian heat source can well represent the real welding as the heat source penetrates into the material.
- Arc voltage and welding speed have a significant effect on the temperature distribution, weld pool size and shape, and weld bead geometry.
- Heat input to the weld pool is transferred rapidly first in the thickness direction of the sheet and then in the width direction to reach uniformed distribution.
- Temperature distributions obtained from the developed model can be used as inputs for the thermo-mechanical analysis of aluminium alloy in gas metal arc welding.

Acknowledgement

The authors would like to acknowledge the technical support provided by Mr. Mohd Saiful Azuar Md. Isa in carrying out the experimental work at the Faculty of Engineering, Universiti Putra Malaysia (UPM).

References

[1] Benyounis, K.Y., Olabi, A.G., Hashmi, M.S.J. (2005). Effect of laser welding parameters on the heat input and weld-bead profile, *Journal of Materials Processing Technology*, Vol. 164-165, 978-985, doi: 10.1016/j.jmatprotec.2005.02.060.

[2] Shanmugam, N.S., Buvanashekaran, G., Sankaranarayasamy, K., Kumar, S.R. (2010). A transient finite element simulation of the temperature and bead profiles of T-joint laser weld, *Materials & Design*, Vol. 31, No. 9, 4528-4542, doi: 10.1016/j.matdes.2010.03.057.

[3] Talabi, S.I., Owolabi, O.B., Adebisi, J.A., Yahaya, T. (2014). Effect of welding variables on mechanical properties of low carbon steel welded joint, *Advances in Production Engineering & Management*, Vol. 9, No. 4, 181-186, doi: 10.14743/apem2014.4.186.

[4] Satheesh, M., Edwin Raja Dhas, J. (2014). Hybrid Taguchi method for optimizing flux cored arc weld parameters for mild steel, *Advances in Production Engineering & Management*, Vol. 9, No. 2, 95-103, doi: 10.14743/apem2014.2.179.

[5] Anca, A., Cardona, A., Risso, A., Fachinotti, V.D. (2011). Finite element modeling of welding process, *Applied Mathematical Modelling*, Vol. 35, No. 2, 688-707, doi: 10.1016/j.apm.2010.07.026.

[6] Sharma, A., Arora, N., Mishra, B. (2015). Mathematical model of bead profile in high deposition welds, *Journal of Material Processing Technology*, Vol. 220, 65-75, doi: 10.1016/j.jmatprotec.2015.01.009.

[7] Chan, B.K.H., Bibby, M.J., Yang, L.J., Chandel, R. (1993). A discussion of algorithms for representing submerged arc weld shape with workpiece edge preparation, In: *Winter Annual Meeting, Manufacturing Science and Engineering*, New Orleans, USA, 873-878.

[8] Kim, G.H., Kang, S.I., Lee, S.B. (1999). A study on the estimate of weld bead shape and the compensation of welding parameters by considering weld defects in horizontal fillet welds, In: *Third International Conference on Knowledge-based Intelligent Information Engineering Systems*, Adelaide, Australia, 212-216, doi: 10.1109/KES.1999.820157.

[9] Datta, S., Bandyopadhyay, A., Pal, P.K. (2008). Modelling and optimization of features of bead geometry including percentage dilution in submerged arc welding using mixture of fresh flux and fused slag, *The International Journal of Advanced Manufacturing Technology*, Vol. 36, No. 11, 1080-1090, doi: 10.1007/s00170-006-0917-4.

[10] Ma, J., Kong, F., Kovacevic, R. (2012). Finite-element thermal analysis of laser welding of galvanized high-strength steel in a zero-gap lap joint configuration and its experimental verification, *Materials & Design*, Vol. 36, 348-358, doi: 10.1016/j.matdes.2011.11.027.

[11] Ribic, B., Palmer, T.A., Debroy, T. (2009). Problems and issues in laser-arc hybrid welding, *International Materials Reviews*, Vol. 54, No. 4, 223-244, doi: 10.1179/174328009X411163.

[12] Uday, M., Ahmad Fauzi, M.N., Zuhailawati, H., Ismail, A.B. (2012). Thermal analysis of friction welding process in relation to the welding of YSZ-alumina composite and 6061 aluminum alloy, *Applied Surface Science*, Vol. 258, No. 20, 8264-8272, doi: 10.1016/j.apsusc.2012.05.035.

[13] Lindgren, L.E. (2001). Finite element modeling and simulation of welding – Part 1: Increased complexity, *Journal of Thermal Stresses*, Vol. 24, No. 2, 141-192, doi: 10.1080/01495730150500442.
[14] Lindgren, L.E. (2001). Finite element modeling and simulation of welding – Part 2: Improved material modeling, *Journal of Thermal Stresses*, Vol. 24, No. 3, 195-231, doi: 10.1080/014957301300006380.
[15] Lindgren, L.E. (2001). Finite element modeling and simulation of welding – Part 3: Efficiency and integration, *Journal of Thermal Stresses*, Vol. 24, No. 4, 305-334, doi: 10.1080/01495730151078117.
[16] Ueda, Y., Yamakawa, T. (1971). Analysis of thermal-elastic stress and strain during welding by finite element method, *Transactions of the Japan Welding Society*, Vol. 2, No. 2, 90-100.
[17] Hibbitt, H.D., Marcal, P.V. (1973). A numerical thermo-mechanical model for the welding and subsequent loading of fabricated structure, *Computers & Structures*, Vol. 3, No. 5, 1145-1174, doi: 10.1016/0045-7949(73)90043-6.
[18] Goldak, J., Chakravarti, A., Bibby, M. (1984). A new finite element model for welding heat sources, *Metallurgical Transactions B*, Vol. 15, No. 2, 299-305, doi: 10.1007/BF02667333.
[19] Hackmair, C., Werner, E., Pönisch, M. (2003). Application of welding simulation for chassis components within the development of manufacturing methods, *Computational Materials Science*, Vol. 28, No. 3-4, 540-547, doi:10.1016/j.commatsci.2003.08.011.
[20] Long, H., Gery, D., Carlier, A., Maropoulos, P.G. (2009). Prediction of welding distortion in butt joint of thin plates, *Materials & Design*, Vol. 30, No. 10, 4126-4135, doi: 10.1016/j.matdes.2009.05.004.
[21] Al-Badour, F., Merah, N., Shuaib, A., Bazoune, A. (2014). Thermo-mechanical finite element model of friction stir welding of dissimilar alloys, *The International Journal of Advanced Manufacturing Technology*, Vol. 72, No. 5, 607-617, doi: 10.1007/s00170-014-5680-3.
[22] Tsirkas, S.A., Papanikos, P., Kermanidis, Th. (2003). Numerical simulation of the laser welding process in butt-joint specimens, *Journal of Materials Processing Technology*, Vol. 134, No. 1, 59-69, doi: 10.1016/S0924-0136(02)00921-4.
[23] Reed, R.C., Stone, H.J., Dye, D., Roberts, S.M., McKenzie, S.G. (2000). Process modelling of the electron beam welding of aeroengine components, In: *Ninth International Symposium on Superalloys*, Pennsylvania, 665-674, doi: 10.7449/2000/Superalloys_2000_665_674.
[24] Afieq, W.M. (2015). *Thermal analysis of weld joint in GMAW process*, Bachelor dissertation, Universiti Putra Malaysia, Malaysia.
[25] Tian, L., Luo, Y., Wang, Y., Wu, X. (2014). Prediction of transverse and angular distortions of gas tungsten arc bead-on-plate welding using artificial neural network, *Materials & Design*, Vol. 54, 458-472, doi: 10.1016/j.matdes.2013.08.082.
[26] Atkins, G., Thiessen, D., Nissley, N., Adonyi, Y. (2002). Welding process effects in weldability testing of steels, *Welding Journal*, Vol. 81, No. 4, 61s-68s.
[27] Ismail, M.I.S., Okamoto, Y., Uno, Y. (2011). Numerical simulation on micro-welding of thin stainless steel sheet by fiber laser, *International Journal of Electrical Machining*, Vol. 16, 9-14.
[28] Yilbas, B.S., Akhtar, S., Shuja, S.Z. (2013). *Laser forming and welding processes*, Springer, New York, doi: 10.1007/978-3-319-00981-0.
[29] Ternik, P., Rudolf, R. (2014). Laminar forced convection heat transfer characteristics from a heated cylinder in water based nanofluids, *International Journal of Simulation Modelling*, Vol. 13, No. 3, 312-322, doi: 10.2507/IJSIMM13(3)5.271.
[30] Ternik, P., Buchmeister, J. (2015). Buoyancy-induced flow and heat transfer of power law fluids in a side heated square cavity, *International Journal of Simulation Modelling*, Vol. 14, No. 2, 238-249, doi: 10.2507/IJSIMM14(2)5.293.
[31] Ternik, P. (2015). Conduction and convection heat transfer characteristics of water-Au nanofluid in a cubic enclosure with differentially heated side walls, *International Journal of Heat and Mass Transfer*, Vol. 80, 368-375, doi: 10.1016/j.ijheatmasstransfer.2014.09.041.
[32] Lin, Q., Liu, J. (2007). Counterexamples to the asymptotic expansion of interpolation in finite elements, *Advances in Computational Mathematics*, Vol. 27, No. 2, 167-177, doi: 10.1007/s10444-007-9030-y.
[33] Asadzadeh, M., Schatz, A.H., Wendland, W. (2009). A new approach to Richardson extrapolation in the finite element method for second order elliptic problems, *Mathematics of Computation*, Vol. 78, 1951-1973, doi: 10.1090/S0025-5718-09-02241-8.
[34] Moraitis, G.A., Labeas, G.N. (2008). Residual stress and distortion calculation of laser beam welding for aluminum lap joints, *Journal of Materials Processing Technology*, Vol. 198, No. 1-2, 260-269, doi: 10.1016/j.jmatprotec.2007.07.013.
[35] Malik, A.M., Qureshi, E.M., Dar, N.U., Khan, I. (2008). Analysis of circumferentially arc welded thin-walled cylinders to investigate the residual stress fields, *Thin-Walled Structure*, Vol. 46, No. 12, 1391-1401, doi: 10.1016/j.tws.2008.03.011.
[36] Mandal, N.R. (2004). *Welding and distortion control*, Alpha Science International Ltd, Pangbourne, England.

APEM journal
Advances in Production Engineering & Management
Volume 11 | Number 1 | March 2016 | pp 38–48
http://dx.doi.org/10.14743/apem2016.1.208
ISSN 1854-6250
Journal home: apem-journal.org
Original scientific paper

A bi-objective inspection policy optimization model for finite-life repairable systems using a genetic algorithm

Ramadan, S.[a,*]

[a]Department of Mechanical and Industrial Engineering, Applied Science Private University, Shafa Badran, Amman, Jordan

ABSTRACT

This paper presents a bi-objective optimization model for finding the optimal number and optimal aperiodic times for the inspections of finite-life repairable systems when the availability of the component and the total maintenance cost are under consideration. The model utilizes the delay-time concept under perfect inspection assumption. The defect arrival process is modelled using the nonhomogeneous Poisson process and the failure times are probabilistic. The solution to this problem is NP-hard, therefore, a mutation-based genetic algorithm has been designed to solve the model. The effectiveness of the model was demonstrated using seven illustrative examples and compared to an existing classical periodic inspection model that uses a fixed number of inspections. The results showed that the proposed model did better (in all of the attributes) than the aperiodic model that using a fixed number of inspections. Furthermore, the results showed that the proposed model gave better results than a single-objective aperiodic model. The proposed model is a general model that can be implemented with different rates of occurrence of defects and different delay-time distributions. Also this model can be extended easily to cover complex systems and imperfect inspection cases.

ARTICLE INFO

Keywords:
Maintenance
Aperiodic inspection
Periodic inspection
Delay-time
Multi-objective optimization
Genetic algorithms

**Corresponding author:*
s_ramadan@asu.edu.jo
(Ramadan, S.)

Article history:
Received 14 September 2015
Revised 29 September 2015
Accepted 19 October 2015

1. Introduction

As equipment age, the failure and deterioration related maintenance costs and interruptions increase; hence, the need for effective maintenance policies become more obvious. Traditionally, corrective maintenance is the most prevailing maintenance type practiced. It was estimated that 80 % of the industry dollars is spent on maintaining chronic failures of machines, systems, and people. Despite this huge figure, corrective maintenance cannot improve the reliability of the machines/systems as the maintenance action is taken after the failure. In the other hand, it was estimated that eliminating many of those chronic failures by implementing an effective maintenance policies can reduce this percentage between 40 % and 60 % [1]. Preventive maintenance (PM) is one of the most widely used maintenance types that can reduce the cost of maintaining machines and systems due to its ability of discovering hidden failures that may constitute up to 40 % of the failure modes in complex industrial systems [2]. Many inspection models were developed in literatures to optimize the inspection process in order to reduce the number of chronic failures. Earlier inspection models aimed to optimize the number of inspections per unit of time by minimizing the total downtime or maximizing the profit which were expressed as a function of number of inspections [3-7]. These models did not discuss the periodicity of the inspections but rather found the optimum number of inspections per unit of time. More recent inspection models were developed based on delay-time concept introduced by [8] which is very

similar to the Potential Failure interval in reliability centered maintenance developed later [2]. Delay-time concept divides the failure process into two stages: defect initialization stage and failure stage and defines the time elapsed between the defect initialization and the corresponding actual failure as the delay-time. This concept is very important in preventive maintenance PM because it shows that there is a time window (equals to the delay-time) that the maintenance crew can detect and fix the defect before it turns into a chronic failure. This concept inspired many researchers to develop optimization inspection models to reduce the number of chronic failures. The essence of those inspection models is to find the optimal periodicity of the inspections that will reduce the expected number of chronic failures. Christer et al. and Baker, used the delay-time concept in the industrial plant to find the periodicity of the inspections where the value of the delay-time was considered probabilistic [9-13]. Wang and Majid [14] used the concept of delay-time in offshore oil platform plant to optimize the periodicity of the inspections by minimize the system downtime. The work of Dawotola et al. [15] used the concept of delay-time in very long cross-country petroleum pipeline system where the periodicity of the inspections was determined by minimizing the total economic loss of failure while taking the human risk and maintenance budget as constraints. Abdel-Hameed [16] implemented increasing jump Markov process to optimize the periodicity of inspections. Okumura et al. [17, 18] proposed a stochastic-process free method for optimizing the discrete time point inspections for single unit system using stochastic processes. Wang [19] proposed two models one for single component and another one for complex component based on delay-time concept and in [20] the author extended the delay-time concept and instead of assuming that the failures can be detected only by inspections, he assumes that the failures can be revealed by themselves. Based on this extension, he proposed an inspection model for two types of inspections and repairs to determine the optimal constant periodicity of the inspections. Later, Wang et al. [21] extended the work of Wang [20] to multi-component multi-failure mode inspection model.

Unfortunately, very little work was devoted to consider the multi-objective optimization of the inspection models under delay-time concept. Under delay-time concept, most of the literatures aimed to optimize the inspection policy based on a single objective namely, minimizing some form of maintenance cost [17, 22-27]. Other objectives are also found in the literatures such as maximizing the availability or the reliability of the system [6, 28, 29].

Few of the studies in the literatures considered both the number of inspections and the timing of these inspections in there models. The majority of them optimized either the number of inspection per unit time [4-7] or considered a constant number of inspections and optimized the times at which the inspections were made [30]. Moreover, a lot of the optimization models in the literatures were solved by a special designed algorithms that can be used only to the corresponding inspection model or algorithms that were time inefficient like enumeration.

In this paper a bi-objective inspection optimization model is considered to optimize the number and the timing of inspections utilizing two objectives: maximizing the availability and minimizing the maintenance cost of the system. The model utilized the delay-time concept under perfect inspection assumption. The defect arrival process is modelled using nonhomogeneous Poisson process and the failure times are probabilistic. Genetic algorithm, which is a generic and efficient optimization algorithm, was used to optimize this model.

The paper contains the following sections: Section 2 shows the notations and the assumptions of the model. Section 3 presents the model formulation based on delay-time concept. Section 4 presents the details of the genetic algorithm used. Section 5 presents the experimentations and discussion, and finally, section 6 concludes.

2. Assumptions and notations

This section lists the assumptions and notations used in this paper. The following assumptions and notations can be explained on the light of Fig. 1 which shows a typical defect-failure-inspection relation under delay-time concept.

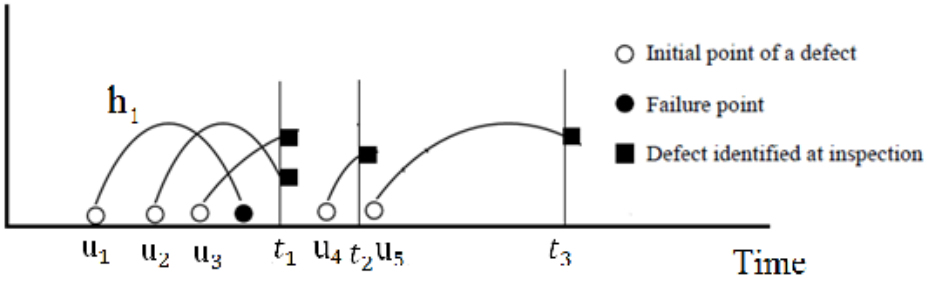

Fig. 1 The relationship between defects, failures, and inspections under the delay-time concept

Consider a system with a finite life L, the objective of this proposed model is to find the optimal inspection policy; i.e., the optimal number of inspections n and the optimal timing for the inspections $\boldsymbol{t}$ to achieve the highest possible availability A_s and the lowest possible maintenance cost C_m for the system. The assumptions underlying the proposed model are as follows:

- The system is treated as single unit.
- One mode of failures (defects) is analyzed and the defects are assumed to be independent.
- The defects arise as a nonhomogenous Poisson process with Rate of Occurrence of Defects (ROCOD) $\lambda(u)$ at time u.
- A failure happens after the initialization of a defect and the corresponding delay-time h is passed.
- The delay-time distribution is independent of the time origin u.
- The probability density function for the delay-time h is $f(h)$ with cumulative density function $F(h)$.
- Inspections are carried out at $\boldsymbol{t} = \{t_1, t_2, t_3, \dots, t_n\}$, hence the decision variables are $\boldsymbol{t}$ and n where $\boldsymbol{t}$ takes discrete values.
- Only one type of inspection is considered and thus the inspections are identical.
- Inspections are perfect in that all the defects present at the time of inspection will be recognized.
- The mean inspection time is d_{ins} during which the system is down.
- The mean time to rectify a defect is d_r during which the system is down.
- The mean time to repair a failure is d_f during which the system is down.
- The average inspection cost is c_{ins}.
- The average rectification cost is c_r.
- The average repairing cost is d_f.
- $E[N_d(t_{i-1}, t_i)]$ represents the expected number of defects in the interval (t_{i-1}, t_i).
- $E\left[N_f(t_{i-1}, t_i)|t_{i-1}\right]$ represnts the expected number of failures in the interval (t_{i-1}, t_i).
- $E[N_r(t_{i-1}, t_i)]$ represents the expected number of rectified defects by inspection i at time t_i.
- A_s denotes the nonparametric availability of the system during its life L.
- C_m denotes the expected maintenance cost of the system during its life L.
- B_m denotes the maintenance budget allocated for the system during its life L.
- SL_{A_s} is the satisfaction level at A_s.
- SL_{C_m} is the satisfaction level at C_m.

3. Model formulation

Consider a nonhomogeneous defect arrivals process with arrival rate given by $\lambda(u)$, then the number of defects in the infinitesimal time $\delta(u)$ is $\lambda(u)\delta(u)$. Integrating $\lambda(u)\delta(u)$ over the interval (t_{i-1}, t_i) gives the expected number of defects in that interval. Mathematically, the expected number of defects in the interval (t_{i-1}, t_i) is

$$E[N_d(t_{i-1}, t_i)] = \int_{t_{i-1}}^{t_i} \lambda(u)du \tag{1}$$

The probability that any of these defects who arose in time u and is in the interval (t_{i-1}, t_i) will develop into a failure in the interval $\big(u, u+\delta(u)\big)$ is $\lambda(u)F(u)\delta(u)$. Integrating λ(u)F(u)δ(u) over the interval (t_{i-1}, t_i) will give the expected number of failures over that interval. Mathematically, the expected number of failures in the interval $(\mathrm{t_{i-1}}, \mathrm{t_i})$ is

$$E\big[N_f(t_{i-1}, t_i)\big] = \int_{t_{i-1}}^{t_i} \lambda(u)F(t_i - u)du \tag{2}$$

Since perfect inspection is assumed, at the i^{th} inspection which is conducted at time t_i, the expected number of rectifications is simply the difference between the expected number of defects arrived in the interval (t_{i-1}, t_i) and the expected number of defects developed into failures, i.e., the expected number of failures, in the same interval. Mathematically the expected number of rectifications in the interval (t_{i-1}, t_i) is

$$E[N_r(t_i)] = E[N_d(t_{i-1}, t_i)] - E\big[N_f(t_{i-1}, t_i)\big] \tag{3}$$

The nonparametric availability of the system can be seen as the ratio between the uptime and the down time. Mathematically the nonparametric availability A_s can be given as

$$A_s = \frac{Uptime}{Uptime + Downtime} \tag{4}$$

The uptime of the system is simply the life time of the system, L, minus the downtime of the system during the system's life. This means that the uptime plus the downtime is the L, the life of the system.

The system downtime is calculated as the sum of four components, namely: the total expected rectification time corresponding to the n inspections; the total expected correction time corresponding to the n inspections, the total time for the n inspections, and finally, the expected correction time corresponding to the period between the last inspection time t_n and the life of the system,L. Mathematically, the expected availability of the system during its life L can be given as

$$A_s = \frac{L - \Big[\sum_{i=1}^{n}\big(d_r E[N_d(t_{i-1}, t_i)] + d_f E\big[N_f(t_{i-1}, t_i)\big]\big) + nd_{ins} + d_f E\big[N_f(t_n, L)\big]\Big]}{L} \tag{5}$$

The system corrective maintenance cost during its life L, is also the sum of four components namely: the total expected rectification cost corresponding to the n inspections; the total expected correction cost corresponding to the n inspection periods, the total cost for the n inspections, and finally, the expected correction cost corresponding to the period between the last inspection time t_n and the life of the system, L. Mathematically, the expected maintenance cost of the system during its life L can be given as

$$C_m = \sum_{i=1}^{n}\big(c_r E[N_d(t_{i-1}, t_i)] + c_f E\big[N_f(t_{i-1}, t_i)\big]\big) + nc_{ins} + c_f E\big[N_f(L, t_n)\big] \tag{6}$$

The two objective functions of the proposed model can be expressed as the total satisfaction level TSL about the inspection policy. The total satisfaction level can be calculated as the weighted average of the maintenance cost satisfaction level SL_{C_m} and the availability satisfaction level SL_{A_s}. To develop the two satisfaction levels, two membership functions were defined: one for A_s (Fig. 2) and one for C_m (Fig. 3).

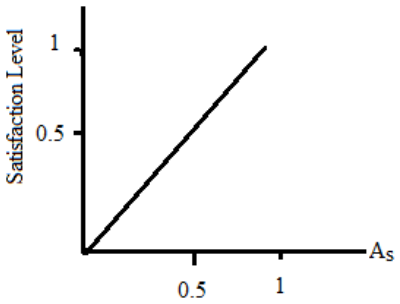

Fig. 2 Membership function for the A_s

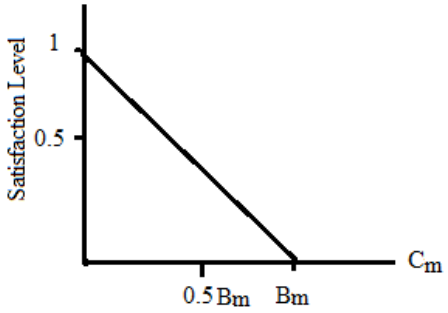

Fig. 3 Membership function for the C_m

Using those two membership functions, the SL_{A_s} and SL_{C_m} are given by

$$SL_{A_s} = A_s \tag{7}$$

$$SL_{C_m} = 1 - \frac{C_m}{B_m} \tag{8}$$

TSL is

$$TSL = wSL_{A_s} + (1 - w)SL_{C_m} \tag{9}$$

Putting all this together, gives the proposed inspection model as

$$max\ TSL$$

subject to

$$\begin{aligned} C_m &\leq B_m \\ t_i &\geq t_{i-1} + d_{ins} \end{aligned} \tag{10}$$

In this model the decision variables are the number of inspections,n, and the inspection times, $\boldsymbol{t}$.The objective function of this mode will maximize the total satisfaction level for the inspection policy, $\langle n, \boldsymbol{t} \rangle$, i.e, find $\langle n, \boldsymbol{t} \rangle$ corresponding to the highest possible availability (highest SL_{A_s}) and lowest possible maintenance cost (highest SL_{C_m}). The constraint $t_i \geq t_{i-1} + d_{ins}$ dictates that the i^{th} inspection should be at least d_{ins} apart from the previous inspection, i.e., the inspection times are discrete. The constraint $C_m \leq B_m$ puts an upper cap on the maintenance cost.

4. Genetic algorithm

Genetic algorithm (GA) is an evolutionary optimization algorithm inspired by Darwin's natural selection theory. It enhances the solutions through successive applications of exploration and exploitation operators. The genetic algorithm encodes the solutions into vectors called chromosomes where each value in the chromosome is called a gene. A fitness function is used to calculate the fitness of each chromosome. The fitness values are used to determine the parents by a step called selection that will generate the next generation of chromosomes. Usually crossover operator is used to generate the chromosomes from the parents for the next generation (called offspring) in a step called reproduction. A mutation operator is used to mutate the new chromosomes generated in the reproduction step. The mutated offspring and some of the parents usually constitute the individuals in the next generation. This evolutionary process (reproduction and selection) terminates when the preset termination criterion is satisfied.

The elements of the genetic algorithm used in this study are presented in the following subsections.

4.1 Chromosome representation

Each chromosome has $L-1$ binary genes. Binary chromosome representation is selected because of its ease of use. Each gene carries two pieces of information: the time (for example a day or a month) and whether an inspection is carried out at this time or not.

Consider the chromosome shown in Fig. 4 for a possible inspection policy.

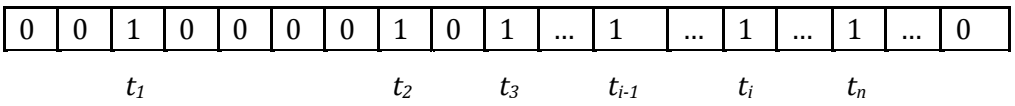

Fig. 4 Chromosome representation for one possible inspection policy (time t_i in days)

This chromosome suggests the use of n inspections. For example the first inspection is in the third day, the second inspection is in the 8th day. This means that there are no inspections between the third day and the 8th day, and the third inspection is in day number 10. Moreover, the first gene and the last gene must always equal to zero because those genes correspond to the fist day and the last day in the system life, which cannot have inspections in them. Decoding this chromosome gives the inspection policy that consists of the number of inspections and timing for the inspections, i.e. $\langle n, \boldsymbol{t} \rangle$.

It should be clear that the possible number of different inspection polices for a L-life system is 2^{L-2} policies which is typically a huge number. For example the possible number of different inspection policies for a 365-day life system is over 7.5E+109 policies.

4.2 Fitness function and selection

The fitness function used in this GA calculates the total satisfaction level. This function is:

$$TSL = w\frac{L - \left[\sum_{i=1}^{n}\left(d_r E[N_d(t_{i-1},t_i)] + d_f E\left[N_f(t_{i-1},t_i)\right]\right) + nd_{ins} + d_f E\left[N_f(t_n,L)\right]\right]}{L} + (1-w)\left[1 - \sum_{i=1}^{n}\left(c_r E[N_d(t_{i-1},t_i)] + c_f E\left[N_f(t_{i-1},t_i)\right]\right) + nc_{ins} + c_f E\left[N_f(L,t_n)\right]\right] \quad (11)$$

In this step, the fitness values for all of the chromosomes in the generation are evaluated and the chromosome with the best fitness value is chosen and selected as the best chromosome. Ties are broken arbitrary.

4.3 Mutation operator and reproduction

In the proposed GA approach, no crossover operator is used; instead, mutation operator with heavy mutation rate is used to explore the sample space. The mutation operator works on the best chromosome found in the generation to produce the offspring as follows:

- Select a random number NG between 2 and $L-1$.
- Scramble the numbers between 2 and $L-1$, which represent the genes numbers in the best chromosome found in the generation, and flip the value of the first NG numbers such that if the gene value equals 1 it will be changes to 0 and vice versa.
- Repeat steps 1 and 2, $NP-1$ times, where NP is the population size, to produce $NP-1$ offspring.
- The best chromosome along with the offspring will be selected to be the population for the next generation based on the fitness value.

5. Experimentations and results

In this section, 7 different examples will be illustrated and solved with the proposed model. The results will be compared with the results obtained by Bi-objective aperiodic model but with fixed number of inspections and with the results of single objective model with variable number of inspections. This comparative analysis is aimed to show the importance of modelling inspection models with variable number of inspections and Bi-objective rather than modelling the inspection models with fixed number of inspections and single objective. Exponential ROCOD $\lambda(t)$ given by $\alpha e^{\beta t}$, α and $\beta > 0$ and exponential delay-time $f(t)$ given by $\gamma e^{-\gamma t}$, $\gamma > 0$ are used traditionally in the literatures such as references [30-33]. For such ROCOD and $f(t)$, the expected number of defects, rectifications, and failures are given as follows:

$$E[N_d(t_{i-1}, t_i)] = \int_{t_{i-1}}^{t_i} \alpha e^{\beta t} dt = \frac{\alpha}{\beta}\left[e^{\beta t_i} - e^{\beta t_{i-1}}\right] \tag{12}$$

$$\begin{aligned} E\left[N_f(t_{i-1}, t_i)\right] &= \int_{t_{i-1}}^{t_i} \lambda(u) F(t_i - u) du = \\ &= \int_{t_{i-1}}^{t_i} \alpha e^{\beta u}\left(1 - e^{-\gamma(t_i - u)}\right) du \\ &= \int_{t_{i-1}}^{t_i} \alpha e^{\beta u} - \alpha e^{\beta u} e^{-\gamma(t_i - u)} du \\ &= \frac{\alpha}{\beta}\left[e^{\beta t_i} - e^{\beta t_{i-1}}\right] - \int_{t_{i-1}}^{t_i} \alpha e^{\beta u} e^{-\gamma t_i} e^{\gamma u} du \\ &= \frac{\alpha}{\beta}\left[e^{\beta t_i} - e^{\beta t_{i-1}}\right] - \alpha e^{-\gamma t_i}\left[\frac{e^{(\beta+\gamma)t_i} - e^{(\beta+\gamma)t_{i-1}}}{(\beta+\gamma)}\right] \end{aligned} \tag{13}$$

$$\begin{aligned} E[N_s(t_i)] &= E[N_d(t_{i-1}, t_i)] - E\left[N_f(t_{i-1}, t_i)\right] \\ &= \alpha e^{-\gamma t_i}\left[\frac{e^{(\beta+\gamma)t_i} - e^{(\beta+\gamma)t_{i-1}}}{(\beta+\gamma)}\right] \end{aligned} \tag{14}$$

Table 1 shows the parameters used in the 7 examples.

Table 1 Parameters used in Examples 1-7

Example #	$\lambda(u)$	$f(h)$	w	*Life* (year)	B_m
1	$\lambda(u) = 0.025e^{(1.8e-2)u}$	$f(h) = 0.0625e^{-0.0625h}$	$w = 0.5$	20	\$5.0E6
2	$\lambda(u) = 0.025$	$f(h) = 0.0625e^{-0.0625h}$	$w = 0.5$	20	\$5.0E6
3	$\lambda(u) = 0.025e^{(1.8e-2)u}$	$f(h) = 0.1e^{-0.1h}$	$w = 0.5$	20	\$5.0E6
4	$\lambda(u) = 0.025$	$f(h) = 0.0625e^{-0.0625h}$	$w = 0.5$	10	\$5.0E6
5	$\lambda(u) = 0.025e^{(1.8e-2)u}$	$f(h) = 0.0625e^{-0.0625h}$	$w = 0{,}0$	20	\$5.0E6
6	$\lambda(u) = 0.025e^{(1.8e-2)u}$	$f(h) = 0.0625e^{-0.0625h}$	$w = 1.0$	20	\$5.0E6
7	$\lambda(u) = 0.025e^{(1.8e-2)u}$	$f(h) = 0.0625e^{-0.0625h}$	$w = 0.5$	20	\$2.5E6

The results for the first example will be discussed in details to show how the model works. The results for the rest of the examples will be listed in Table 2 for comparison.

Fig. 5 shows the evolution of the *TSL* values throughout the generations using the proposed model. The figure shows that the algorithm converged to a value of 0.9400. This convergence happened after 120 generations and stayed for the rest of the generations through the generation number 150. The processing time was 0.57 seconds with population size of 10 chromosomes and 150 generations.

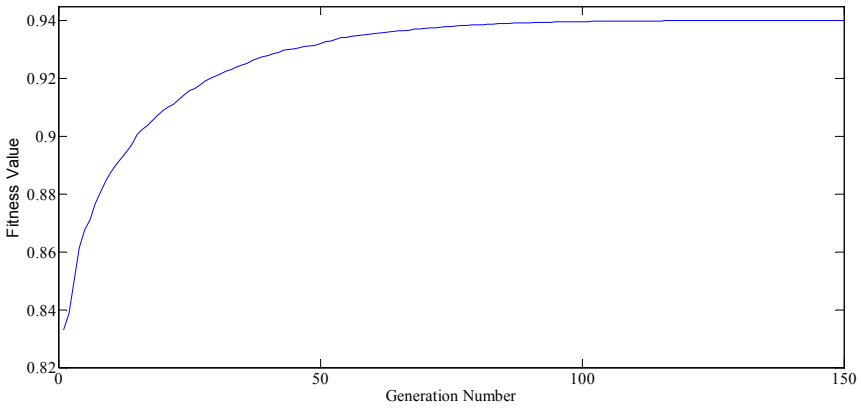

Fig. 5 The evolution of the TSL value throughout the generations using the proposed model

The best inspection policy produced by the proposed model for Example 1 consisted of 123 inspections at the following timing (in days):

t = { 156	350	537	742	893	1095	1288	1437	1547	1703
1887	1960	2080	2165	2266	2341	2486	2530	2613	2678
2747	2839	2917	3016	3097	3170	3291	3365	3435	3509
3559	3627	3712	3775	3859	3924	3960	4025	4061	4140
4195	4261	4295	4355	4418	4460	4509	4571	4606	4682
4748	4820	4880	4921	4971	5001	5043	5085	5125	5170
5193	5254	5273	5332	5373	5417	5465	5524	5563	5613
5651	5696	5745	5769	5813	5834	5869	5891	5927	5952
5978	6011	6035	6064	6092	6103	6149	6180	6209	6236
6276	6317	6342	6364	6396	6426	6445	6467	6497	6514
6530	6571	6608	6625	6654	6681	6694	6735	6762	6800
6832	6846	6886	6911	6936	6982	6999	7020	7048	7075
7087	7112	7127 }							

Fig. 6 shows a histogram for the number of inspections in each of the twenty years. The histogram shows that the number of inspections increased with the life of the system. For example in the first 1200 days of the system life, the model suggested 6 inspections while in the last 1200 days of the system life the model suggested to have 51 inspections. This increase in the number of inspections coincides with the fact that the system is aging. As the system ages, the number of defects increases and the delay-time of the defects decreases which force the model to assign more inspections toward the end of the system life.

Table 2 shows the results of the 7 examples for the proposed model along with the results for the aperiodic model with fixed number of inspections where the number of inspections was 30 inspections. The table shows that the proposed model is better, in all of the attributes, than the aperiodic model with fixed number of periods except for Example 2 where the number of inspections is equal. Basically, in Example 2, the two models are equivalent. Example 4 shows that the proposed model chose 12 inspections with lower maintenance cost and higher TSL than the aperiodic model with the fixed number of inspections 30. Moreover, the rest of the examples (except Example 2) show that even the number of inspections is higher in the proposed model than the number of inspections in the aperiodic model with fixed number of inspections, both the maintenance cost and the availability is better in the proposed model. These results show that treating the number of inspections as a variable, that need to be optimized in the inspection model, is better than treating it as a constant in the model as this will enhance the maintenance cost and the availability of the system simultaneously.

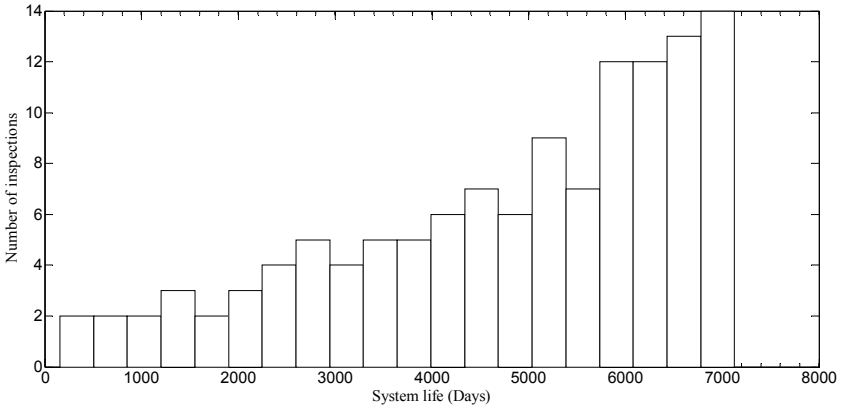

Fig. 6 A histogram for the number of inspections in the twenty years of life

Comparing the results of Examples 1, 5, and 6 for the proposed model, one can see that the number of inspections chosen by the model is significantly different. In Example 5, where the objective of the model was to maximize the availability of the system alone, the number of inspections was significantly higher than the number of inspections in Example 6 where the objective was to minimize the maintenance cost only. Moreover the *TSL* for example 5 was lower than the *TSL* in Example 6. The average of *TSL*s of Example 5 and Example 6 is almost the same as the *TSL* in Example 1 where the two objectives were considered. Moreover the average number of inspections for the two examples was almost the same as the number of inspections in Example 1 but the average cost of the two examples was higher than the average cost in Example 1.

To better understand what happened in Examples 1, 5, and 6 and why it happened. Consider Fig. 7 which shows the relation between the A_s and C_m. The figure shows that there may be more than one value of A_s for the same value of C_m. This result can be understood on the light of that different inspection policies may have the same cost but different effect on the availability of the system. For this reason, it is not wise to use maintenance cost as the only objective in the inspection models. On the same taken, using availability as the only objective in the inspection model may result in choosing an expensive inspection policy when we can have the same availability using other inspection policies that have lower costs. This result emphasizes the importance of treating the inspection-policy optimization problem as a multi-objective optimization problem rather than a single objective problem.

By comparing the results of Example 1 and the results of Example 3, it is easy to see that the increase in the delay-time rate caused an increase in the number of inspections (to increase the availability of the system) but this increase also increased the maintenance cost, the matter that caused a decrease in the *TSL*. This result is expected because the increase in the delay-time rate means that the defects will turn into failures faster and thus more inspections are needed to prevent the defects from turning into failures and hence reducing the availability of the system.

Table 2 The results of the 7 examples for the proposed model along with the results for the aperiodic model with 30 inspections

	Example 1	Example 2	Example 3	Example 4	Example 5	Example 6	Example 7
	Results for the proposed model						
A_s, SL_{A_s}	0.9305	0.9903	0.9231	0.9908	N/A	0.9313	0.9295
C_m	2.53e+05	4.58e+04	2.99e+05	2.298e+04	2.52e+05	2.67e+05	2.54e+05
SL_{C_m}	0.9495	0.9908	0.9401	0.9954	0.9496	N/A	0.8985
TSL	0.9400	0.9906	0.9316	0.9931	0.9496	0.9313	0.9140
n	120	30	134	12	138	91	127
	Results for the aperiodic model with fixed number of inspections (30 inspections)						
A_s, SL_{A_s}	0.9096	0.9898	0.8882	0.9875	N/A	0.9085	0.9086
C_m	4.75e+05	4.87e+04	6.48e+05	2.57e+04	4. 80e+05	4.89e+05	4.84e+05
SL_{C_m}	0.9050	0.9903	0.8703	0.9949	0.9040	N/A	0.8064
TSL	0.9073	0.9900	0.8792	0.9912	0.9040	0.9085	0.8575
n	30	30	30	30	30	30	30

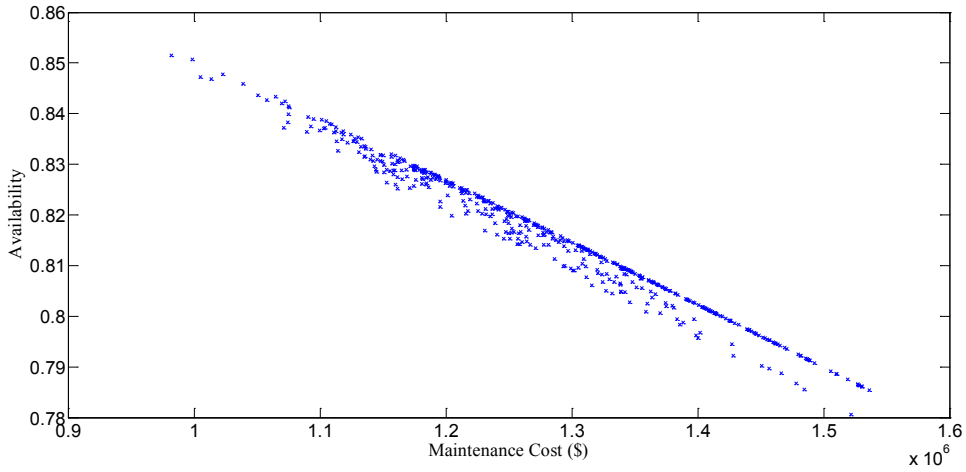

Fig. 7 The relation between the A_s and C_m

The proposed model responded to the increase in the delay-time rate by increasing the number of inspections but this also increased the maintenance cost as well. The model chose the optimal inspections number that compromised between the availability of the system and the maintenance cost of the system

6. Conclusion

In this paper an aperiodic inspection model is proposed and solved using mutation-based Genetic algorithm. The proposed inspection model is based on delay-time concept and nonhomogeneous Poisson process of defect arrivals rather than renewal theory and periodic inspection modelling that are used classically. The proposed model also optimizes the number of inspections and the timing of inspections simultaneously rather than optimizing either the number of inspections or the timing of inspections as in the case of the majority of the available inspection models. Moreover, the proposed model uses two objectives, namely: system availability and maintenance cost, to optimize the inspection policy whereas the available inspection models use only one objective.

The results showed that the proposed model is better (in all of the attributes) than the aperiodic model that uses fixed number of inspections. Moreover, the results showed that using two objectives (system availability and maintenance cost) in the inspection models rather than one objective, can improve the quality of the inspection policy in terms of system availability and maintenance cost.

The proposed model is a general model that can be implemented with different ROCOD and different delay-time distributions. Also this model can be extended easily to cover complex systems and imperfect inspection cases.

Acknowledgement

The author is grateful to the Applied Science Private University, Amman, Jordan, for the full financial support granted to this research (Grant No. DRGS-2015).

References

[1] Dhillon, B.S. (2002). *Engineering maintenance: A modern approach*, CRC press, Boca Raton, USA, doi: 10.1201/9781420031843.
[2] Moubray J. (1997). *Reliability-centered Maintenance II*, (2nd edition), Industrial Press, New York, USA.
[3] Barlow, E.E., Proschan, F., Hunter, L.C. (1965). *Mathematical theory of reliability*, Wiley, New York-London-Sydney, doi: 10.1002/bimj.19660080409.
[4] Wild, R. (1985). *Essentials of production and operations management*, Holt, Rinehart & Winston, London, UK.

[5] Dhillon, B.S. (1988). *Mechanical reliability: Theory, models, and applications*, American Institute of Aeronautics and Astronautics, Washington, D.C., USA.
[6] Jardine, A.K.S. (1973). *Maintenance, replacement and reliability*, Pitman Publishing, London, UK.
[7] Dhillon, B.S. (1983). *Systems reliability, maintainability, and management*, Petrocelli Books, New York, USA.
[8] Christer, A.H. (1976). Innovative decision making, In: *Proceedings of the NATO Conference on the Role and Effectiveness of Theories of Decision in Practice*, Hodder & Stoughton, 368-377.
[9] Christer, A.H., Waller, W.M. (1984). Delay time models of industrial inspection maintenance problems, *The Journal of the Operational Research Society*, Vol. 35, 401-406, doi: 10.1057/jors.1984.80.
[10] Christer, A.H. (1987). Delay-time model of reliability of equipment subject to inspection monitoring, *The Journal of the Operational research Society*, Vol. 38, No. 4, 329-334, doi: 10.2307/2582056.
[11] Baker, R.D., Christer, A.H. (1994). Review of delay-time OR modelling of engineering aspects of maintenance, *European Journal of Operational Research*, Vol. 73, No. 3, 407-422, doi: 10.1016/0377-2217(94)90234-8.
[12] Christer, A.H. (1999). Developments in delay time analysis for modelling plant maintenance, *Journal of Operational Research Society*, Vol. 50, 1120-1137, doi: 10.1057/palgrave.jors.2600837.
[13] Christer, A.H., Wang, W., Baker, R.D., Sharp, J. (1995). Modelling maintenance practice of production plant using the delay-time concept, *IMA Journal of Management Mathematics,* Vol. 6, No. 1, 67-84, doi: 10.1093/imaman/6.1.67.
[14] Wang, W., Majid, H.B.A. (2000). Reliability data analysis and modelling of offshore oil platform plant, *Journal of Quality in Maintenance Engineering*, Vol. 6, No. 4, 287-295, doi: 10.1108/13552510010346824.
[15] Dawotola, A.W., Trafalis, T.B., Mustaffa, Z., van Gelder, P.H.A.J.M., Vrijling, J.K. (2013). Risk-based maintenance of a cross-country petroleum pipeline system, *Journal of Pipeline Systems Engineering and Practice*, Vol. 4, No. 3, 141-148, doi: 10.1061/(ASCE)PS.1949-1204.0000121.
[16] Abdel-Hameed, M. (1995). Correction to: 'Inspection and maintenance policies of devices subject to deterioration', *Advances in Applied Probability*, Vol. 27, No. 2, p. 584.
[17] Okumura, S., Jardine, A.K.S., Yamashina, H. (1996). An inspection policy for a deteriorating single-unit system characterized by a delay-time model, *International Journal of Production Research*, Vol. 34, No. 9, 2441-2460, doi: 10.1080/00207549608905037.
[18] Okumura, (1997). An inspection policy for deteriorating processes using delay-time concept, *International Transactions in Operational Research*, Vol. 4, No. 5-6, 365-375.
[19] Wang, W. (2008). Delay time modelling, In: Kobbacy, K.A.H., Murthy, D.N.P. (eds.), *Complex system maintenance handbook*, Springer Series in Reliability Engineering, Springer, London, 345-370, doi: 10.1007/978-1-84800-011-7_14.
[20] Wang, W. (2009). An inspection model for a process with two types of inspections and repairs, *Reliability Engineering & System Safety*, Vol. 94, No. 2, 526-533, doi. 10.1016/j.ress.2008.06.010.
[21] Wang, W., Banjevic, D., Pecht, M. (2010). A multi-component and multi-failure mode inspection model based on the delay time concept, *Reliability Engineering and System Safety*, Vol. 95, No. 8, 912-920, doi: 10.1016/j.ress.2010.04.004.
[22] Taghipour, S., Banjevic, D., Jardine, A.K.S. (2010). Periodic inspection optimization model for a complex repairable system, *Reliability Engineering & System Safety,* Vol. 95, No. 9, 944-952, doi: 10.1016/j.ress.2010.04.003.
[23] Taghipour, S., Banjevic, D. (2011*). Periodic inspection optimization models for a repairable system subject to hidden failures*, *IEEE Transactions on Reliability*, Vol. 60, No. 1, 275-285, doi: 10.1109/TR.2010.2103596.
[24] Taghipourab, S., Banjevic, D. (2012). Optimum inspection interval for a system under periodic and opportunistic inspections, *IIE Transactions*, Vol. 44, No. 11, 932-948, doi: 10.1080/0740817X.2011.618176.
[25] Kakade, V., Valenzuela, J.F., Smith, J.S. (2004). An optimization model for selective inspection in serial manufacturing systems, *International Journal of Production Research*, Vol. 42, No. 18, 3891-3909, doi: 10.1080/00207540410001704014.
[26] Golmakani, H.R., Moakedi, H. (2012). Periodic inspection optimization model for a multi-component repairable system with failure interaction, *The International Journal of Advanced Manufacturing Technology,* Vol. 61, No. 1, 295-302, doi: 10.1007/s00170-011-3693-8.
[27] Wang, W., Christer, A.H. (2003). Solution algorithms for a nonhomogeneous multi-component inspection model, *Computers & Operations Research,* Vol. 30, No. 1, 19-34, doi: 10.1016/S0305-0548(01)00074-0.
[28] Chan, G.K., Asgarpoor, S. (2006). Optimum maintenance policy with Markov processes, *Electric Power Systems Research,* Vol. 76, No. 6-7, 452-456, doi: 10.1016/j.epsr.2005.09.010.
[29] Von Alven, W.H. (1964). *Reliability Engineering*, Prentice-Hall, Englewood Cliffs, New Jersey, USA.
[30] Nazemi, E., Shahanaghi, K. (2015). Developing an inspection optimization model based on the delay-time concept, *Journal of Industrial Engineering*, Vol. 2015, Article ID 843137, 7 pages, doi: 10.1155/2015/843137.
[31] Ben-Daya, M., Duffuaa, S.O., Raouf, A., Knezevic, J., Ait-Kadi, D. (2009). *Handbook of maintenance management and engineering*, Springer, London, UK, doi: 10.1007/978-1-84882-472-0.
[32] Christer, A.H., Wang, W. (1995). A delay-time-based maintenance model of a multi-component system, *IMA Journal of Management Mathematics*, Vol. 6, No. 2, 205-222, doi: 10.1093/imaman/6.2.205.
[33] Wang, W., Majid, H.B.A. (2000). Reliability data analysis and modelling of offshore oil platform plant, *Journal of Quality in Maintenance Engineering*, Vol. 6, No. 4, 287-295, doi: 10.1108/13552510010346824.

APEM journal
Advances in Production Engineering & Management
Volume 11 | Number 1 | March 2016 | pp 49–58
http://dx.doi.org/10.14743/apem2016.1.209
ISSN 1854-6250
Journal home: apem-journal.org
Original scientific paper

Integration of SWOT and ANP for effective strategic planning in the cosmetic industry

Al-Refaie, A.[a,*], **Sy, E.**[b], **Rawabdeh, I.**[a], **Alaween, W.**[c]

[a]Department of Industrial Engineering, The University of Jordan, Amman, Jordan
[b]Ateneo de Manila University, Metro Manila, Philippines
[c]Department of Industrial Engineering, The University of Jordan, Jordan

ABSTRACT

Typically, the decision making processes in cosmetics firms are greatly affected by internal and external factors, which as a result affect firms' success. In this research, the Strengths, Weakness, Opportunities, and Threat (SWOT) analysis was used to identify those factors that affect a cosmetics firm's success and consequently lists the feasible strategy alternatives. The analytic network process (ANP) was adopted for calculating the relative importance for each SWOT factors and sub-factors, while taking into consideration the dependency among SWOT factors, as well as among sub-factors. Utilizing the importance values in the super-matrix, the most preferred strategy in a cosmetic industry is identified, which is to open-up new markets on European market. In conclusion, the SWOT and ANP integration may provide great assistance to strategic planners in determining the best strategy alternative that fulfils the firm's desired objectives.

ARTICLE INFO

Keywords:
Cosmetic industry
Analytic network process (ANP)
SWOT analysis
Strategic planning

**Corresponding author:*
abbas.alrefai@ju.edu.jo
(Al-Refaie, A.)

Article history:
Received 9 January 2015
Revised 10 September 2015
Accepted 5 January 2016

1. Introduction

Strategic management is a collection of actions and decisions taken in order to achieve organization's goals and objectives. Decision making process is greatly affected by internal and external factors. Systematic identification and analysis of the effects of such factors on organization success has received significant research attention [1-8]. The Strengths-Weakness-Opportunities-Threats (SWOT) technique is frequently used to analyse internal and external factors, assess the feasible alternative strategies, and then to determine the best one that helps an organization in achieving its desired objectives and goals. Nevertheless, the SWOT analysis as a qualitative tool does not numerically evaluate the effect of each factor on selected strategies [9-11].

The analytic hierarchy process (AHP) method [12-14] is a powerful technique which assists analysts in selecting the best decision among multiple decisions by structuring the decision problem in a hierarchically structure at different levels. In AHP, each level consists of finite number of decision elements, where the upper level of the hierarchy represents the overall goal, while the lower level represents all possible alternatives and the intermediate levels shape the decision criteria and sub-criteria [15-17]. The AHP allows the assessment of factors, which considered as criteria and the alternative strategies by giving them relative weights. Next, pairwise comparisons are carried out between all factors by assigning weights between one (equal importance) to nine (absolutely more important), whereas reciprocal values are assigned to the inverse comparison. Then, for each factor a pairwise comparison is performed between strate-

gies using a scale between one and nine. Finally, the integration between relative weight of factors and strategies are utilized to identify the overall weight of each strategy [18].

The AHP method assumes that there are unidirectional relationships between elements of different decision levels along the hierarchy and uncorrelated elements within each cluster as well as between clusters [19]. As a result, AHP is not appropriate for models that deal with interdependent relationships in AHP. The analytic network process (ANP) is introduced to solve this problem [20-23]. The comparison between AHP and ANP tools is depicted in Fig. 1.

ANP method is an improved version of AHP, which provides more accurate results in complicated problems. In the ANP method and after clearly defined factors, the pairwise comparisons are performed as done by the AHP method; in addition, the dependencies among factors should be examined in pairwise manner. As a final step, the weighted score for each strategy is determined and then used to identify the best strategy.

This research integrates SWOT analysis and ANP technique to determine the best strategy that results in improving the performance of a Jordanian cosmetics sector. The remaining of this research is organized as follows. Section two presents SWOT analysis. Section three introduces the ANP technique. Implementation of the integrated approach is performed in section four. Finally, conclusions are summarized in section five.

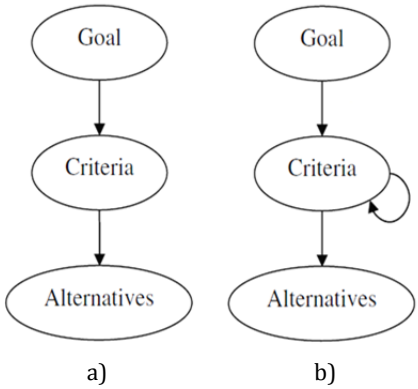

Fig. 1 Hierarchy and network structure: a) AHP, and b) ANP

2. SWOT analysis

The SWOT matrix treats an organization's strengths and weaknesses as internal factors, whereas the threats and opportunities, as external factors. These factors are utilized to identify and formulate strategies by matching the key internal and external factors. The matching between internal and external factors, what is called TOWS, is the most difficult and challenging part in SWOT analysis. TOWS matrix is utilized to develop four types of strategies. These strategies are shown in Fig. 2.

Internal / External	Strengths (S) 1,..., s	Weakness (W) 1,..., w
Opportunities (O) 1,..., o	SO strategies	WO Strategies
Threats (T) 1,..., t	ST Strategies	WT Strategies

Fig. 2 SWOT matrix

The Strengths-opportunities (SO) strategies utilize internal strengths of an organization to take advantage of external opportunities, weaknesses-opportunities (WO) strategies improve internal weaknesses by taking advantage of external opportunities, strengths-threats (ST) strategies use strengths of organization to avoid or minimize the effect of external threats, and weaknesses-threats (WT) strategies are defensive tactics aimed at reducing internal weaknesses and avoiding external threats.

3. ANP analysis

The ANP is used to determine the dependencies and interrelations among factors using four main steps:

Step 1: Clearly state and define the decision model as a network structure shown in Fig. 1.b. Once the goal or objective of the decision model is stated, it would further be decomposed into criteria, sub-criteria, and so on until alternatives level is reached.

Step 2: Establish pairwise comparison matrices and priority vectors. In each factor pairs of decision elements are compared with respect to their relative importance. Then, the factors themselves are compared pairwise with respect to their contribution to the main goal. Furthermore, the interdependencies among elements of each factor are examined pairwise. The pairwise comparison is done by assigning relative importance values (a_{ij}) as shown in Table 1. However, the reciprocal ($a_{ji} = 1/a_{ij}$) of this value is assigned to the inverse comparison.

Table 1 Preference scale as represented by Saaty (1996)

Weight	Definition	Description
1	Equal importance	Factor *i* and *j* are of equally important
3	Moderate importance	Factor *i* is weakly more important than *j*
5	Strong importance	Factor *i* strongly more important than *j*
7	Very strong importance	Factor *i* is very strongly more important than *j*
9	Absolute importance	Factor *i* is absolutely more important than *j*
2, 4, 6, 8	Intermediate values	Represent compromise between the priorities

The pairwise comparison matrix *A*, is represented as follows:

$$A = \begin{bmatrix} 1 & a_{12} & \cdots & a_{1(n-1)} & a_{1n} \\ 1/a_{21} & 1 & & a_{2(n-1)} & a_{2n} \\ \vdots & & \ddots & & \\ 1/a_{1(n-1)} & \cdots & & 1 & a_{(n-1)n} \\ 1/a_{1n} & 1/a_{2n} & \cdots & 1/a_{(n-1)n} & 1 \end{bmatrix} \quad (1)$$

An estimate of the relative importance of the compared factors is determined using Eq. 2.

$$Aw = \lambda_{max} w \quad (2)$$

where *w* is the desired to estimate eigenvector and λ_{max} is the largest Eigen value of *A*.

Step 3: Determine the relative importance of all components with dependency effects and then create the super-matrix. The super-matrix adjusts the relative weights in individual matrices to form a new ''overall'' matrix with the eigenvectors of the adjusted relative weights. That is, the eigenvectors obtained in step 2 are grouped and placed in the appropriate positions in the super matrix in a hierarchy manner as goal, factors, sub-factors and alternatives as follows:

$$W = \begin{bmatrix} 0 & 0 & 0 & 0 \\ W_{21} & 0 & 0 & 0 \\ 0 & W_{32} & 0 & 0 \\ 0 & 0 & W_{43} & I \end{bmatrix} \tag{3}$$

where each entry in W is a matrix. The W_{21} is a matrix which represents the impact of the goal on the factors, W_{32} is a matrix that represents the impact of the factors on each of the sub-factor, W_{43} represents the impact of the sub-factors on each of the alternatives, and I is the identity matrix. If there is any dependency among the factors of W, then W_{22} would be non-zero matrix, and so on. All interdependences can be represented in the same manner.

Step 4: Calculate the weights of alternatives from the normalized super-matrix.

Step 5: Select the alternative that corresponds to the largest priority as the most preferred alternative.

4. Cosmetics industry

The integration of the SWOT and ANP analysis was implemented in cosmetics industry in Jordan and is described as follows. The key internal factors (strengths and weakness) and the most external factors (opportunities and threats) are listed in Table 2. The corresponding ANP structure for cosmetics is shown in Fig. 2. The pairwise comparisons between these factors are presented in Table 3. Then, the matrix W_1, represents the Eigenvector that represents for the SWOT factors is expressed as:

$$W_1 = \begin{bmatrix} 0.547 \\ 0.135 \\ 0.272 \\ 0.047 \end{bmatrix} \tag{4}$$

The dependency among the SWOT factors is analysed by identifying the impact of each factor on the others in pairwise comparison as shown in Table 4. Consequently, the dependency matrix W_2, of the SWOT factors is written as:

$$W_2 = \begin{bmatrix} 1.000 & 0.649 & 0.768 & 0.768 \\ 0.587 & 1.000 & 0.153 & 0.153 \\ 0.324 & 0.295 & 1.000 & 0.079 \\ 0.089 & 0.057 & 0.079 & 1.000 \end{bmatrix} \tag{5}$$

Utilizing Eqs. 4 and 5, the matrix, $W_{factors}$, contains the relative importance of the SWOT factors is determined by multiplying the relative importance matrix W_1, under the assumption of independency by the relative importance matrix W_2, considering the dependency among factors. That is:

$$W_{factors} = W_1 \times W_2 = \begin{bmatrix} 1.000 & 0.649 & 0.768 & 0.768 \\ 0.587 & 1.000 & 0.153 & 0.153 \\ 0.324 & 0.295 & 1.000 & 0.079 \\ 0.089 & 0.057 & 0.079 & 1.000 \end{bmatrix} \times \begin{bmatrix} 0.547 \\ 0.135 \\ 0.272 \\ 0.047 \end{bmatrix} = \begin{bmatrix} 0.880 \\ 0.505 \\ 0.493 \\ 0.125 \end{bmatrix} \tag{6}$$

In Eq. 6, it is noted that the largest importance weight (= 0.880) corresponds to the strengths factor, whereas the smallest weight (0.125) associated with the threats. There is significant difference between the relative weight for each factor with and without considering the dependencies.

Table 2 TOWS matrix for the cosmetic company

		Internal Factors		
		Strength	Weakness	
		1. Human expertise and financial resources. 2. Strong and well-known brand name. 3. Depending on neutral material.	1. Loss of trust from different supply chain parties. 2. Falling in utilizing e-commerce capabilities. 3. Price is expensive. 4. Innovation skills and strong research and development. 5. Better products quality relative to rivals.	
External Factors	**Opportunities**	1. Growing trend in cosmetics industry with 10 % annually. 2. Internet technology is used dramatically to cut cost. 3. Availability of Dead sea mud and salts.	Developing new products consist of neutral material (especially eye makeup).	Utilizing e-trade to marketing their products.
	Threats	1. Increasing import of European products. 2. Increasing cosmetic surgery. 3. Rising taxes of cosmetic products. 4. Competitors are rapidly imitate new product.	Open new market in the European countries by exporting.	Provide different price level to gain multi-segments.

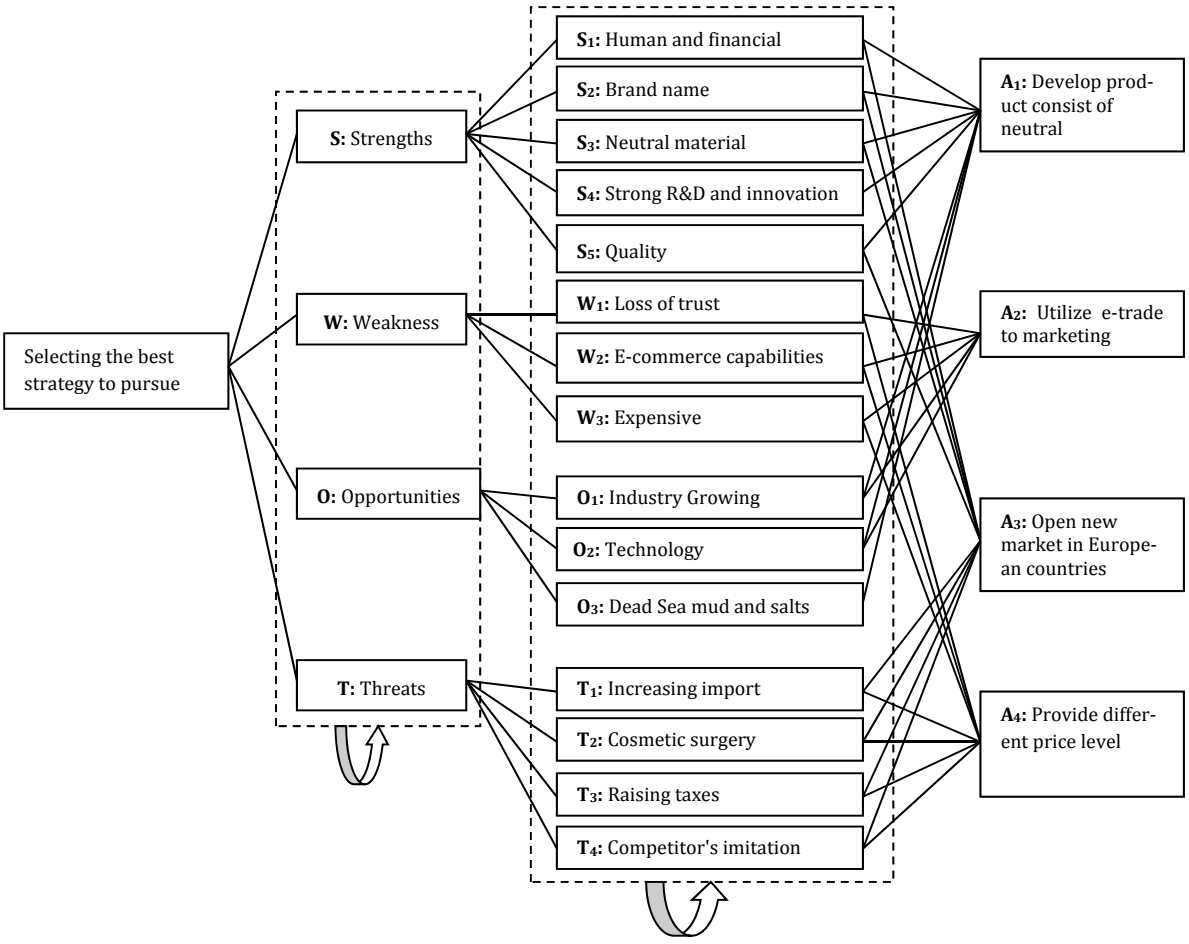

Fig. 3 The ANP model for cosmetics case

Table 3 Pairwise comparison of SWOT factors by assuming independency

SWOT factors	Strengths	Weakness	Opportunities	Threats	4th root of product of values	Eigenvector
Strengths	1	5	3	7	3.200	0.547
Weakness	0.20	1	0.50	4	0.795	0.135
Opportunities	0.33	2	1	9	1.561	0.272
Threats	0.14	0.25	0.11	1	0.269	0.047
				Total	5.825	

Table 4 Dependence matrix of SWOT factors

With respect to	Factors	Weakness	Opportunities	Threats	Importance
Strengths	Weakness	1	2	6	0.587
	Opportunities	0.5	1	4	0.324
	Threats	0.17	0.25	1	0.089
Weakness	Strengths	1	3	9	0.649
	Opportunities	0.33	1	7	0.295
	Threats	0.11	0.14	1	0.057
Opportunities	Strengths	1	9	7	0.768
	Weakness	0.11	1	3	0.153
	Threats	0.14	0.33	1	0.079
Threats	Strengths	1	7	3	0.768
	Weakness	0.14	1	0.2	0.153
	Opportunities	0.33	5	1	0.079

Table 5 Pairwise comparison for SWOT sub-factors

Sub factors	S_1	S_2	S_3	S_4	S_5	W_1	W_2	W_3	O_1	O_2	O_3	T_1	T_2	T_3	T_4	Importance
S_1	1	0.50	4	1	3											0.277
S_2	2	1	0.50	4	2											0.243
S_3	0.25	2	1	9	0.50											0.262
S_4	1.00	0.25	0.11	1	3											0.135
S_5	0.33	0.50	0.33	1	1											0.083
W_1						1	2	0.33								0.230
W_2						0.50	1	0.2								0.122
W_3						3.00	5	1								0.648
O_1									1	8	1					0.533
O_2									0.13	1	0.50					0.117
O_3									1.00	2	1					0.351
T_1												1	3	5	7	0.575
T_2												0.33	1	0.50	2	0.142
T_3												0.20	2	1	4	0.215
T_4												0.14	0.50	0.25	1	0.068

Next, the pairwise comparison among the sub-factors with their corresponding importance values for each SWOT factor is shown in Table 5.

The weighted vectors for the sub-factors, $W_{sf(S)}$, $W_{sf(W)}$, $W_{sf(O)}$, and $W_{sf(T)}$, for the SWOT factors strengths, weaknesses, opportunities, and threats, respectively, are expressed as:

$$W_{sf(S)} = \begin{bmatrix} 0.277 \\ 0.243 \\ 0.262 \\ 0.135 \\ 0.083 \end{bmatrix} \quad W_{sf(W)} = \begin{bmatrix} 0.230 \\ 0.122 \\ 0.648 \end{bmatrix} \quad W_{sf(O)} = \begin{bmatrix} 0.533 \\ 0.117 \\ 0.351 \end{bmatrix} \quad W_{sf(T)} = \begin{bmatrix} 0.575 \\ 0.142 \\ 0.215 \\ 0.068 \end{bmatrix} \tag{7}$$

The weights for the sub-factors W_{sf} are calculated by multiplying the weight of the each SWOT factor in $W_{factors}$ by the corresponding weights of sub-factors. These weights are represented by the following vector:

$$W_{sf} = \begin{bmatrix} 0.277 \times 0.88 = 0.244 \\ 0.243 \times 0.88 = 0.214 \\ 0.262 \times 0.88 = 0.231 \\ 0.135 \times 0.88 = 0.119 \\ 0.083 \times 0.88 = 0.073 \\ 0.230 \times 0.505 = 0.116 \\ 0.122 \times 0.505 = 0.062 \\ 0.648 \times 0.505 = 0.327 \\ 0.533 \times 0.493 = 0.263 \\ 0.117 \times 0.493 = 0.058 \\ 0.351 \times 0.493 = 0.173 \\ 0.575 \times 0.125 = 0.072 \\ 0.142 \times 0.125 = 0.018 \\ 0.215 \times 0.125 = 0.027 \\ 0.068 \times 0.125 = 0.009 \end{bmatrix} \tag{8}$$

To determine the overall weights for sub-factors, the relative weights among SWOT sub-factors are determined by using pairwise comparison matrix. Table 6 shows the pairwise comparisons for the sub-factors with respect to human and financial resources (S_1). The summary of importance values with respect to each of the other sub-factors are displayed in Table 7.

Table 6 Pairwise comparison for sub factors with respect to human and financial resources (S_1)

Sub factors	S_2	S_3	S_4	S_5	W_1	W_2	W_3	O_1	O_2	O_3	T_1	T_2	T_3	T_4	Importance
S_2	1	5	1	6	6	7	1	5	9	6	4	2	3	4	0.167
S_3	0.20	1	3	6	1	5	7	2	4	3	4	9	1	2	0.120
S_4	1.00	0.33	1	5	7	9	2	1	3	3	1	4	3	1	0.115
S_5	0.17	0.17	0.20	1	2	3	7	2	5	2	2	3	4	2	0.069
W_1	0.17	1.00	0.14	0.50	1	5	9	5	7	6	5	2	5	6	0.103
W_2	0.14	0.20	0.11	0.33	0.20	1	4	6	7	9	4	1	7	7	0.082
W_3	1.00	0.14	0.50	0.14	0.11	0.25	1	9	1	2	4	9	6	8	0.083
O_1	0.20	0.50	1.00	0.50	0.20	0.17	0.11	1	3	4	6	8	3	9	0.066
O_2	0.11	0.25	0.33	0.20	0.14	0.14	1.00	0.33	1	7	9	3	2	3	0.048
O_3	0.17	0.33	0.33	0.50	0.17	0.11	0.50	0.25	0.14	1	1	2	4	6	0.029
T_1	0.25	0.25	1.00	0.50	0.20	0.25	0.25	0.17	0.11	1.00	1	1	7	8	0.039
T_2	0.50	0.11	0.25	0.33	0.50	1.00	0.11	0.13	0.33	0.50	1.00	1	4	9	0.034
T_3	0.33	1.00	0.33	0.25	0.20	0.14	0.17	0.33	0.50	0.25	0.14	0.25	1	5	0.025
T_4	0.25	0.50	1.00	0.50	0.17	0.14	0.13	0.11	0.33	0.17	0.13	0.11	0.20	1	0.019

Table 7 Pairwise comparisons between sub-factors

Sub factors	S_1	S_2	S_3	S_4	S_5	W_1	W_2	W_3	O_1	O_2	O_3	T_1	T_2	T_3	T_4
S_1	-	0.192	0.183	0.186	0.187	0.149	0.126	0.125	0.133	0.135	0.154	0.166	0.157	0.146	0.140
S_2	0.167	-	0.127	0.137	0.124	0.124	0.138	0.121	0.122	0.113	0.102	0.127	0.155	0.123	0.122
S_3	0.120	0.119	-	0.089	0.089	0.094	0.102	0.102	0.097	0.097	0.093	0.098	0.107	0.091	0.084
S_4	0.115	0.104	0.095	-	0.072	0.078	0.092	0.101	0.108	0.110	0.100	0.096	0.089	0.107	0.121
S_5	0.069	0.068	0.068	0.067	-	0.096	0.099	0.096	0.100	0.102	0.093	0.081	0.078	0.086	0.084
W_1	0.103	0.108	0.110	0.111	0.091	-	0.092	0.091	0.090	0.083	0.089	0.088	0.086	0.088	0.090
W_2	0.082	0.080	0.077	0.085	0.096	0.103	-	0.080	0.081	0.085	0.084	0.066	0.065	0.072	0.076
W_3	0.083	0.082	0.091	0.081	0.092	0.092	0.092	-	0.069	0.068	0.072	0.062	0.063	0.066	0.066
O_1	0.066	0.060	0.063	0.059	0.068	0.072	0.068	0.070	-	0.042	0.051	0.053	0.047	0.047	0.047
O_2	0.048	0.037	0.037	0.035	0.039	0.038	0.043	0.044	0.030	-	0.037	0.035	0.032	0.036	0.037
O_3	0.029	0.037	0.031	0.039	0.038	0.040	0.039	0.041	0.034	0.035	-	0.036	0.029	0.037	0.039
T_1	0.039	0.035	0.036	0.035	0.026	0.029	0.031	0.036	0.037	0.039	0.036	-	0.034	0.035	0.035
T_2	0.034	0.030	0.032	0.028	0.027	0.025	0.026	0.034	0.037	0.037	0.036	0.036	-	0.040	0.039
T_3	0.025	0.027	0.027	0.026	0.028	0.027	0.028	0.029	0.034	0.034	0.032	0.033	0.039	-	0.022
T_4	0.019	0.020	0.022	0.023	0.023	0.031	0.024	0.030	0.030	0.021	0.020	0.022	0.019	0.025	-

Then, the weight matrix W_3, for the sub-factors is expressed as:

$$W_3 = \begin{bmatrix} 1.00 & 0.19 & 0.18 & 0.19 & 0.15 & 0.13 & 0.13 & 0.13 & 0.13 & 0.14 & 0.15 & 0.17 & 0.16 & 0.15 & 0.14 \\ 0.17 & 1.00 & 0.13 & 0.17 & 0.12 & 0.12 & 0.14 & 0.12 & 0.12 & 0.11 & 0.10 & 0.13 & 0.16 & 0.12 & 0.12 \\ 0.12 & 0.12 & 1.00 & 0.09 & 0.09 & 0.09 & 0.10 & 0.10 & 0.10 & 0.10 & 0.09 & 0.10 & 0.11 & 0.09 & 0.08 \\ 0.12 & 0.10 & 0.10 & 1.00 & 0.07 & 0.08 & 0.09 & 0.10 & 0.11 & 0.11 & 0.10 & 0.10 & 0.09 & 0.11 & 0.12 \\ 0.07 & 0.07 & 0.07 & 0.07 & 1.00 & 0.10 & 0.10 & 0.10 & 0.10 & 0.10 & 0.09 & 0.08 & 0.08 & 0.09 & 0.08 \\ 0.10 & 0.11 & 0.11 & 0.11 & 0.09 & 1.00 & 0.09 & 0.09 & 0.09 & 0.08 & 0.09 & 0.09 & 0.09 & 0.09 & 0.09 \\ 0.08 & 0.08 & 0.08 & 0.09 & 0.10 & 0.10 & 1.00 & 0.08 & 0.08 & 0.09 & 0.08 & 0.07 & 0.07 & 0.07 & 0.08 \\ 0.08 & 0.08 & 0.09 & 0.08 & 0.09 & 0.09 & 0.09 & 1.00 & 0.07 & 0.07 & 0.07 & 0.06 & 0.06 & 0.07 & 0.07 \\ 0.07 & 0.06 & 0.06 & 0.06 & 0.07 & 0.07 & 0.07 & 0.07 & 1.00 & 0.04 & 0.05 & 0.05 & 0.05 & 0.05 & 0.05 \\ 0.05 & 0.04 & 0.04 & 0.04 & 0.04 & 0.04 & 0.04 & 0.04 & 0.03 & 1.00 & 0.04 & 0.04 & 0.03 & 0.04 & 0.04 \\ 0.03 & 0.04 & 0.03 & 0.04 & 0.04 & 0.04 & 0.04 & 0.04 & 0.03 & 0.04 & 1.00 & 0.04 & 0.03 & 0.04 & 0.04 \\ 0.04 & 0.04 & 0.04 & 0.04 & 0.03 & 0.03 & 0.03 & 0.04 & 0.04 & 0.04 & 0.04 & 1.00 & 0.03 & 0.04 & 0.04 \\ 0.03 & 0.03 & 0.03 & 0.03 & 0.03 & 0.03 & 0.03 & 0.03 & 0.04 & 0.04 & 0.04 & 0.04 & 1.00 & 0.04 & 0.04 \\ 0.03 & 0.03 & 0.03 & 0.03 & 0.03 & 0.03 & 0.03 & 0.03 & 0.03 & 0.03 & 0.03 & 0.03 & 0.04 & 1.00 & 0.02 \\ 0.02 & 0.02 & 0.02 & 0.02 & 0.02 & 0.03 & 0.02 & 0.03 & 0.03 & 0.02 & 0.02 & 0.02 & 0.02 & 0.03 & 1.00 \end{bmatrix} \quad (9)$$

Then, the matrix that contains the overall weights of sub-factors $W_{sf\ (overall)}$, is created as follows:

$$W_{sf(overall)} = W_3 \times W_{sf} = \begin{bmatrix} 0.516 \\ 0.449 \\ 0.413 \\ 0.309 \\ 0.235 \\ 0.300 \\ 0.221 \\ 0.461 \\ 0.372 \\ 0.133 \\ 0.238 \\ 0.141 \\ 0.083 \\ 0.084 \\ 0.057 \end{bmatrix} \quad (10)$$

Furthermore, the evaluation of the alternative strategies is performed to determine the best alternative. To do so, the strategies are compared pairwise based on each sub-factors. For illustration, for the first sub-factor S_1, human experts and financial resources, the pairwise comparison among the four alternatives is displayed in Table 8.

Table 8 Pairwise comparison for the alternative strategies based on S_1

Alternative strategies	A_1	A_2	A_3	A_4	Importance
Developing new products (A_1)	1	5	0.5	7	0.329
Utilizing e-commerce (A_2)	0.2	1	0.14	0.5	0.059
Opening new market in Europe (A_3)	2	7	1	9	0.537
Providing different price level (A_4)	0.14	2	0.11	1	0.074

Similarly, the pairwise comparison for the proposed alternative strategies is performed with respect to each of the sub-factors S_1 to T_4. The resulted matrix W_4, of importance values are listed in Eq. 11.

$$W_4 = \begin{bmatrix} 0.329 & 0.514 & 0.461 & 0.583 & 0.404 & 0.121 & 0.139 & 0.209 & 0.537 & 0.121 & 0.426 & 0.209 & 0.127 & 0.045 & 0.242 \\ 0.059 & 0.156 & 0.058 & 0.042 & 0.249 & 0.466 & 0.543 & 0.429 & 0.191 & 0.612 & 0.054 & 0.121 & 0.059 & 0.413 & 0.087 \\ 0.537 & 0.262 & 0.416 & 0.274 & 0.263 & 0.079 & 0.251 & 0.066 & 0.205 & 0.134 & 0.411 & 0.621 & 0.177 & 0.236 & 0.366 \\ 0.074 & 0.068 & 0.064 & 0.101 & 0.084 & 0.334 & 0.067 & 0.296 & 0.066 & 0.041 & 0.109 & 0.050 & 0.637 & 0.306 & 0.305 \end{bmatrix} \quad (11)$$

The second step of alternative evaluation is to calculate the overall weight for each strategy alternative W_{st}, by multiplying importance weight matrix of the alternative strategies $W_{st\ (overall)}$, by the overall weight for sub-factors W_4, as given by Eq. 12.

$$W_{st} = W_4 \times W_{sf(overall)} = \begin{bmatrix} 0.404 \\ 0.680 \\ 0.962 \\ 0.557 \end{bmatrix} \quad (12)$$

Finally, based on the obtained values in Eq. 12, the best strategy that the cosmetic firm should pursue is to open new market in European countries (A_3, weight is 0.962) and exporting cosmetic products that mainly consist of neutral material.

5. Conclusion

Strategic management is collection of decisions adopted to achieve goals and objectives of an organization. This research successfully integrated the SWOT analysis and ANP analysis to assess the feasibility of alternative strategies and identify the best alternative that improves the performance of a Jordanian cosmetics firm. The importance of each SWOT factor is first determined with and without dependency. The super-matrix is created that contains matrices of importance values for factors, sub-factors, and alternatives. Based on the results of SWOT and ANP integration, the best strategy that cosmetic firm should follow is to open new market in European countries. In conclusion, this integration may provide great assistance to strategy planners in selecting the best strategy from a collection of potential feasible strategy alternatives that may bring significant performance improvement to firms in a wide range of applications.

References

[1] Al-Refaie, A. (2014). Examining factors affect supply chain collaboration in Jordanian organizations, *Journal of Management Analytics*, Vol. 1, No. 4, 317-337, doi: 10.1080/23270012.2014.991357.

[2] Al-Refaie, A., Al-Tahat, M. (2014). Effects of knowledge management and organizational learning on firm performance, *Journal of Nature Science and Sustainable Technology*, Vol. 8, No. 3, 369-390.

[3] Al-Refaie, A., Thyabat, A. (2014). Effect of just-in-time selling strategy on firms' performance in Jordan, *International Journal of Business Performance Management*, Vol. 16, No. 1, 1-18, doi: 10.1504/IJBPM.2015.066020.

[4] Al-Refaie, A., Hanayneh, B. (2014). Influences of TPM, TQM, Six Sigma practices on firms performance in Jordan, *International Journal of Productivity and Quality Management*, Vol. 13, No. 2, 219-234, doi: 10.1504/IJPQM.2014.059174.

[5] Al-Refaie, A., Li, M.H., Ko, J.H. (2012). Factors affecting customer linking capabilities and customer satisfaction in CRM: Evidence from Jordanian hotels, *International Journal of Customer Relationship Marketing and Management*, Vol. 3, No. 4, 16-30, doi: 10.4018/jcrmm.2012100102.

[6] Al-Refaie, A., Al-Tahat, M.D., Bata, N. (2014). CRM/e-CRM effects on banks performance and customer-bank relationship quality, *International Journal of Enterprise Information Systems*, Vol. 10, No. 2, 62-80, doi: 10.4018/ijeis.2014040104.
[7] Al-Refaie, A., Jalham, I.S., Li, M.H.C. (2012). Factors influencing the repurchase intention and customer satisfaction: A case of Jordanian telecom companies, *International Journal of Productivity and Quality Management*, Vol. 10, No. 3, 374-387, doi: 10.1504/IJPQM.2012.048754.
[8] Al-Refaie, A. (2015). Effects of human resource management on hotel performance using structural equation modeling, *Computers in Human Behavior*, Vol. 43, 293-303, doi: 10.1016/j.chb.2014.11.016.
[9] Dyson, R.G. (2004). Strategic development and SWOT analysis at the University of Warwick, *European Journal of Operational Research*, Vol. 152, No. 3, 631-640, doi: 10.1016/S0377-2217(03) 00062-6.
[10] Kahraman, C., Demirel, N.Ç., Demirel, T. (2007). Prioritization of e-Government strategies using a SWOT-AHP analysis: The case of Turkey, *European Journal of Information Systems*, Vol. 16, 284-298, doi: 10.1057/palgrave.ejis.3000679.
[11] Houben, G., Lenie, K., Vanhoof, K. (1999). A knowledge-based SWOT-analysis system as an instrument for strategic planning in small and medium sized enterprises, *Decision Support Systems*, Vol. 26, No. 2, 125-135, doi: 10.1016/S0167-9236(99)00024-X.
[12] Saaty, T.L. (1980). *The analytic hierarchy process*, McGraw-Hill, New York, USA.
[13] Saaty, T.L. (2008). Decision making with the analytic hierarchy process, *International Journal of Services Sciences*, Vol. 1, No. 1, 83-98, doi: 10.1504/IJSSCI.2008.017590.
[14] Saaty, T.L. (1996). *Decision making with dependence and feedback: The analytic network process*, RWS Publications, Pittsburgh, USA.
[15] Ertay, T., Ruan, D., Tuzkaya, U.R. (2006). Integrating data envelopment analysis and analytic hierarchy for the facility layout design in manufacturing systems, *Information Sciences*, Vol. 176, No. 3, 237-262, doi: 10.1016/j.ins. 2004.12.001.
[16] Mathiyazhagan, K., Diabat, A., Al-Refaie, A., Xu, L. (2015). Application of analytical hierarchy process to evaluate pressures to implement green supply chain management, *Journal of Cleaner Production*, Vol. 107, 229-236, doi: 10.1016/j.jclepro.2015.04.110.
[17] Goussous, J., Al-Refaie, A. (2014). Evaluation of a green building design using LCC and AHP techniques, *Life Science Journal*, Vol. 11, No. 8s, 29-40.
[18] Kurttila, M., Pesonen, M., Kangas, J., Kajanus, M. (2000). Utilizing the analytic hierarchy process (AHP) in SWOT analysis – A hybrid method and its application to a forest-certification case, *Forest Policy and Economics*, Vol. 1, No. 1, 41-52, doi: 10.1016/S1389-9341(99)00004-0.
[19] Chung, S.H., Lee, A.H.I., Pearn, W.L. (2005). Analytic network process (ANP) approach for product mix planning in semiconductor fabricator, *International Journal of Production Economics*, Vol. 96, No. 1, 15-36, doi: 10.1016/j.ijpe.2004.02.006.
[20] Cheng, E.W.L., Li, H. (2007). Application of ANP in process models: An example of strategic partnering, *Building and Environment*, Vol. 42, No. 1, 278-287, doi: 10.1016/j.buildenv.2005.07.031.
[21] Wu, W.W., Lee, Y.T. (2007). Selecting knowledge management strategies by using the analytic network process, *Expert Systems with Applications*, Vol. 32, No. 3, 841-847, doi: 10.1016/j.eswa.2006.01.029.
[22] Bayazit, O., Karpak, B. (2007). An analytical network process-based framework for successful total quality management (TQM): An assessment of Turkish manufacturing industry readiness, *International Journal of Production Economics*, Vol. 105, No. 1, 79-96, doi: 10.1016/j.ijpe.2005.12.009.
[23] Lin, Y.H., Chiu, C.C, Tsai, C.H. (2008). The study of applying ANP model to assess dispatching rules for wafer fabrication, *Expert Systems with Applications*, Vol. 34, No. 3, 2148-2163, doi: 10.1016/j.eswa.2007.02.033.

APEM journal
Advances in Production Engineering & Management
Volume 11 | Number 1 | March 2016 | pp 59–69
http://dx.doi.org/10.14743/apem2016.1.210
ISSN 1854-6250
Journal home: apem-journal.org
Professional paper

Aluminium hot extrusion process capability improvement using Six Sigma

Ketan, H.[a,*], **Nassir, M.**[a]

[a]Mechanical Engineering Department, University of Baghdad, Baghdad, Iraq

ABSTRACT

In this work, the Six Sigma (Define-Measure-Analyse-Improve-Control) DMAIC methodology has been followed to explain the original problem of lowering extrusion process variation and improving the process capability based on the determined Critical Quality Characteristics (CQC). The extrusion process charter worksheet is recognized, a SIPOC (Supplier-Input-Process-Output-Customer) chart is constructed and a Pareto chart is drawn in the Define phase of the methodology. Measurement data are collected, verifying process stability and verifying process normality by using $\overline{X}$-R charts and normality test, respectively. Process capacity index, sigma levels, defects per million opportunities (DPMO) determination in the measure phase using a Histogram. During Analyse phase, Cause and Effect diagram are established to determine their likelihood for the root cause of aluminium extrusion defective products. The suggested solutions are installed in the improve phase. In the Control phase, all tools are applied in the Measure phase are repeated to determine the improvement level. The DMAIC methodology has been applied in the (Ur state company for engineering industries)/(aluminium extrusion factory). The Minitab 16 Software is used for calculations and plot charts. The results for the internal dimension (X1) of the corner section product indicate a reduction in DPMO from 536804 to 185795.09, sigma level is improved from 1.4 to 2.4, process yield (Y) is improved from 46 % to 81 %, and profit is improved from ID 127.000 to ID 223.000 per 1000 kg.

ARTICLE INFO

Keywords:
Aluminium extrusion process
Six Sigma
DMAIC
Critical quality characteristics
Profit

**Corresponding author:*
hussket@yahoo.com
(Ketan, H.)

Article history:
Received 21 April 2014
Revised 3 September 2015
Accepted 20 October 2015

1. Introduction

Six Sigma was used by Motorola in 1987 [1]. Therefore of a series of changes in the quality area beginning in the late 1970s, with determined ten-fold advance drives [2]. The top-level organization management along with CEO Robert Galvin developed a theory called Six Sigma [3, 4]. From 1987 to 1997, Motorola got a fivefold increase in sales with income climbing nearly 20 percent per year, cumulative investments at $14 billion and stock price gain compounded to a once a year rate of 21.3 % [5].

In 1994, Six Sigma was started as a business initiative to produce high-level results, improve work processes, expand all employees' skills and change the culture [6]. GE determined in 1995 to apply Six Sigma throughout the entire companies. CEO Jack Welch led the organization during this implementation, and many distributions of GE experienced notable improvements in quality through those years [7]. Universal Electric reported that $300 million supplied in 1997 in Six Sigma send between $400 million and $500 million savings, with further incremental limits of $100 million to $200 million [8, 9].

In early 1997, Samsung and LG set in Korea started to establish Six Sigma under their comp organizations. The outcomes were surprisingly good in those organizations. For example, Samsung SDI, which is an organization under Samsung set, reported that the cost investments by Six Sigma planner totalled $150 million [10, 11]. Sigma is the letter in the Greek alphabet utilized to indicate standard deviation, a statistical mensuration of variation, the exclusion to expected results. The standard deviation can be thought of like a comparison among expected results in a group of procedures, against those that not succeed. The measurement of standard deviation illustrates that rates of defects, or exceptions, are calculable [7, 12]. Six Sigma is arithmetical term that refers to 3.4 defects per million (or 99.99966 % accuracy), which is as close as anyone is probable to obtain to perfect [5, 13]. A defect any effect that falls short of the customer's requirements or expectations [7].

Six Sigma methods use defects per unit (DPU) like a measurement tool. DPU is a good method to determine the quality of product or a process. The defects are generally relation between the time and the cost. The sigma value additional shows the frequency at which failures happen; as a result, as upper sigma value means the lower defect possibility. The defect is definite as the displeasure of the customer. Therefore, as sigma level raises, cycle time and cost reduce and at the same time customer satisfaction raises [6].

In Six Sigma method there are two tools namely: DMAIC and DFSS. The overall method to solve problem by DMAIC method consist of: translation of a practical problem into a statistical problem, discover a statistical solution, and then translation of that statistical solution into a practical solution and implementation appropriately in the industry [14].

Gijo et al. [15] shows the application of the Six Sigma method in decreasing defects in a fine grinding process of an automotive company, The DMAIC (Define-Measure-Analyse-Improve-Control) method to solve the original problem of decreasing process improving and variation the process yield. The purpose of the Six Sigma method resulted in decrease of defects in the fine grinding process from 16.6 % to 1.19 %.

Hung et al. [16] showed how a food company in Taiwan can use a systematic and disciplined method to go towards the aim of Six Sigma quality level. The DMAIC phases are used to reduce the defect rate of small custard buns by 70 % from the baseline to its entitlement. After the development actions were implemented through a six-month period this fell to under 0.141 %. Mandahawi et al. [17] studies a procedure development study applied at a local paper manufacturing support on customized lean Six Sigma method. The DMAIC methodology and various lean tools are used to streamline processes and enhance production. Gupta [18] showed a quality development study applied at a yarn manufacturing company's foundation on Six Sigma methodologies. The DMAIC task management-methodology and various tools are used to streamline processes and enhance production. Defects rate of textile goods in the yarn manufacturing process is so essential in industry point of view.

2. DMAIC methodology phases application

DMAIC is closed-loop method that removes non-productive steps, oftentimes concentrate on new measurements, and used technology for continuous development. Achievement of DMAIC method took place in five phases. Problem classification and definition takes in defining phase. After recognizing main processes, their performance is determined by measure phase with the assist of data collection. Origin causes of the problem are establishing out in the analysis phase. Solutions to implement problem and solving them are in improving phase. Development is maintained in control phase. The following case is taken from production line that produces aluminium products in in the (Ur state company for engineering industries) and particularly to (aluminium extrusion factory) [14].

2.1 Define phase

Define the extrusion process at dissimilar angles with the help of tools as the extrusion process charter worksheet and Pareto chart as shown below.

Drafting the extrusion process charter worksheet

This extrusion process charter worksheet outlines the purpose, objectives, and scope of the project as shown in Table 1.

Table 1 Extrusion process worksheet

Project title	Extrusion process capability improvement using Six Sigma
Business case	Extrusion factory in Ur state company for engineering industries produces varying amounts of typical aluminium products. Depending on the data recorded for the marketing department as shown in Table 2. It illustrates the increase of defects percentage due to the appearance of defects in products so that the records for the year 2012 will be taking due to the lack of the production rate.
Problem statement	Appearance defects in aluminium products and this has led to lower production rate as shown in the Table 2.
Goal statement	Improve extrusion process capability to reduce extrusion defects that appear frequently and in large quantities in the typically aluminium products, increase production costs, reduce inventory planes, raise profit and get better satisfaction for customer.

Table 2 Sales of aluminium products for years 2010 to 2012

Year	Production quantity (× 1000 kg)	Production sold (× 1000 kg)	Production defective (%)	Annual income (× ID 1000)
2010	67.837	60.836	10	270.325
2011	92.342	82.854	10.5	365.000
2012	313.005	268.501	14	1.182.00

Developing process map (SIPOC Diagram)

The SIPOC diagram of this work describing the supplier, input, process, output and customer are as shown in Table 3.

Table 3 Supplier-Input-Process-Output-Customer (SIPOC) diagram

Supplier	Input	Process	Output	Customer
1 – Raw material store 2 – Dies store 3 – Adjuvants store (Graphite pens) 4 – Sutton company	1 – Aluminum alloy 6063. – Dimensions (Billet diameter ø178-198 mm and length *L* 400-700 mm) – Standard specification (ASTM-B221 Iraqi standard 1730) 2 – Physical properties 3 – Chemical composition 4 – Hydraulic fluid	1 – Preheating process 2 – Extrusion process 3 – Quenching process 4 – Stretching process 5 – Cut-off process 6 – Artificial aging 7 – Packaging process	1 – Square section 2 – Rectangular section 3 – Joint section 4 –Swing doors section 5 – Structural section 6 – Furniture section 7 –T-section 8 – Angles section 9 – Round section 10 – Corner section	1 – Directorate General of Electricity Distribution Rusafa 2 – Directorate General of Electricity Distribution Karkh 3 – Directorate General of Electricity Distribution Euphrates 4 – Directorate General of Electricity Distribution South 5 – Directorate General of Electricity Distribution center 6 – Directorate General for power

Project selection

In this step the aluminium products and extrusion defects are selected and by using the data in the records of quality control department in extrusion factory for the year 2012. Initially, Pareto

chart in Fig. 1 should be used to select only the vital aluminium products that have the highest cumulative percentage as a key product. Finally, Pareto chart in Fig. 2 should be used to select only the vital extrusion defects that have the highest cumulative percentage as a key defect.

According to results from the Pareto charts in Fig. 1 and Fig. 2, the corner section product has the polygon with high defective rate (0.32) with percent (17.8), and the dimensional deflection defect has the high defective count (19923) with percent (45.2), respectively.

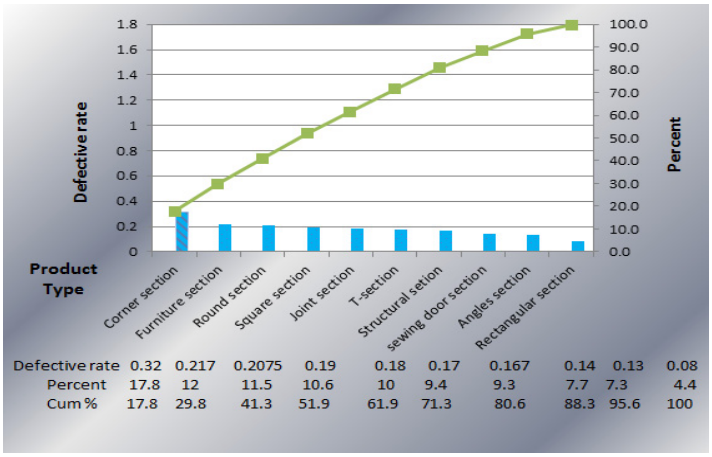

Fig. 1 Pareto chart of aluminium product type

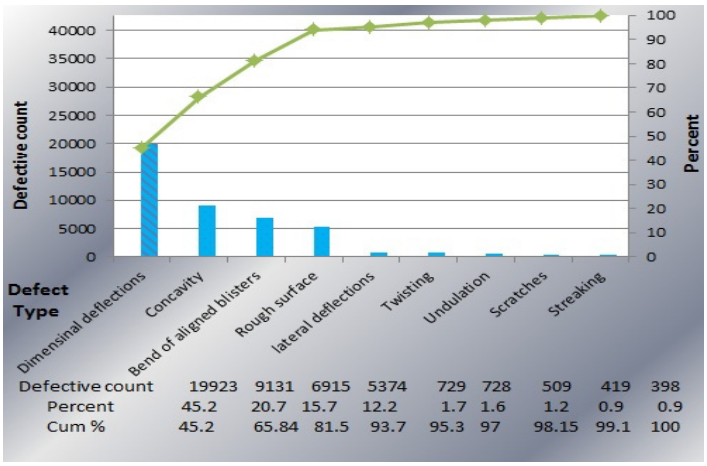

Fig. 2 Pareto chart of defect type

2.2 Measure phase

In this phase, corner section product is selected to execute the research methodology based on the results of Pareto charts in the previous phase. Critical Quality Characteristic (X1) with dimension specification ($36.7^{\pm 0.46}$) for corner section product in Fig. 3 is selected, due to its importance. Since any deviation from the required specification of (X1) will lead to the emergence of more defect products rejected by the customer. Measurements of 15 samples have been taken, each sample consist of 5 items from the packaging operation.

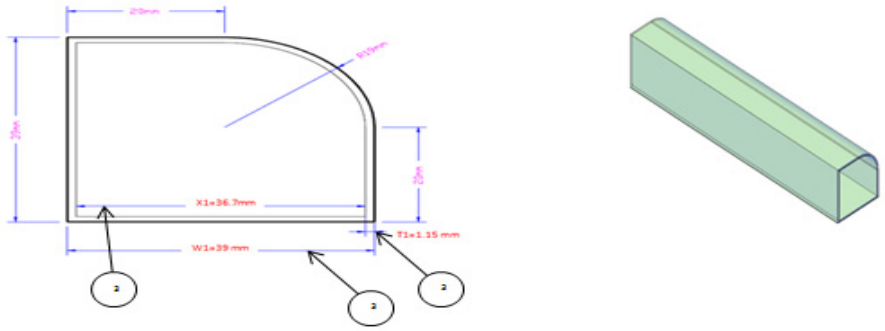

No.	Characteristics name	Signs	Tolerances (mm)
1	Section width	W1	$39^{\pm 0.54}$
2	The internal dimension of the section	X1	$36.7^{\pm 0.28}$
3	Section thickness	T1	$1.15^{\pm 0.17}$

Fig. 3 Corner section of the product

Analyzing the samples data by $\overline{X}$-R charts to determine if the extrusion process is under statistical control or not. Minitab 16 software is used to draw $\overline{X}$-R charts as shown in Fig. 4.

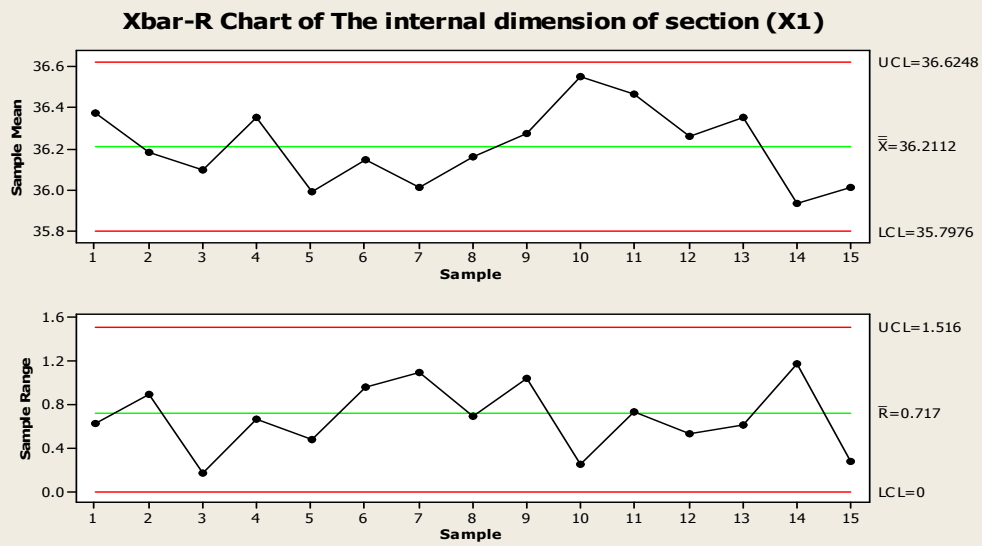

Fig. 4 $\overline{X}$-R charts for internal dimension of section (X1) before improvement

In Fig. 4 we can notice internal dimension (X1) of corner section product in stable state because no points out of the control limits of $\overline{X}$-R charts.

The Anderson-Darling test is used to determine the normality of internal dimension (X1) samples data of corner section product. Minitab 16 software is used for this purpose and the results are shown in Fig. 5. It is appear that (X1) samples data is normally distributed because the P-value of 0.212 is bigger than the critical value of 0.05.

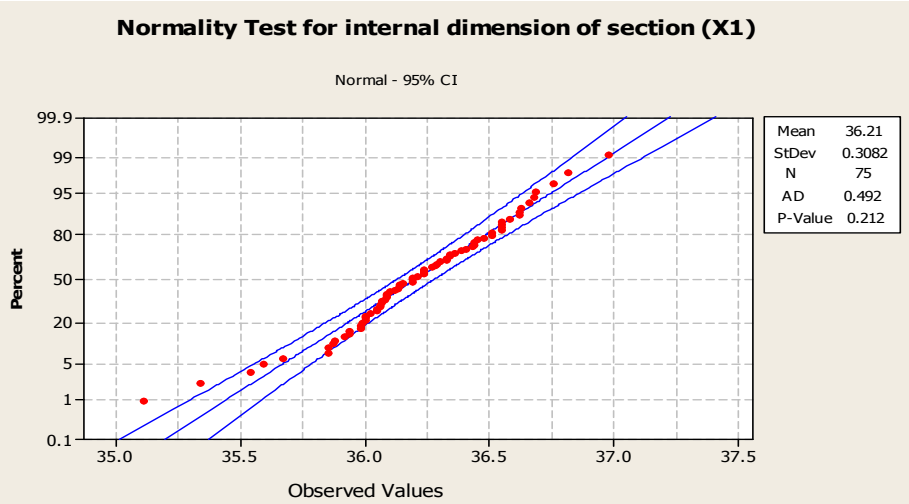

Fig. 5 Normality test for internal dimension of section (X1) before improvement

Based on the results of normality test, it is found that data for X1 are normally distributed. Therefore, process capability can be measured by using process capability analysis using histogram as shown in Fig. 6. Sigma level, yield (Y), defects per 1000 kg, and profit can be calculated by using following equations and the results in Table 4 as follows [2]:

$$\text{Sigma level} = 3 \cdot Cpk + 1.5 \tag{1}$$

$$Y = e^{-DPMO} \tag{2}$$

$$\text{Defects per 1000 kg} = DPMO \cdot W \tag{3}$$

$$W = V \cdot \rho \tag{4}$$

$$V = A \cdot L \tag{5}$$

$$\text{Profit} = (1 - \text{Defects per 1000 kg}) \cdot \text{Profit margin} \tag{6}$$

L is length of corner section product (6 m), A is area of corner section product (165 mm^2), V is volume of corner section product, W is weight of corner section product, ρ is alloys 6063 density (2685 kg/m^3), $DPMO$ is defects per million opportunities, and profit margin is ID 275.000.

Table 4 Results for calculations extrusion process measures of internal dimension (X1) of corner section of the product before improvement

Extrusion process measures	Measure value
C_p	0.46
C_{pk}	-0.03
Sigma level	1.4
DPMO	536804
Yield (Y)	46 %
Defects per 1000 kg	0.536804
Profit per 1000 kg	ID 127.000
Σ	0.329759
$\overline{X}$	36.2112

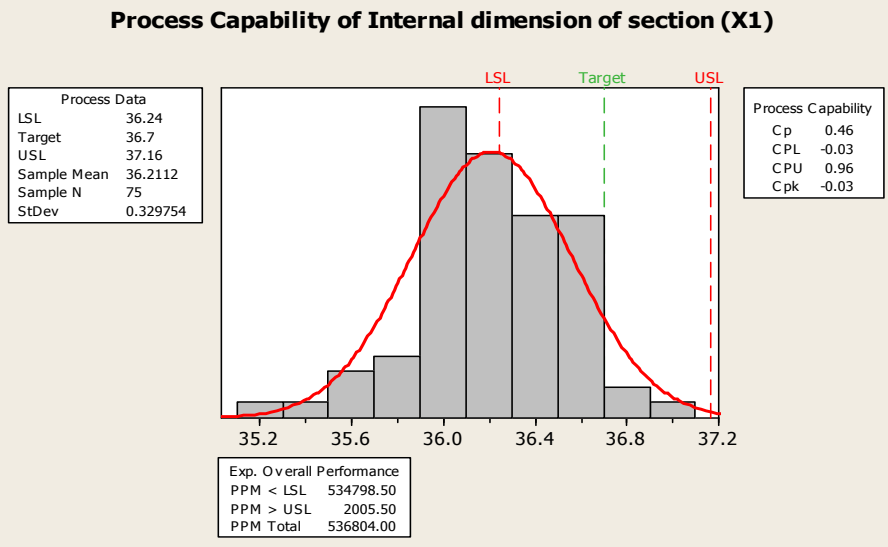

Fig. 6 Process capability of internal dimension of section (X1) before improvement

2.3. Analysis phase

This phase includes causes and effect diagram tool for analysis the previous results obtained from measure phase.

Cause and effect analysis

This step expresses the possible causes identified which have the most impact on the extrusion process. Fig. 7 for dimensional deflection defect presents a chain of causes and effects.

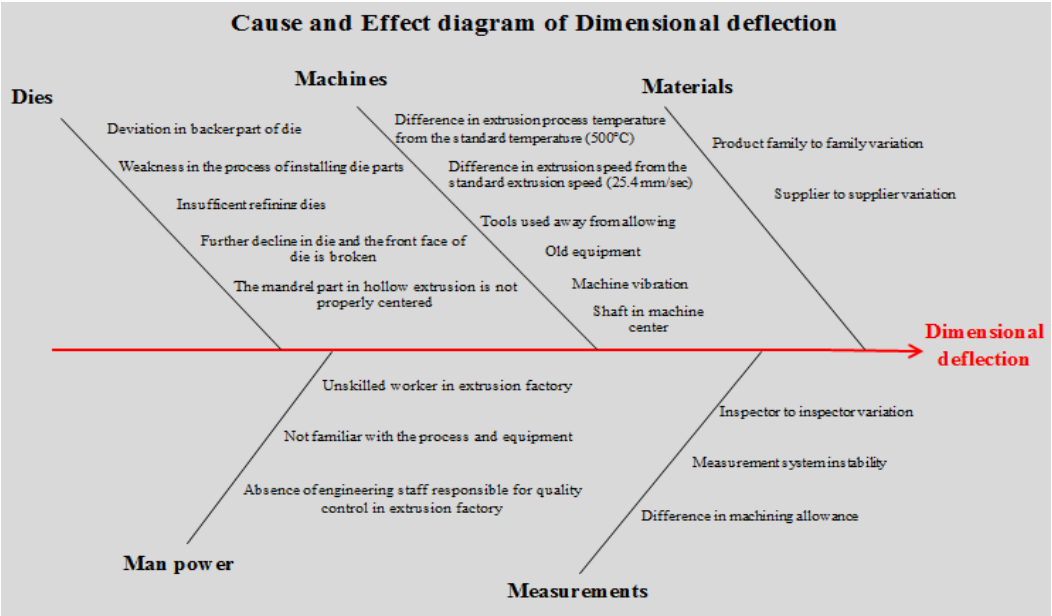

Fig. 7 Process capability of internal dimension of section (X1) before improvement

2.4 Improve phase

The improve phase is the fourth step in DMAIC methodology phases and its objective is to implement and find measures that would solve the aluminium products defects. Cause and suggested solution are shown in Table 5.

Table 5 Cause and suggested solution

Cause	Suggested solution
1 – Difference in extrusion process temperature from the standard temperature. 2 – Unskilled workers in extrusion factory. 3 – Absence of engineering staff to monitor the production line in every step of the extrusion process. 4 – Further decline in die and the front face of die is broken. 5 – Deviation in backer. 6 – Weakness in the process of assembly die parts. 7 – Insufficient refining dies.	1 – Monitoring the extrusion process temperature (control the die temperature and billet preheating temperature) by thermocouple device as shown in Fig. 8. 2 – Workers must engage in training sessions before overseeing the extrusion process. 3 – Creating a staff of quality control specialist. 4 – Replacement of the old die with a new die and check the front face of the die. 5 – Checking the process of assembly and grinding of die parts (mandrel and backer) as shown in Fig. 9, Fig. 10, and Fig. 11.

Fig. 8 Thermocouple device

Fig. 9 Parts of corner section die

Fig. 10 Corner section die after assembly

Fig. 11 Corner section die after grinding process

2.5 Control phase

The extrusion process will be test by finding the values of PCIs (Process capability indices), Sigma level, DPMO, Yield (Y) and profit after improvement. Therefore, new data of 15 samples with sample size 5 have been collected from the aluminium extrusion process. Then the entire steps in measure phase are repeated. The collected data and the details of the steps and calculations are shown in Table 6 and Figs. 12, 13, and 14.

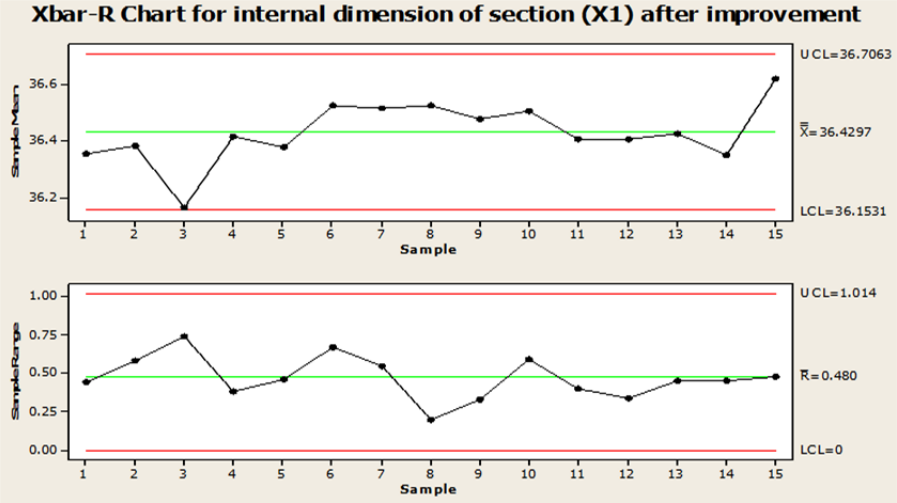

Fig. 12 $\overline{X}$-R charts for internal dimension of section (X1) after improvement

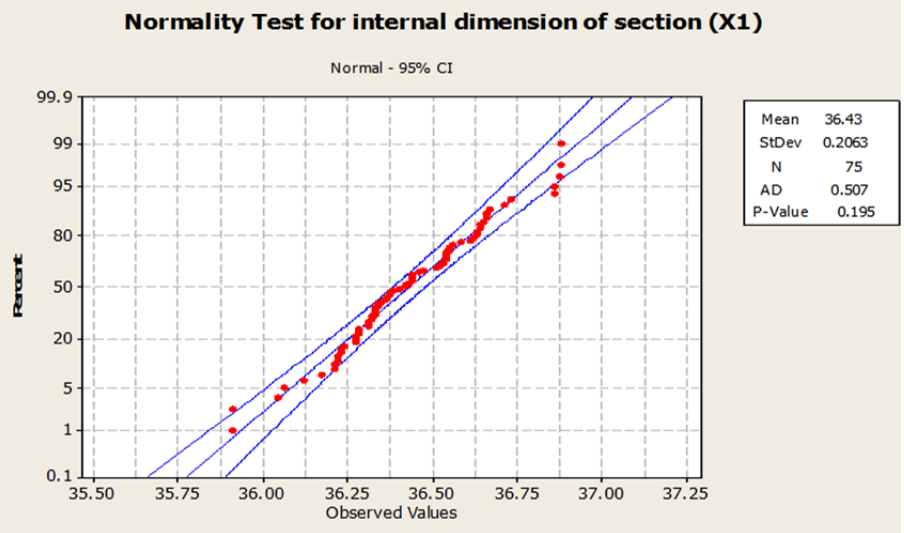

Fig 13 Normality test for internal dimension of section (X1) after improvement

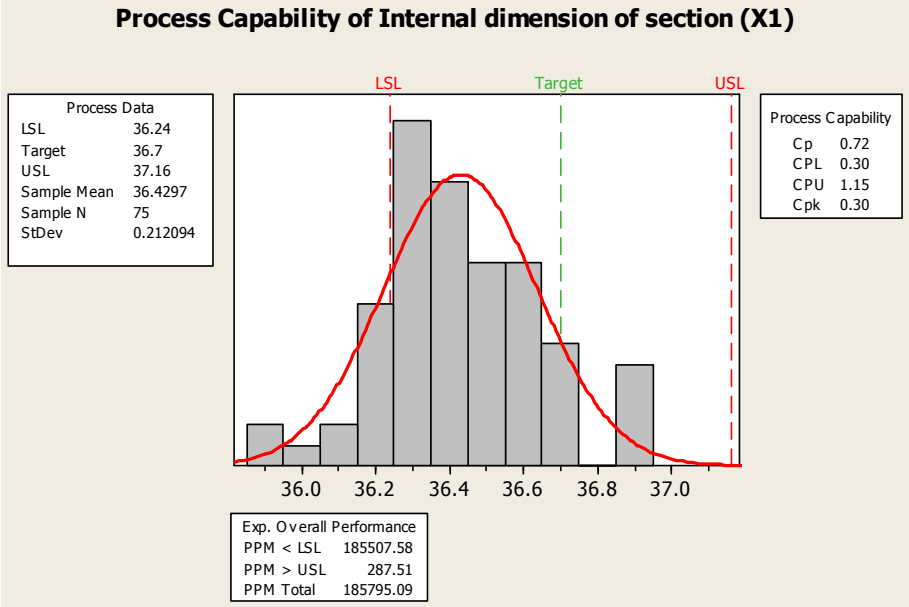

Fig 14 Process capability of internal dimension of section (X1) after improvement

Table 6 Results for calculations extrusion process measures of internal dimension of section (X1) after improvement

Extrusion process measures	Measure value
C_p	0.72
C_{pk}	0.3
Sigma level	2.4
DPMO	185795.09
Yield (Y)	81 %
Defect per 1000 kg	0.18579509
Profit per 1000 kg	223.000
Σ	0.212094
$\overline{X}$	36.4297

3. Results and discussion

The results of extrusion process measures PCIs (Process capability indices), sigma levels, and DPMO values before and after improvement shown in Table 4 and Table 6. The improvement of performance measures are as following: C_p value has been increased from 0.5 to 0.74 which means that the process capability is sufficient and the specification width greater than the process spread. The value of C_{pk} has increased from –0.032 to 0.306 which means that the standard deviation has decreased from 0.3082 to 0.208125. The process yield is increase to 36 % items without defects. The value of sigma level has increased from 1.4 to 2.42 which means reduction in defect products, so that DPMO value has been reduced from 536804 to 185795.09 and the profit increased from ID 127.000 to ID 226.000 per 1000 kg.

4. Conclusions and recommendations for future work

The conclusions and recommendations that are drawn from this work are as follows:

- Profits of implementation DMAIC methodology are accomplished in expression of cost decrease and remove aluminium products defects.
- The values for process capability measures (C_p, C_{pk}) indicate the ability to process improves or not. If the values are less than 1.0 as for CQC (X1) this situation point out the process mean deviation for aluminium product design specification (target value).
- The extrusion process mean increased, the extrusion process dispersion decreased and the process extrusion very nearer to target value.
- Based on the results, the sigma levels values increased depending on the implemented suggested solution. Therefore, this improvement is not sufficient to reach the value of six sigma level.
- The results prove that the DMAIC methodology is effective in estimation, analysis and improvement process capability of data that are normally distributed.
- Study the process capability improvement (DMAIC methodology) by using simulation technique to test and improve the effectiveness of suggested solution before they are implemented.
- The possibility of the DMAIC methodology application in the other aluminium products and other product defects were not able to study in this work due to the limitation of research time.

Acknowledgement

Our grateful to the staff members of quality control, dies manufacturing departments and staff of extrusion factory in UR state company for engineering industries in Iraq for their support to accomplish this research work. Finally, thanks are devoted to head and staff members of the department of mechanical engineering of Baghdad University for all facilities offered.

References

[1] García, F.R. (2014). *Six Sigma implementation within the building construction industry: A case study of the research building construction*, Master of science thesis, University Polytechnic of Valencia, School of Architecture, Valencia, Spain.
[2] Desale, S.V., Deodhar S.V. (2013). Lean Six Sigma principal in construction: A literature review related to conclusions, *International Journal of Emerging Technology and Advanced Engineering*, Vol. 3, No. 5, 531-535.
[3] El Santty, M.I., Tharwat A.A., Zein Eldin, R.A. (2013). Multi objective Six Sigma methodology: Application on chromojet printing, *American Journal of Research Communication*, Vol. 1, No. 7, 100-115.
[4] Park, S.H. (2003). *Six Sigma for quality and productivity promotion*, Productivity Series 32, Asian Productivity Organization, Tokyo, Japan.
[5] Khan, O.H. (2005). *A study of critical success factors for Six Sigma implementation in UK organizations*, Master of science dissertation, Bradford University, School of Management, UK.
[6] Aksoy, B., Orbak, Â.Y. (2009). Reducing the quantity of reworked parts in a robotic arc welding process, *Quality and Reliability Engineering International*, Vol. 25, No. 4, 495-512, doi: 10.1002/qre.985.

[7] Thomsett, M.C. (2004). *Getting started in Six Sigma*, John Wiley & Sons, Inc., Hoboken, New Jersey, USA.
[8] Farahmand, K., Grajales, J.V.M., Hamidi, M. (2010). Application of Six Sigma to gear box manufacturing, *International Journal of Modern Engineering*, Vol. 11, No. 1, 12-19.
[9] Basu, R., Wright, J.N. (2003). *Quality beyond Six Sigma*, Butterworth-Heinemann, Oxford, UK.
[10] Jodi, M.R. (2014). *Casting process improvements based on Six Sigma with simulation modelling*, Ph.D. thesis, Baghdad University, Mechanical department, Iraq.
[11] Prasad, K.G.D., Subbaiah, K.V., Padmavathi, G. (2012). Application of Six Sigma methodology in an engineering educational institution, *International Journal of Emerging Sciences*, Vol. 2, No. 2, 222-237.
[12] Mahanti, R., Antony, J. (2005). Confluence of Six Sigma, simulation and software development, *Managerial Auditing Journal*, Vol. 20, No. 7, 739-762, doi: 10.1108/02686900510611267.
[13] Habibi, A., Rezapour, A. (2015). The ability of implementation of Six Sigma in government hospitals of Babol, *DU Journal, Humanities and Social Sciences*, Vol. 8, No. 6, 41-63.
[14] Khekale, S.N., Chatpalliwar, A.S., Thakur, N.V. (2010). Minimization of cord wastages in belt industry using DMAIC, *International Journal of Engineering Science and Technology*, Vol. 2, No. 8, 3687-3694.
[15] Gijo, E.V., Scaria, J., Antony, J. (2011). Application of Six Sigma methodology to reduce defects of a grinding process, *Quality and Reliability Engineering International*, Vol. 27, No. 8, 1221-1234, doi: 10.1002/qre.1212.
[16] Hung, H.C., Sung, M.H. (2011). Applying Six Sigma to manufacturing processes in the food industry to reduce quality cost, *Scientific Research and Essays*, Vol. 6, No. 3, 580-591.
[17] Mandahawi, N., Fouad, R.H., Obeidat, S. (2012). An application of customized Lean Six Sigma to enhance productivity at a paper manufacturing company, *Jordan Journal of Mechanical & Industrial Engineering*, Vol. 6, No. 1, 103-109.
[18] Gupta, N., Bharti, P.K. (2013). Implementation of Six Sigma for minimizing the defects rate at a yarn manufacturing company, *International Journal of Engineering Research and Applications*, Vol. 3, No. 2, 1000-1011.

Calendar of events

- 5th International Conference on Industrial Technology and Management, Paris, France, March 17-18, 2016.
- 18th International Conference on Engineering Systems Modeling, Simulation and Analysis, Boston, USA, April 25-26, 2016.
- 3rd International Conference New Technologies NT-2016, Mostar, Bosnia and Herzegovina, May 13-14, 2016.
- 6th CIRP Conference on Assembly Technologies and Systems, Gothenburg, Sweden, May 16-17, 2016.
- 49th CIRP Conference on Manufacturing Systems, Stuttgart, Germany, May 25-27, 2016.
- 14th Annual Industrial Simulation Conference, Bucharest, Romania, June 6-8, 2016.
- 3rd CIRP Conference on Surface Integrity, Charlotte, NC, USA, June 8-10, 2016.
- International Symposium on Green Manufacturing and Applications, Bali, Indonesia, June 21-25, 2016.
- 8th IFAC Conference on Manufacturing Modelling, Management and Control, Troyes, France, June 28-30, 2016.
- 28th European Conference on Operational Research, Poznan, Poland, July 3-6, 2016.
- 10th CIRP Conference on Intelligent Computation in Manufacturing Engineering, Gulf of Naples, Italy, July 20-22, 2016.
- International Conference on Design and Production Engineering, Berlin, Germany, July 25-26, 2016.
- 27th DAAAM International Symposium, Mostar, Bosnia and Herzegovina, October 26-29, 2016.
- 3rd International Conference on Mechatronics, Automation and Manufacturing, Tokyo, Japan, October 29-31, 2016.

Notes for contributors

General

Articles submitted to the *APEM journal* should be original and unpublished contributions and should not be under consideration for any other publication at the same time. Manuscript should be written in English. Responsibility for the contents of the paper rests upon the authors and not upon the editors or the publisher. Authors of submitted papers automatically accept a copyright transfer to *Production Engineering Institute*, *University of Maribor*. For most up-to-date information on publishing procedure please see the *APEM journal* homepage *apem-journal.org*.

Submission of papers

A submission must include the corresponding author's complete name, affiliation, address, phone and fax numbers, and e-mail address. All papers for consideration by *Advances in Production Engineering & Management* should be submitted by e-mail to the journal Editor-in-Chief:

Miran Brezocnik, Editor-in-Chief
UNIVERSITY OF MARIBOR
Faculty of Mechanical Engineering
Production Engineering Institute
Smetanova ulica 17, SI – 2000 Maribor
Slovenia, European Union
E-mail: editor@apem-journal.org

Manuscript preparation

Manuscript should be prepared in *Microsoft Word 2007* (or higher version) word processor. *Word .docx* format is required. Papers on A4 format, single-spaced, typed in one column, using body text font size of 11 pt, should have between 8 and 12 pages, including abstract, keywords, body text, figures, tables, acknowledgements (if any), references, and appendices (if any). The title of the paper, authors' names, affiliations and headings of the body text should be in *Calibri* font. Body text, figures and tables captions have to be written in *Cambria* font. Mathematical equations and expressions must be set in *Microsoft Word Equation Editor* and written in *Cambria Math* font. For detail instructions on manuscript preparation please see instruction for authors in the *APEM journal* homepage *apem-journal.org*.

The review process

Every manuscript submitted for possible publication in the *APEM journal* is first briefly reviewed by the editor for general suitability for the journal. Notification of successful submission is sent. After initial screening, and checking by a special plagiarism detection tool, the manuscript is passed on to at least two referees. A double-blind peer review process ensures the content's validity and relevance. Optionally, authors are invited to suggest up to three well-respected experts in the field discussed in the article who might act as reviewers. The review process can take up to eight weeks. Based on the comments of the referees, the editor will take a decision about the paper. The following decisions can be made: accepting the paper, reconsidering the paper after changes, or rejecting the paper. Accepted papers may not be offered elsewhere for publication. The editor may, in some circumstances, vary this process at his discretion.

Proofs

Proofs will be sent to the corresponding author and should be returned within 3 days of receipt. Corrections should be restricted to typesetting errors and minor changes.

Offprints

An e-offprint, i.e., a PDF version of the published article, will be sent by e-mail to the corresponding author. Additionally, one complete copy of the journal will be sent free of charge to the corresponding author of the published article.

APEM journal

Advances in Production Engineering & Management

Production Engineering Institute (PEI)
University of Maribor
APEM homepage: apem-journal.org

Volume 11 | Number 1 | March 2016 | pp 1-72

Contents

ISSN 1854-6250

apem-journal.org